July 14, 2023 Docket No. 052-050

U.S. Nuclear Regulatory Commission
ATTN: Document Control Desk
One White Flint North
11555 Rockville Pike
Rockville, MD 20852-2738

SUBJECT: NuScale Power, LLC Submittal of Responses to NRC RSIs on Topical Report, "Methodology for the Determination of the Onset of Density Wave Oscillations (DWO)," TR-131981, Revision 0

REFERENCES:
1. NuScale Power, LLC, TR-131981-P, Revision 0, "Methodology for the Determination of the Onset of Density Wave Oscillations (DWO)," December 30, 2022. (ML22364A333)
2. NRC letter to NuScale Power, LLC, "Audit Plan for U.S. Nuclear Regulatory Commission Requests for Supplemental Information Identification of Specific Information Requirements – NuScale Standard Design Approval Application," March 22, 2023 (ML23067A298)

This letter provides NuScale's responses to the NRC Requests for Supplemental Information (RSIs) on topical report, "Methodology for the Determination of the Onset of Density Wave Oscillations," TR-131981, Revision 0 (Reference 1).

This letter contains NuScale's responses to the following RSI questions from the NRC, which were transmitted separately from Reference 2 in an RSI Audit Spreadsheet on Wednesday, March 22, 2023:

- RSI-1
- RSI-2
- RSI-3
- RSI-4
- RSI-5
- RSI-6
- RSI-7
- RSI-8
- RSI-9
- RSI-10
- RSI-11
- RSI-12
- RSI-13
- RSI-14
- RSI-15
- RSI-16
- RSI-17

The NRC accessed RSI responses containing markups to Reference 1 via the electronic reading room (eRR) prior to this transmittal. The RSI responses in Enclosure 1 and Enclosure 2 have been updated to be consistent with TR-131981-P, Revision 1, which is being transmitted separately. Compared to the RSI responses on the eRR, the RSI responses transmitted herein contain technical changes to Section 4.3.7, Figure 8-29, Figure 8-41, and Figure 10-10. All other changes are editorial in nature and do not affect the technical aspects of the RSI responses that were provided via the eRR.

Enclosure 1 contains the proprietary version of the RSI responses. NuScale requests that the proprietary version be withheld from public disclosure in accordance with the requirements of 10 CFR § 2.390. The enclosed affidavit (Enclosure 3) supports this request. The proprietary

version has also been deemed to contain Export Controlled Information. This information must be protected from disclosure per the requirements of 10 CFR § 810. Enclosure 2 contains the nonproprietary version of the RSI responses.

This letter makes no regulatory commitments and no revisions to any existing regulatory commitments.

If you have any questions, please contact Thomas Griffith at 541-452-7813 or tgriffith@nuscalepower.com.

Sincerely,

Mark W. Shaver
Acting Director, Regulatory Affairs
NuScale Power, LLC

Distribution: Michael Dudek, NRC
Getachew Tesfaye, NRC
Bruce Bavol, NRC

Enclosure 1: NuScale Responses to NRC RSIs on “Methodology for the Determination of the Onset of Density Wave Oscillations (DWO)”, TR-131981, Revision 0, proprietary version
Enclosure 2: NuScale Responses to NRC RSIs on “Methodology for the Determination of the Onset of Density Wave Oscillations (DWO)”, TR-131981, Revision 0, nonproprietary version
Enclosure 3: Affidavit of Mark W. Shaver, AF-145426

Enclosure 1:

NuScale RSI Responses to NRC Audit Questions on “Methodology for the Determination of the Onset of Density Wave Oscillations (DWO)”, TR-131981, Revision 0, proprietary version

NuScale Power, LLC
1100 NE Circle Blvd., Suite 200 Corvallis, Oregon 97330 Office 541.360.0500 Fax 541.207.3928
www.nuscalepower.com

Enclosure 2:

NuScale RSI Responses to NRC Audit Questions on “Methodology for the Determination of the Onset of Density Wave Oscillations (DWO)”, TR-131981, Revision 0, nonproprietary version

Response to Request for Additional Information
Docket: 99902078

RAI No.: RSI
Date of RAI Issue: 03/27/2023

NRC Question No.: RSI-1

52.137, Contents of Applications; Technical Information, (a)(2) requires “A description and analysis of the structures, systems, and components (SSCs) of the facility, with emphasis upon performance requirements, the bases, with technical justification, upon which these requirements have been established, and the evaluations required to show that safety functions will be accomplished,” and (b) “An application for approval of a standard design, which differs significantly from the light-water reactor designs of plants that have been licensed and in commercial operation before April 18, 1989,or uses simplified, inherent, passive, or other innovative means to accomplish its safety functions, must meet the requirements of 10 CFR 50.43(e).” Further, from 50.43(e) “Applications for a design certification, combined license, manufacturing license, or operating license that propose nuclear reactor designs which differ significantly from light-water reactor designs that were licensed before 1997, or use simplified, inherent, passive, or other innovative means to accomplish their safety functions, will be approved only if: (1)(i) The performance of each safety feature of the design has been demonstrated through either analysis, appropriate test programs, experience, or a combination thereof; (ii) Interdependent effects among the safety features of the design are acceptable, as demonstrated by analysis, appropriate test programs, experience, or a combination thereof; and (iii) Sufficient data exist on the safety features of the design to assess the analytical tools used for safety analyses over a sufficient range of normal operating conditions, transient conditions, and specified accident sequences, including equilibrium core conditions”. The NRC staff needs to assess the NRELAP5 ability to predict the required phenomena in order to conclude that code results adequately reflect the phenomena over the applicable range of conditions. The application for the DWO LTR is missing the following digital files: the measurement data and boundary conditions that include, at a minimum, primary and secondary side flows, bypass flows, temperatures, thermocouple measurements in the tubes, testing tube strain measurement data (or coaxial, but angularly separate, measurements with thermocouples), absolute and

differential pressure measurements, and heat loss. {{

}}[2(b)] These data files are necessary and considered a gap in the LTR application because without it the application would not be considered technically sufficient for the staff to review and the information presented is not sufficient to support the conclusions drawn by the LTR regarding NRELAP's ability to adequately predict the onset of DWO. The test data is required to compare the NRELAP predictions to the actual test results.

NuScale Response:

Proprietary Class 1 density wave oscillation (DWO) data was generated in 2022 testing at Società Informazioni Esperienze Termoidrauliche S.p.A. (SIET) TF-2. The following test data files in .bin format are on digital versatile disc for NRC use during the audit of the DWO topical report, TR-131981-P.

Table A {{ }}[2(b),ECI]

{{

}}[2(b),ECI]

{{

}}[2(b),ECI]

{{

}}2(b),ECI

{{

}}2(b),ECI

Figure 1 {{ }}(b),ECI

{{

}}2(b),ECI

Figure 2 {{ }}2(b),ECI

In addition, the following tables provide information to supplement the data files outlined in Table A.

- Table B contains a summary of the SIET TF-2 DWO test data.
- Table C identifies the critical measurements for the SIET TF-2 DWO test program.
- Table D identifies the critical instruments for the SIET TF-2 DWO test program.
- Table E contains the steady state set point confirmation criteria for the SIET TF-2 DWO test program.
- Table F contains DWO onset initiation and return to stability methods for the SIET TF-2 DWO test program.

The test facility piping and instrumentation diagram and the instrumentation diagrams for Row 1, Row 3, and Row 5 are attached to this response.

Table B {{ }}2(b),ECI

{{

}}2(b),ECI

Table B {{ }}2(b),ECI

{{

}}2(b),ECI

Table B {{ }}2(b),ECI

{{

}}2(b),ECI

Table C {{ }}2(b),ECI

{{

}}2(b),ECI

Table D {{ }}2(b),ECI

{{

}}2(b),ECI

Table D {{ }}2(b),ECI

{{

}}2(b),ECI

Table D {{ }}2(b),ECI

{{

}}2(b),ECI

{{

}}2(b),ECI

Table E {{ }}2(b),ECI

{{

}}2(b),ECI

{{

}}2(b),ECI

{{

}}2(b),ECI

Table F {{ }}2(b),ECI
{{

}}2(b),ECI

{{

}}2(b),ECI

Impact on Topical Report:

There are no impacts to Topical Report TR-131981, Methodology for the Determination of the Onset of Density Wave Oscillations (DWO), as a result of this response.

Figures:
NuScale Helical Coil Steam Generator Tests TF2 Fluid Heated Facility P&ID Loops

{{

}}2(b),ECI

{{

}}2(b),ECI

{{

}}2(b),ECI

{{

}}2(b),ECI

Response to Request for Additional Information
Docket: 99902078

RAI No.: RSI
Date of RAI Issue: 03/27/2023

NRC Question No.: RSI-2

The scope of what the DWO LTR seeks approval for is internally conflicting in various sections, and significant content is missing from the LTR for various types of approvals mentioned in the LTR. Although the title of the LTR would indicate the focus is only on the determination of the onset of DWO, the abstract states, "NuScale Power, LLC (NuScale) is requesting the Nuclear Regulatory Commission (NRC) review and approval to use the Steam Generator (SG) Density Wave Oscillation (DWO) Evaluation Model (EM) described herein for analyses of such oscillations during normal and off-normal operating conditions at reactor power levels between 20 and 100 percent nominal," and "[t]his EM provides a methodology for analyzing secondary-side instabilities in the NPM SG design, addresses identification of potential DWOs within the SG tubes, and provides information about such transients to support downstream stress and fatigue analysis of applicable portions of the reactor coolant system integral reactor pressure vessel and steam generator." This is also reflected in the executive summary. Further, sections 3 and 4 of the LTR indicate that both {{

}}$^{2(a),(c)}$. However, the purpose of this section of the LTR is more limited in scope and states, "[t]his evaluation model (EM) provides a validated method for calculating the margin to onset of density wave oscillations (DWO) in steam generator (SG) tubes that use an inlet flow restrictor (IFR) device. This report is used to size the inlet flow restrictor (IFR) resistance for the NuScale Power Module (NPM) to demonstrate thermal hydraulic stability between 20 percent and 100 percent reactor power (nominal), and to inform the design of nonsafety-related secondary-side control systems." This is a much more limited scope than that reflected in the abstract, executive summary, and portions of sections 3 and 4 of the LTR. Multiple clarification calls with NuScale have not resulted in any clarity as to the intended scope of the LTR, and as noted above, the docketed information is internally conflicting. If the abstract, executive summary and portions of sections 3 and 4 are indicative of the intent to qualify the methodology for broader calculations and analysis of the magnitude of the effects of DWO for downstream

design and licensing purposes, then the LTR is missing additional justification for the application of the method to produce those FoMs and the uncertainty analysis must be updated to reflect these additional FoMs.

NuScale Response:

The following sections of TR-131981-P, Revision 0, are revised as indicated in the attached markup:

- Abstract
- Executive Summary
- 1.1 Purpose
- 3.1 NuScale Power Module Steam Generator Operation (editorial to define an acronym whose definition was removed from Section 1.1)
- 3.2 Evaluation Model Requirements and Figures of Merit
- 11.0 Results/Conclusions

Note that changes to Section 3 are used to address request for supplemental information (RSI) 3.

Note that Section 4 is discussed in this RSI; however, changes to Section 4 are addressed in response to RSI-5, asking for clarification on the phenomena identification and ranking table. The response to RSI-5 is consistent with the changes in the attached markup to TR-131981-P, Revision 0.

In summary, the changes to TR-131981-P, Revision 0, state that the primary objective of the density wave oscillation (DWO) topical report is to obtain approval of the evaluation methodology (EM) to use NRELAP5 to predict the onset of DWO between 20 percent and 100 percent nominal reactor power in the NuScale Power Module (NPM-20) for the purpose of demonstrating margin to DWO onset within the expected operational domain. Clarification is also added to explain the example calculations in Appendix B and their purpose, which is only to provide example calculations showing how the NRELAP5 model can be used to predict onset of DWO in the NPM-20.

During the meeting to address RSI 1 on April 19, 2023, the NRC requested that NuScale outline how the safety of the NPM-20 is assured in case of possible DWO instability during any point of

operation. The consideration of DWO in operational and transient analysis space will be addressed in the responses to RSI-4, RSI-12, RSI-13, RSI-14, RSI-15, RSI-16, and RSI-17.

{{

}}2(a),(c)

{{

}}2(a),(c)

There was an additional set of clarifying questions on this RSI transmitted on May 11, 2023. The questions are in italics with responses following each question.

- *The RSI response states that the secondary objective of the topical report is approval of methodology to inform secondary side control system design. The RSI topical report markup states "This EM provides a methodology for analyzing secondary-side instabilities in the US460 NPM design. This EM also addresses identification of the onset of potential DWOs within the SG tubes for determining secondary side control feedback and for evaluating a preferred operating domain."*

  Please provide clarification for the scope of the topical report with respect to the markup that states the EM provides a methodology for analyzing secondary side instabilities. Clarify if only the onset of DWO is considered for secondary side control system design, or if a broader analysis of DWO is included in the scope, as implied by the first sentence.

  The statement in the Abstract, Executive Summary, and Section 1.1 Purpose of TR-131981-P is revised in the attached markup to clarify the scope. TR-131981-P is only seeking approval of an EM to predict DWO onset using NRELAP5 for the NPM-20.

- *The RSI response states clarification is also added to explain the example calculations in Appendix B and their purpose, which is to provide example calculations showing how the NRELAP5 model can be used to predict onset of DWO in the NPM.*

  The RSI topical report markup states (1) "Sample calculations for the NPM demonstrate that DWO onset does not occur in the NPM SG at nominal or off-nominal, steady-state operation at 100 percent power if the integral flow restrictor (IFR) loss coefficient is {{ }}2(a),(c)*. The sample calculation also evaluates DWO onset at off-nominal, 100 percent power conditions", (2) "The sample calculations demonstrate that the IFR loss coefficient (Kinlet) and expected operating conditions can be used to prevent onset of DWO at nominal and off-nominal operating conditions at 100 percent nominal power." (3) "The results of the sample calculation show that margin to DWO onset is possible at nominal and off-nominal 100 percent power conditions" and (4) "The sample results show that DWO onset does not occur in the NPM SG at the nominal or*

off-nominal, steady state 100 percent power level if the minimum IFR loss coefficient value is {{ }}[2(a),(c)].

Please provide clarification that the sample calculation results are not used to conclude that the SDAA NPM design will not experience DWO at nominal or off-nominal, steady-state operation at 100 percent power. Clarify whether the scope of the topical report requests the staff to make a finding that the SDAA NPM design does not experience DWO at nominal or off-nominal, steady-state operation at 100 percent power.

As stated in the Abstract of TR-131981-P, the sample calculation in Appendix B is for illustrative purposes to aid the reader's understanding of the context of the application of the DWO evaluation methodology. As stated in the Executive Summary of TR-131981-P, sample calculations are provided to demonstrate application of the EM in an NPM-20 steam generator model. As stated in Section 11.0, Results, of TR-131981-P, the sample calculation in Appendix B demonstrates application of the DWO evaluation methodology in an NPM-20 NRELAP5 model configured to predict DWO onset following the DWO evaluation methodology.

Impact on Topical Report:

Topical Report TR-131981, Methodology for the Determination of the Onset of Density Wave Oscillations (DWO), has been revised as described in the response above and as shown in the markup provided in this response.

Abstract

RSI-2

NuScale Power, LLC (NuScale) is requesting ~~the~~ Nuclear Regulatory Commission (NRC) review and approval to use the ~~Steam Generator (SG)~~ Density Wave Oscillation (DWO) Evaluation Model (EM) described herein for analyses of ~~such oscillations~~the onset of DWO in the NuScale Power Module (NPM-20) in the US460 design during normal and off-normal operating conditions at nominal reactor power levels between 20 percent and 100 percent ~~nominal~~. Use of this EM outside of ~~this power range~~these limitations requires justification.

RSI-2

The ~~SG~~ DWO ~~EM~~evaluation model uses the proprietary NRELAP5 system analysis code. The NRELAP5 code includes models and correlations for heat transfer and pressure drop for the ~~NuScale Power Module (~~NPM-20~~)~~ helical coil steam generator (SG). Extensive NRELAP5 validation was performed to ensure the DWO ~~EM~~evaluation model is applicable for important phenomena and processes. The validation suite includes separate effects test (SET) and integral effects test (IET) data developed specifically for the NPM-20 application.

RSI-2

This EM addresses identification of the onset of potential DWOs within the SG tubes for evaluating a preferred operating domain. This EM is not used to verify safety-related functions of structures, systems, and components (SSC).~~This EM provides a methodology for analyzing secondary side instabilities in the NPM SG design, addresses identification of potential DWOs within the SG tubes, and provides information about such transients to support downstream stress and fatigue analysis of applicable portions of the reactor coolant system integral reactor pressure vessel and steam generator.~~

RSI-2

Although not required because this method is not used to verify safety-related functions of SSC, this ~~SG~~ DWO ~~EM~~evaluation method follows the guidance provided in “Transient and Accident Analysis Methods,” Regulatory Guide (RG) 1.203. Key aspects of ~~this~~ RG 1.203 that are addressed include:

RSI-2

- development of the DWO phenomena identification and ranking table (PIRT)~~,~~
- assessment of separate effects and integral~~-~~ effects DWO tests~~,~~
- quantification of code uncertainty based on comparisons to test data~~,~~
- EM development~~,~~
- EM adequacy assessment using bottom-up assessment of NRELAP5 models and correlations, and top-down assessment of NRELAP5 models for mass, momentum, and energy conservation, and numerical solution techniques~~.~~
- integral effects test facility scaling~~.~~

RSI-2

Uncertainty quantification and margin evaluation applies to the NRELAP5 analysis of DWO onset for the NPM-20.

RSI-2

For illustrative purposes to aid the reader's understanding of the context of the application of this ~~SG~~ DWO ~~EM, a~~evaluation method sample calculations of the implemented EM using NRELAP5 ~~is~~are provided. ~~C~~Sample calculations for the NPM-20 ~~SG are performed at 100 percent power~~demonstrate that DWO onset does not occur in the NPM-20 steam generator at nominal or off-nominal steady-state operation at 100 percent power if the inlet flow restrictor (IFR) loss coefficient is {{ }}$^{2(a),(c)}$. Example calculations illustrate~~Results show~~ that a {{ }}$^{2(a),(c)}$ exists at ~~this~~100 percent power.

Executive Summary

RSI-2

NuScale Power, LLC (NuScale) is requesting Nuclear Regulatory Commission (NRC) review and approval to use the ~~Steam Generator (SG)~~ Density Wave Oscillation (DWO) Evaluation Model (EM) described in this topical report for analyses of ~~steam generator oscillations~~DWO onset prediction during ~~normal~~nominal and off-~~normal~~nominal operating conditions at reactor power levels between 20 percent and 100 percent ~~nominal~~. Although not required because this EM is not used to verify safety-related functions of systems, structures, and components (SSC), this ~~SG~~ DWO ~~EM~~evaluation model is consistent with the guidance provided in "Transient and Accident Analysis Methods," Regulatory Guide (RG) 1.203 (Reference 12.1), ~~since~~because it contains industry best practices for EM development. This topical report is not intended to provide final design values or results; rather, it contains ~~example values~~sample calculations using the EM for illustrative purposes to aid the reader's understanding of the context of the application of the ~~SG~~ DWO ~~EM~~evaluation model.

RSI-2

NuScale developed a small modular reactor (SMR) design that supports operation of multiple NuScale Power Modules (NPM-20s) at a specific site. Each NPM-20 is an advanced, light-water, integrated pressurized water reactor (PWR) using natural circulation for the primary coolant flow. Within each NPM-20 there are two independent helical coil steam generators (SG) in the upper outer annulus of the primary reactor pressure vessel (RPV). Each SG consists of a large number of helical tubes connected in parallel to common feedwater (FW) plenums at the bottom~~,~~ and common steam plenums at the top. Each SG tube has ~~at its inlet~~ an inlet flow restrictor ~~device~~(IFR) that is sized to provide secondary-side hydraulic resistance within the single-phase region to enhance secondary flow stability.

RSI-2

Systems that utilize convective boiling flow, such as the NPM-20 steam generators~~SGs~~ can be found in a variety of industrial applications, including boiling water reactors, steam boilers, heat exchangers, and condensers. Such systems offer the advantage of high heat transfer rates at moderate temperature differences. A drawback ~~though~~ is that these systems are susceptible to thermally-~~-~~induced two-phase DWO~~s~~ that require additional engineering design to ~~overcome~~address. For the NuScale Power Module (NPM-20) ~~SG~~steam generators, secondary-side fluid boiling within the tubes creates conditions potentially prone to parallel tube DWO. Hydraulic sizing of the tube ~~inlet flow restrictor~~IFR is important to ensuring acceptable flow stability ~~along with reasonable constraints to power operation~~.

RSI-2

~~NuScale previously submitted to the NRC a design certification application (DCA) for review and approval of a 12 NPM power plant design. Upon final review and final ACRS meetings, it was determined that a Combined Operating License (COL) item was required to close portions of the reactor coolant system integral reactor pressure vessel and steam generator fatigue analysis to address potential impact of DWO to SG lifetime. A COL item 3.9-14 was created to address these concerns, it states:~~

> ~~*A COL applicant that references the NuScale Power Plant design certification will develop an evaluation methodology for the analysis of secondary-side instabilities in the steam generator design. This methodology will address the identification of potential density wave oscillations*~~

~~*in the steam generator tubes, and qualification of the applicable portions of the reactor coolant system integral reactor pressure vessel and steam generator given the occurrence of density wave oscillations, including the effects of reverse fluid flows within the tubes.*~~

RSI-2

This EM is used to identify the onset of potential DWO within the SG tubes for evaluating a preferred operating domain. The qualification of applicable portions of the reactor coolant system (RCS) integral RPV and SG given the occurrence of DWO is outside the scope of this topical report. This EM is not used to verify safety-related functions of SSC.~~This SG DWO EM provides a methodology for analyzing secondary side instabilities in the NPM SG design, addresses identification of potential DWOs within the SG tubes, and provides information about such transients to support downstream stress and fatigue analysis of applicable portions of the reactor coolant system integral reactor pressure vessel and steam generator. The methodology for evaluating SG integrity from a thermal fatigue perspective is outside the scope of this report.~~

RSI-2

This ~~SG~~ DWO ~~EM~~evaluation model uses the NuScale-proprietary NRELAP5 computer code as the computational tool. This software was derived from the Idaho National Laboratory (INL) RELAP5-3D© computer code. It includes the necessary models for characterization of the NPM-20 hydrodynamics, heat transfer between structures and fluids, modeling of fuel, reactor kinetics models, and control systems. The NRELAP5 code includes models and correlations for heat transfer and pressure drop for the NPM-20 helical coil SG.

RSI-2

Validation and verification of the ~~SG~~ DWO ~~EM~~evaluation model was conducted following the principles and guidance in the Evaluation Model Development and Assessment Process (EMDAP) of RG 1.203. A phenomena identification and ranking table (PIRT)~~,~~ that identifies the important phenomena and processes impacting ~~SG~~ DWO~~,~~ was developed. Seventeen phenomena were identified as important to DWO, ~~and thus important to capture~~ which were considered in the ~~SG~~ DWO ~~EM~~evaluation model. Six of these important phenomena have a low knowledge level (level = 2)~~,~~ and require~~d~~ assessment against test data.

RSI-2

Extensive NRELAP5 code assessment was performed to ensure applicability of the ~~SG~~ DWO ~~EM~~evaluation model for the important PIRT phenomena over the range of conditions encountered in the NPM-20. The validation tests included separate effects test (SET) and integral~~-~~ effects ~~DWO~~ test~~s~~ (IET) performed at the Società Informazioni Esperienze Termoidrauliche S.p.A. (SIET) TF-1 facility in 2013~~6 and new~~ and at SIET TF-2 in 2015, as well as DWO tests performed at the SIET TF-2 facility in 2022. Additional validation was conducted using an external database obtained from Polytechnic University of Milan (POLIMI). For TF-1 and TF-2 testing, predicted-to-measured values of DWO onset are in reasonable-to-excellent agreement. For POLIMI, which has longer tubes and a tighter helix than the NPM-20 ~~SG~~steam generator, NRELAP5 predictions of DWO onset are conservative.

RSI-2

The EM adequacy for analysis of DWO ~~analysis of~~onset for the NPM-20 ~~SGs~~ is demonstrated through bottom-up and top-down evaluations performed with NRELAP5 for high-ranking PIRT phenomena~~,~~ and through NRELAP5 validation against relevant test data. For the bottom-up assessment, adequacy of the models and correlations in NRELAP5 are examined by considering their pedigree, applicability, and fidelity to appropriate fundamental or ~~separate effects test~~SET

data, and scalability to the ~~SG~~ DWO onset conditions. Integral or top-down performance is assessed by evaluating the mathematical models for mass, momentum, and energy conservation; numerical solution techniques employed; and integral effects test predictions of TF-2 where integral system response is present. The conclusion drawn from the bottom-up and top-down assessments is that the EM is adequate for the purpose of predicting ~~SG~~ DWO onset for the NPM-20.

RSI-2

An uncertainty analysis ~~is carried out using~~uses TF-1 and TF-2 test~~DWO~~ data. Using a 95 percent confidence interval, the NRELAP5 uncertainty in predicting helical coil SG tube pressure drop and heat transfer is calculated. When highly conservative biasing parameter uncertainty is applied to TF-2 NRELAP5 models, NRELAP5 uncertainty for predicting DWO onset is calculated to be {{ }}$^{2(a),(c)}$. This uncertainty is then applied to the NPM-20 ~~SG~~steam generator DWO onset analysis calculations.

RSI-2

~~A s~~Sample calculations ~~is~~are provided to demonstrate application of the EM in an NPM-20 ~~SG DWO~~steam generator model. These~~is~~ sample calculations demonstrate~~s~~ that appropriate NRELAP5 modeling can be used to predict DWO onset~~, with consideration of an inlet flow restrictor~~. The sample calculations provide context for the reader's understanding of the application of the DWO evaluation model. The sample calculations demonstrate that the IFR loss coefficient (K_{inlet}) ~~loss~~ and expected operating conditions can be used to prevent onset of DWO at nominal and off-nominal operating conditions at 100 percent nominal power. This methodology application also illustrates how to determine margin to DWO onset, apply code uncertainty, and account for the effect of deviations from nominal conditions in DWO onset predictions. The results of the sample calculations show that margin to DWO onset is possible at ~~all~~ nominal ~~power levels at and above 20 percent power,~~ and ~~at~~ off-nominal 100 percent power conditions~~ that are reasonably expected to be bounded by the final control system design and nominal trip setpoints.~~

1.0 Introduction

1.1 Purpose

RSI-2

~~This evaluation model (EM) provides a validated method for calculating the margin to onset of density wave oscillations (DWO) in steam generator (SG) tubes that use an inlet flow restrictor (IFR) device. This report is used to size the inlet flow restrictor (IFR) resistance for the NuScale Power Module (NPM) to demonstrate thermal hydraulic stability between 20 percent and 100 percent reactor power (nominal), and to inform the design of nonsafety-related secondary side control systems.~~This evaluation model (EM) addresses identification of the onset of potential density wave oscillations (DWO) within the steam generator (SG) tubes in the NuScale Power Module (NPM-20) design for evaluating a preferred operating domain. This EM is not used to verify safety-related functions of structures, systems, and components (SSC).

1.2 SG DWO Stability Evaluation Model Scope

RSI-2

The scope of this ~~evaluation model (~~EM~~)~~ is limited to the NPM-20 steam generator ~~(SG)~~ and nominal reactor power levels between 20 percent and 100 percent. Use of this EM for components other than the SG or outside of the nominal 20 percent to 100 percent power range requires further justification.

RSI-2

~~Although not required,~~ This method is not used to verify safety-related functions of SSC; therefore, Regulatory Guide (RG) 1.203 is not required. However, this EM is consistent with the guidance in "Transient and Accident Analysis Methods," ~~Regulatory Guide (~~RG~~)~~ 1.203 (Reference 12.1)~~, since~~ because it contains industry best practices for thermal-hydraulic (T-H) EM development. As such, this report describes the ~~NuScale SG~~NPM-20 steam generator design and operation, phenomena identification and ranking table (PIRT), and NRELAP5 input model, correlations, and applicability to ~~SG~~ DWO onset analysis. ~~In addition, t~~This report also summarizes NRELAP5 assessments against separate effects test (SET) and integral effects test (IET) data~~. A~~ and presents an uncertainty analysis and DWO onset margin methodology ~~is presented~~.

RSI-2

Qualification of NPM-20 structural components, such as the integral reactor pressure vessel (RPV) and SG, given the occurrence of DWO are outside of the scope of this report~~, but are taken into consideration as part of the ASME component lifetime fatigue analysis.~~

1.3 Abbreviations

RSI-2

Table 1-1 Abbreviations

Term	Definition
1-D	one-dimensional
~~ACRS~~	~~Advisory Committee on Reactor Safeguards~~
ASME	American Society of Mechanical Engineers

RSI-2

Figure 3-1 NuScale Power Module Cut Away

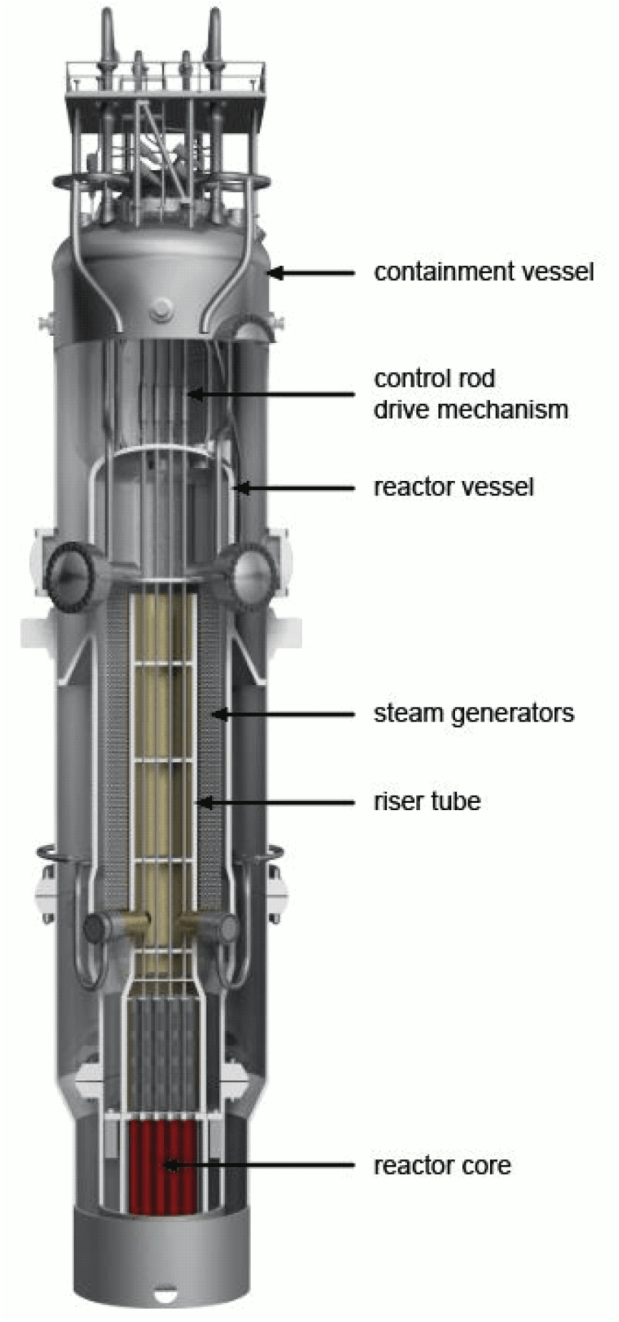

3.2 Evaluation Model Requirements and Figures of Merit

RSI-2, RSI-3

This EM provides a validated method for calculating the margin to the onset of density wave oscillations in the NPM-20 ~~SG~~steam generator tubes that use an ~~tube~~ IFR ~~device~~. ~~It is used to size IFR resistance for the NPM to demonstrate thermal hydraulic stability between 20 percent and 100 percent reactor power (nominal).~~

RSI-2, RSI-3

In order to evaluate SG stability with respect to DWO onset, the following figure~~s~~ of merit (FoM~~s~~) ~~are~~is selected:

1. DWO onset

RSI-2, RSI-3

2. ~~DWO flow change amplitude~~
3. ~~DWO flow rate frequency~~

RSI-2, RSI-3

Two supplemental FoMs are used:

1. DWO flow change amplitude
2. DWO flow rate frequency

RSI-2, RSI-3

Because the three FoMs are inextricably linked to the DWO phenomena, the use of DWO flow change amplitude and DWO flow rate frequency must be considered in order to accurately predict onset of DWO related to instabilities in the NPM-20 helical coil SG. For this DWO onset EM~~methodology~~, reasonable-to-excellent agreement is needed for prediction of DWO onset (FoM~~s~~ 1) because DWO onset prediction is the purpose of the DWO evaluation model.~~,~~ ~~while m~~Minimal agreement is needed for flow change amplitude~~,~~ and flow rate frequency (FoMs 2 and 3) because these FoMs can have higher uncertainty and still support the accurate prediction of DWO onset and ensure that the DWO onset is attributable to the correct phenomena.

RSI-2, RSI-3

The calculation of margin is performed using realistic operating parameters that are used by non-safety~~-~~-related secondary~~-~~-side control systems for monitoring and control of power production.

RSI-2, RSI-3

This report provides a description of the NuScale ~~SG~~ DWO ~~EM~~evaluation model. The following steps are used to develop the EM. ~~They are:~~

- ~~D~~determining the requirements for the EM
- ~~D~~developing an assessment base consistent with the determined requirements
- ~~D~~developing the EM
- ~~A~~assessing the adequacy of the EM

11.0 Results/Conclusions

RSI-2

This topical report presents the EM used to evaluate DWO in the NPM-20 ~~HCSG~~ during ~~normal~~nominal and off-nominal~~normal~~ operating conditions. Although not required, this DWO ~~EM~~evaluation model is consistent with guidance provided in the EMDAP of "Transient and Accident Analysis Methods," Regulatory Guide 1.203.

RSI-2

The DWO ~~EM~~evaluation model uses the proprietary NRELAP5 code as the computational tool. NRELAP5 includes the necessary models for the characterization of the NPM-20 hydrodynamics, heat transfer between structures and fluids, modeling of fuel, reactor kinetics models, and control systems. Additional models and correlations are added to model the NPM-20 helical coil SG configuration.

RSI-2

Validation and verification of the EM and NRELAP5 code are conducted using a well-established process. A PIRT, which identifies the important phenomena and processes for HCSG stability, is developed. A total of 17 phenomena are identified as high- ranked and thus important to capture in the DWO ~~EM~~evaluation model.

RSI-2

Extensive NRELAP5 code validation is performed to ensure that the EM is applicable for the important phenomena and processes over the range encountered in NPM-20 operation. The validation suite includes SETs and IETs developed and run specifically for the NPM-20 SG application. The FoM for ~~IETs are~~the DWO evaluation model is DWO onset~~, DWO flow period, and DWO flow amplitude~~.

RSI-2

The SETs were performed at the TF-1 facility. TF-1 provided data on pressure drop and heat transfer for the secondary- side. TF-1 also provided DWO test data with DWO onset, DWO flow period, and DWO flow amplitude. Both SETs and IETs were performed at the TF-2 facility. TF-2 SETs provided data on primary-side heat transfer and pressure drop. TF-2 also provided DWO test data with DWO onset, DWO flow period, and DWO flow amplitude. Additional validation of NRELAP5 is carried out with an external DWO database obtained from POLIMI. The POLIMI DWO test data validation shows that NRELAP5 is conservative in predicting DWO onset for a non-prototypical HCSGs with longer tubes and a tighter helix.

RSI-2

The NRELAP5-based ~~SG~~ DWO ~~EM~~evaluation model is evaluated for applicability to analyze DWO in the NPM-20. The applicability of NRELAP5 for high- ranked~~ing~~ phenomena is demonstrated by comparing NRELAP5 predictions to data from SETs and IETs. Reasonable-to-excellent agreement obtained via comparison establishes the applicability of NRELAP5 to accurately predict DWO onset phenomena at both the SETs and IETs.

RSI-2

Uncertainty analysis is carried out based on TF-1 SET data and on TF-2 DWO ~~IET~~integral effects test data. Using a 95 percent confidence interval, the {{

}}2(a),(c), respectively. When highly conservative biasing parameter uncertainty is applied to TF-2 DWO NRELAP5 models, the NRELAP5 uncertainty for predicting DWO onset is ~~calculated at~~ {{

}}2(a),(c)

RSI-2

This~~e~~ report also contains the methodology for evaluating margin to DWO onset in the NPM-20 at normal and off-normal operating conditions and is applied for NPM-20 nominal reactor power levels between 20 percent and 100 percent ~~nominal~~. The sample calculations in Appendix B demonstrate~~s~~ application of the DWO ~~EM~~evaluation model in an NPM-20 NRELAP5 model configured to predict DWO onset following the DWO evaluation model.~~NPM SG DWO NRELAP5 model.~~ The sample results show that DWO onset does not occur in the NPM-20 helical coil SG at the nominal or off-nominal, steady--state 100 percent power level if the minimum IFR ~~loss coefficient~~K_{inlet} value is {{

}}2(a),(c) Results are conservatively biased for code uncertainty. Margin to DWO onset is demonstrated at nominal and~~power levels and at~~ off-nominal 100 percent power conditions. ~~that are reasonably expected to be bounded by the final control system design and nominal trip setpoints.~~

RSI-2

The ~~evaluation model~~EM developed herein has an established pedigree and is determined to be adequate for downstream NPM-20 ~~SG~~ analysis for DWO onset. ~~Use of NRELAP5 for accurate prediction of DWO flow period and DWO flow amplitude requires additional evaluation, which may involve nodalization changes and/or methodology improvement.~~

Response to Request for Additional Information
Docket: 99902078

RAI No.: RSI
Date of RAI Issue: 03/27/2023

NRC Question No.: RSI-3

The DWO LTR indicates that for some FOMs, the agreement between the model's calculated results and the testing results only needs to be "minimal". Therefore, if approval is sought for the methodology to produce FoMs for licensing purposes (see item above on the inconsistencies in scope of approval requested for this LTR) for which the agreement between the EM and the validation basis is "minimal," additional justification for this approach is missing.

NuScale Response:

NuScale is requesting approval of a methodology to predict density wave oscillation (DWO) onset for the US460 design NuScale Power Module (NPM-20) in TR-131981-P; however, the phenomena of DWO onset, DWO flow amplitude, and DWO flow frequency are interrelated due to the physics involved and are used as Figures of Merit (FoMs) with varying requirements for agreement, depending on their use in TR-131981-P.

{{

}}2(a),(c)

{{

}}2(a),(c)

Impact on Topical Report:

Topical Report TR-131981, Methodology for the Determination of the Onset of Density Wave Oscillations (DWO), has been revised as described in the response above and as shown in the markup provided in this response.

Abstract

RSI-2

NuScale Power, LLC (NuScale) is requesting ~~the~~ Nuclear Regulatory Commission (NRC) review and approval to use the ~~Steam Generator (SG)~~ Density Wave Oscillation (DWO) Evaluation Model (EM) described herein for analyses of ~~such oscillations~~the onset of DWO in the NuScale Power Module (NPM-20) in the US460 design during normal and off-normal operating conditions at nominal reactor power levels between 20 percent and 100 percent ~~nominal~~. Use of this EM outside of ~~this power range~~these limitations requires justification.

RSI-2

The ~~SG~~ DWO ~~EM~~evaluation model uses the proprietary NRELAP5 system analysis code. The NRELAP5 code includes models and correlations for heat transfer and pressure drop for the ~~NuScale Power Module (~~NPM-20~~)~~ helical coil steam generator (SG). Extensive NRELAP5 validation was performed to ensure the DWO ~~EM~~evaluation model is applicable for important phenomena and processes. The validation suite includes separate effects test (SET) and integral effects test (IET) data developed specifically for the NPM-20 application.

RSI-2

This EM addresses identification of the onset of potential DWOs within the SG tubes for evaluating a preferred operating domain. This EM is not used to verify safety-related functions of structures, systems, and components (SSC).~~This EM provides a methodology for analyzing secondary side instabilities in the NPM SG design, addresses identification of potential DWOs within the SG tubes, and provides information about such transients to support downstream stress and fatigue analysis of applicable portions of the reactor coolant system integral reactor pressure vessel and steam generator.~~

RSI-2

Although not required because this method is not used to verify safety-related functions of SSC, this ~~SG~~ DWO ~~EM~~evaluation method follows the guidance provided in “Transient and Accident Analysis Methods,” Regulatory Guide (RG) 1.203. Key aspects of ~~this~~ RG 1.203 that are addressed include:

RSI-2

- development of the DWO phenomena identification and ranking table (PIRT)~~,~~
- assessment of separate effects and integral~~-~~ effects DWO tests~~,~~
- quantification of code uncertainty based on comparisons to test data~~,~~
- EM development~~,~~
- EM adequacy assessment using bottom-up assessment of NRELAP5 models and correlations, and top-down assessment of NRELAP5 models for mass, momentum, and energy conservation, and numerical solution techniques~~.~~
- integral effects test facility scaling~~.~~

RSI-2

Uncertainty quantification and margin evaluation applies to the NRELAP5 analysis of DWO onset for the NPM-20.

RSI-2

For illustrative purposes to aid the reader's understanding of the context of the application of this ~~SG~~ DWO ~~EM, a~~evaluation method sample calculations of the implemented EM using NRELAP5 ~~is~~are provided. ~~C~~Sample calculations for the NPM-20 ~~SG are performed at 100 percent power~~demonstrate that DWO onset does not occur in the NPM-20 steam generator at nominal or off-nominal steady-state operation at 100 percent power if the inlet flow restrictor (IFR) loss coefficient is {{ }}$^{2(a),(c)}$. Example calculations illustrate~~Results show~~ that a {{ }}$^{2(a),(c)}$ exists at ~~this~~100 percent power.

Executive Summary

RSI-2

NuScale Power, LLC (NuScale) is requesting Nuclear Regulatory Commission (NRC) review and approval to use the ~~Steam Generator (SG)~~ Density Wave Oscillation (DWO) Evaluation Model (EM) described in this topical report for analyses of ~~steam generator oscillations~~DWO onset prediction during ~~normal~~nominal and off-~~normal~~nominal operating conditions at reactor power levels between 20 percent and 100 percent ~~nominal~~. Although not required because this EM is not used to verify safety-related functions of systems, structures, and components (SSC), this ~~SG~~ DWO ~~EM~~evaluation model is consistent with the guidance provided in "Transient and Accident Analysis Methods," Regulatory Guide (RG) 1.203 (Reference 12.1), ~~since~~because it contains industry best practices for EM development. This topical report is not intended to provide final design values or results; rather, it contains ~~example values~~sample calculations using the EM for illustrative purposes to aid the reader's understanding of the context of the application of the ~~SG~~ DWO ~~EM~~evaluation model.

RSI-2

NuScale developed a small modular reactor (SMR) design that supports operation of multiple NuScale Power Modules (NPM-20s) at a specific site. Each NPM-20 is an advanced, light-water, integrated pressurized water reactor (PWR) using natural circulation for the primary coolant flow. Within each NPM-20 there are two independent helical coil steam generators (SG) in the upper outer annulus of the primary reactor pressure vessel (RPV). Each SG consists of a large number of helical tubes connected in parallel to common feedwater (FW) plenums at the bottom~~,~~ and common steam plenums at the top. Each SG tube has ~~at its inlet~~ an inlet flow restrictor ~~device~~(IFR) that is sized to provide secondary-side hydraulic resistance within the single-phase region to enhance secondary flow stability.

RSI-2

Systems that utilize convective boiling flow, such as the NPM-20 steam generators~~SGs~~ can be found in a variety of industrial applications, including boiling water reactors, steam boilers, heat exchangers, and condensers. Such systems offer the advantage of high heat transfer rates at moderate temperature differences. A drawback ~~though~~ is that these systems are susceptible to thermally-~~-~~induced two-phase DWO~~s~~ that require additional engineering design to ~~overcome~~address. For the NuScale Power Module (NPM-20) ~~SG~~steam generators, secondary-side fluid boiling within the tubes creates conditions potentially prone to parallel tube DWO. Hydraulic sizing of the tube ~~inlet flow restrictor~~IFR is important to ensuring acceptable flow stability ~~along with reasonable constraints to power operation~~.

RSI-2

~~NuScale previously submitted to the NRC a design certification application (DCA) for review and approval of a 12 NPM power plant design. Upon final review and final ACRS meetings, it was determined that a Combined Operating License (COL) item was required to close portions of the reactor coolant system integral reactor pressure vessel and steam generator fatigue analysis to address potential impact of DWO to SG lifetime. A COL item 3.9-14 was created to address these concerns, it states:~~

> ~~*A COL applicant that references the NuScale Power Plant design certification will develop an evaluation methodology for the analysis of secondary-side instabilities in the steam generator design. This methodology will address the identification of potential density wave oscillations*~~

~~*in the steam generator tubes, and qualification of the applicable portions of the reactor coolant system integral reactor pressure vessel and steam generator given the occurrence of density wave oscillations, including the effects of reverse fluid flows within the tubes.*~~

RSI-2

This EM is used to identify the onset of potential DWO within the SG tubes for evaluating a preferred operating domain. The qualification of applicable portions of the reactor coolant system (RCS) integral RPV and SG given the occurrence of DWO is outside the scope of this topical report. This EM is not used to verify safety-related functions of SSC.~~This SG DWO EM provides a methodology for analyzing secondary side instabilities in the NPM SG design, addresses identification of potential DWOs within the SG tubes, and provides information about such transients to support downstream stress and fatigue analysis of applicable portions of the reactor coolant system integral reactor pressure vessel and steam generator. The methodology for evaluating SG integrity from a thermal fatigue perspective is outside the scope of this report.~~

RSI-2

This ~~SG~~ DWO ~~EM~~evaluation model uses the NuScale-proprietary NRELAP5 computer code as the computational tool. This software was derived from the Idaho National Laboratory (INL) RELAP5-3D© computer code. It includes the necessary models for characterization of the NPM-20 hydrodynamics, heat transfer between structures and fluids, modeling of fuel, reactor kinetics models, and control systems. The NRELAP5 code includes models and correlations for heat transfer and pressure drop for the NPM-20 helical coil SG.

RSI-2

Validation and verification of the ~~SG~~ DWO ~~EM~~evaluation model was conducted following the principles and guidance in the Evaluation Model Development and Assessment Process (EMDAP) of RG 1.203. A phenomena identification and ranking table (PIRT)~~,~~ that identifies the important phenomena and processes impacting ~~SG~~ DWO~~,~~ was developed. Seventeen phenomena were identified as important to DWO, ~~and thus important to capture~~ which were considered in the ~~SG~~ DWO ~~EM~~evaluation model. Six of these important phenomena have a low knowledge level (level = 2)~~,~~ and require~~d~~ assessment against test data.

RSI-2

Extensive NRELAP5 code assessment was performed to ensure applicability of the ~~SG~~ DWO ~~EM~~evaluation model for the important PIRT phenomena over the range of conditions encountered in the NPM-20. The validation tests included separate effects test (SET) and integral~~-~~ effects ~~DWO~~ test~~s~~ (IET) performed at the Società Informazioni Esperienze Termoidrauliche S.p.A. (SIET) TF-1 facility in 2013~~6 and new~~ and at SIET TF-2 in 2015, as well as DWO tests performed at the SIET TF-2 facility in 2022. Additional validation was conducted using an external database obtained from Polytechnic University of Milan (POLIMI). For TF-1 and TF-2 testing, predicted-to-measured values of DWO onset are in reasonable-to-excellent agreement. For POLIMI, which has longer tubes and a tighter helix than the NPM-20 ~~SG~~steam generator, NRELAP5 predictions of DWO onset are conservative.

RSI-2

The EM adequacy for analysis of DWO ~~analysis of~~onset for the NPM-20 ~~SGs~~ is demonstrated through bottom-up and top-down evaluations performed with NRELAP5 for high-ranking PIRT phenomena~~,~~ and through NRELAP5 validation against relevant test data. For the bottom-up assessment, adequacy of the models and correlations in NRELAP5 are examined by considering their pedigree, applicability, and fidelity to appropriate fundamental or ~~separate effects test~~SET

data, and scalability to the ~~SG~~ DWO onset conditions. Integral or top-down performance is assessed by evaluating the mathematical models for mass, momentum, and energy conservation; numerical solution techniques employed; and integral effects test predictions of TF-2 where integral system response is present. The conclusion drawn from the bottom-up and top-down assessments is that the EM is adequate for the purpose of predicting ~~SG~~ DWO onset for the NPM-20.

RSI-2

An uncertainty analysis ~~is carried out using~~uses TF-1 and TF-2 test~~DWO~~ data. Using a 95 percent confidence interval, the NRELAP5 uncertainty in predicting helical coil SG tube pressure drop and heat transfer is calculated. When highly conservative biasing parameter uncertainty is applied to TF-2 NRELAP5 models, NRELAP5 uncertainty for predicting DWO onset is calculated to be {{ }}$^{2(a),(c)}$. This uncertainty is then applied to the NPM-20 ~~SG~~steam generator DWO onset analysis calculations.

RSI-2

~~A s~~Sample calculations ~~is~~are provided to demonstrate application of the EM in an NPM-20 ~~SG DWO~~steam generator model. These~~is~~ sample calculations demonstrate~~s~~ that appropriate NRELAP5 modeling can be used to predict DWO onset~~, with consideration of an inlet flow restrictor~~. The sample calculations provide context for the reader's understanding of the application of the DWO evaluation model. The sample calculations demonstrate that the IFR loss coefficient (K_{inlet}) ~~loss~~ and expected operating conditions can be used to prevent onset of DWO at nominal and off-nominal operating conditions at 100 percent nominal power. This methodology application also illustrates how to determine margin to DWO onset, apply code uncertainty, and account for the effect of deviations from nominal conditions in DWO onset predictions. The results of the sample calculations show that margin to DWO onset is possible at ~~all~~ nominal ~~power levels at and above 20 percent power,~~ and ~~at~~ off-nominal 100 percent power conditions~~ that are reasonably expected to be bounded by the final control system design and nominal trip setpoints.~~

1.0 Introduction

1.1 Purpose

RSI-2

~~This evaluation model (EM) provides a validated method for calculating the margin to onset of density wave oscillations (DWO) in steam generator (SG) tubes that use an inlet flow restrictor (IFR) device. This report is used to size the inlet flow restrictor (IFR) resistance for the NuScale Power Module (NPM) to demonstrate thermal hydraulic stability between 20 percent and 100 percent reactor power (nominal), and to inform the design of nonsafety-related secondary side control systems.~~This evaluation model (EM) addresses identification of the onset of potential density wave oscillations (DWO) within the steam generator (SG) tubes in the NuScale Power Module (NPM-20) design for evaluating a preferred operating domain. This EM is not used to verify safety-related functions of structures, systems, and components (SSC).

1.2 SG DWO Stability Evaluation Model Scope

RSI-2

The scope of this ~~evaluation model (~~EM~~)~~ is limited to the NPM-20 steam generator ~~(SG)~~ and nominal reactor power levels between 20 percent and 100 percent. Use of this EM for components other than the SG or outside of the nominal 20 percent to 100 percent power range requires further justification.

RSI-2

~~Although not required,~~ This method is not used to verify safety-related functions of SSC; therefore, Regulatory Guide (RG) 1.203 is not required. However, this EM is consistent with the guidance in "Transient and Accident Analysis Methods," ~~Regulatory Guide (~~RG~~)~~ 1.203 (Reference 12.1)~~, since~~ because it contains industry best practices for thermal-hydraulic (T-H) EM development. As such, this report describes the ~~NuScale SG~~NPM-20 steam generator design and operation, phenomena identification and ranking table (PIRT), and NRELAP5 input model, correlations, and applicability to ~~SG~~ DWO onset analysis. ~~In addition, t~~This report also summarizes NRELAP5 assessments against separate effects test (SET) and integral effects test (IET) data~~. A~~ and presents an uncertainty analysis and DWO onset margin methodology ~~is presented~~.

RSI-2

Qualification of NPM-20 structural components, such as the integral reactor pressure vessel (RPV) and SG, given the occurrence of DWO are outside of the scope of this report~~, but are taken into consideration as part of the ASME component lifetime fatigue analysis.~~

1.3 Abbreviations

RSI-2

Table 1-1 Abbreviations

Term	Definition
1-D	one-dimensional
~~ACRS~~	~~Advisory Committee on Reactor Safeguards~~
ASME	American Society of Mechanical Engineers

RSI-2

Figure 3-1 NuScale Power Module Cut Away

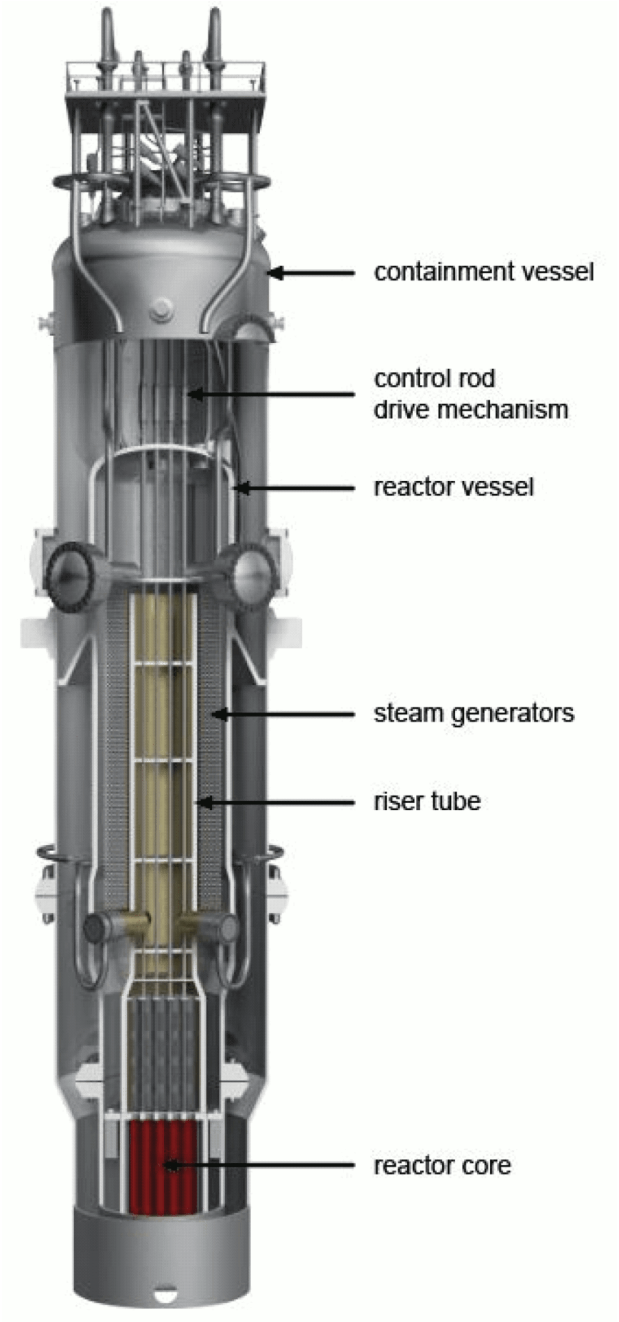

3.2 Evaluation Model Requirements and Figures of Merit

RSI-2, RSI-3

This EM provides a validated method for calculating the margin to the onset of density wave oscillations in the NPM-20 ~~SG~~steam generator tubes that use an ~~tube~~ IFR ~~device~~. ~~It is used to size IFR resistance for the NPM to demonstrate thermal hydraulic stability between 20 percent and 100 percent reactor power (nominal).~~

RSI-2, RSI-3

In order to evaluate SG stability with respect to DWO onset, the following figure~~s~~ of merit (FoM~~s~~) ~~are~~is selected:

1. DWO onset

RSI-2, RSI-3

2. ~~DWO flow change amplitude~~
3. ~~DWO flow rate frequency~~

RSI-2, RSI-3

Two supplemental FoMs are used:

1. DWO flow change amplitude
2. DWO flow rate frequency

RSI-2, RSI-3

Because the three FoMs are inextricably linked to the DWO phenomena, the use of DWO flow change amplitude and DWO flow rate frequency must be considered in order to accurately predict onset of DWO related to instabilities in the NPM-20 helical coil SG. For this DWO onset EM~~methodology~~, reasonable-to-excellent agreement is needed for prediction of DWO onset (FoM~~s~~ 1) because DWO onset prediction is the purpose of the DWO evaluation model.~~,~~ ~~while m~~Minimal agreement is needed for flow change amplitude~~,~~ and flow rate frequency (FoMs 2 and 3) because these FoMs can have higher uncertainty and still support the accurate prediction of DWO onset and ensure that the DWO onset is attributable to the correct phenomena.

RSI-2, RSI-3

The calculation of margin is performed using realistic operating parameters that are used by non-safety~~-~~-related secondary~~-~~-side control systems for monitoring and control of power production.

RSI-2, RSI-3

This report provides a description of the NuScale ~~SG~~ DWO ~~EM~~evaluation model. The following steps are used to develop the EM. ~~They are:~~

- ~~D~~determining the requirements for the EM
- ~~D~~developing an assessment base consistent with the determined requirements
- ~~D~~developing the EM
- ~~A~~assessing the adequacy of the EM

11.0 Results/Conclusions

RSI-2

This topical report presents the EM used to evaluate DWO in the NPM-20 ~~HCSG~~ during ~~normal~~nominal and off-nominal~~normal~~ operating conditions. Although not required, this DWO ~~EM~~evaluation model is consistent with guidance provided in the EMDAP of "Transient and Accident Analysis Methods," Regulatory Guide 1.203.

RSI-2

The DWO ~~EM~~evaluation model uses the proprietary NRELAP5 code as the computational tool. NRELAP5 includes the necessary models for the characterization of the NPM-20 hydrodynamics, heat transfer between structures and fluids, modeling of fuel, reactor kinetics models, and control systems. Additional models and correlations are added to model the NPM-20 helical coil SG configuration.

RSI-2

Validation and verification of the EM and NRELAP5 code are conducted using a well-established process. A PIRT, which identifies the important phenomena and processes for HCSG stability, is developed. A total of 17 phenomena are identified as high- ranked and thus important to capture in the DWO ~~EM~~evaluation model.

RSI-2

Extensive NRELAP5 code validation is performed to ensure that the EM is applicable for the important phenomena and processes over the range encountered in NPM-20 operation. The validation suite includes SETs and IETs developed and run specifically for the NPM-20 SG application. The FoM for ~~IETs are~~the DWO evaluation model is DWO onset~~, DWO flow period, and DWO flow amplitude~~.

RSI-2

The SETs were performed at the TF-1 facility. TF-1 provided data on pressure drop and heat transfer for the secondary- side. TF-1 also provided DWO test data with DWO onset, DWO flow period, and DWO flow amplitude. Both SETs and IETs were performed at the TF-2 facility. TF-2 SETs provided data on primary-side heat transfer and pressure drop. TF-2 also provided DWO test data with DWO onset, DWO flow period, and DWO flow amplitude. Additional validation of NRELAP5 is carried out with an external DWO database obtained from POLIMI. The POLIMI DWO test data validation shows that NRELAP5 is conservative in predicting DWO onset for a non-prototypical HCSGs with longer tubes and a tighter helix.

RSI-2

The NRELAP5-based ~~SG~~ DWO ~~EM~~evaluation model is evaluated for applicability to analyze DWO in the NPM-20. The applicability of NRELAP5 for high- ranked~~ing~~ phenomena is demonstrated by comparing NRELAP5 predictions to data from SETs and IETs. Reasonable-to-excellent agreement obtained via comparison establishes the applicability of NRELAP5 to accurately predict DWO onset phenomena at both the SETs and IETs.

RSI-2

Uncertainty analysis is carried out based on TF-1 SET data and on TF-2 DWO ~~IET~~integral effects test data. Using a 95 percent confidence interval, the {{

}}2(a),(c), respectively. When highly conservative biasing parameter uncertainty is applied to TF-2 DWO NRELAP5 models, the NRELAP5 uncertainty for predicting DWO onset is ~~calculated at~~ {{

}}2(a),(c)

RSI-2

This~~e~~ report also contains the methodology for evaluating margin to DWO onset in the NPM-20 at normal and off-normal operating conditions and is applied for NPM-20 nominal reactor power levels between 20 percent and 100 percent ~~nominal~~. The sample calculations in Appendix B demonstrate~~s~~ application of the DWO ~~EM~~evaluation model in an NPM-20 NRELAP5 model configured to predict DWO onset following the DWO evaluation model.~~NPM SG DWO NRELAP5 model.~~ The sample results show that DWO onset does not occur in the NPM-20 helical coil SG at the nominal or off-nominal, steady--state 100 percent power level if the minimum IFR ~~loss coefficient~~K_{inlet} value is {{

}}2(a),(c) Results are conservatively biased for code uncertainty. Margin to DWO onset is demonstrated at nominal and~~power levels and at~~ off-nominal 100 percent power conditions. ~~that are reasonably expected to be bounded by the final control system design and nominal trip setpoints.~~

RSI-2

The ~~evaluation model~~EM developed herein has an established pedigree and is determined to be adequate for downstream NPM-20 ~~SG~~ analysis for DWO onset. ~~Use of NRELAP5 for accurate prediction of DWO flow period and DWO flow amplitude requires additional evaluation, which may involve nodalization changes and/or methodology improvement.~~

Response to Request for Additional Information
Docket: 99902078

RAI No.: RSI
Date of RAI Issue: 03/27/2023

NRC Question No.: RSI-4

The DWO LTR requests approval for a method of demonstrating that instability is unlikely in the range of operation between 20-100% power. However, the information provided in the LTR is lacking the description and consideration within this method that a variety of power, flow and temperature conditions in individual steam generator (SG) tubes are permitted by Technical Specifications and plant operations for any given power level. The LTR is further missing description and appropriate consideration of other operational realities permitted by Technical Specifications and expected during the course of operation, including steam generator tube plugging and fouling, equipment out of service, such as feedwater heaters, single SG operation, or significantly imbalanced SG operation due to something like plugging.

NuScale Response:

{{

}}2(a),(c)

{{

}}2(a),(c)

{{

}}2(a),(c)

{{

}}2(a),(c)

{{

}}2(a),(c)

The attached changes to Section 10 of TR-131981-P, Revision 0, outline the global sensitivity analysis and the relative influence and bias direction of each parameter listed above (Table 10-6).

While not explicitly evaluated as part of the global sensitivity analysis, the appropriate treatment for additional operational considerations uses the sensitivity analysis results for the parameters listed above as outlined below.

- {{

}}2(a),(c)

There was an additional clarifying question on this RSI transmitted on June 16, 2023. The question is in italics with the response following the question. Note that the clarifying questions on RSI-12 and RSI-13 contain this same response and that the responses to RSI-4, RSI-12, and RSI-13 should be considered together to address the operating band considered for DWO.

The response only included a description of the impact of some operational realities within a small band of variation, but did not include appropriate consideration of all potential operational realities in that no markups were provided that would then place analytical or operational controls on those parameters that would then ensure the methodology appropriately constrains operation to that which is supported by analysis (and the small bands of variation considered).

The objective of this additional information is to clarify the systematic construction of the global sensitivity analysis for DWO onset, which represents the full range of the anticipated NPM-20 operating domain using the following combination of inputs:

- {{

}}2(a),(c)

Table 10-6 of TR-131981-P provides the summary of significant system parameter biases necessary to ensure a conservative DWO onset calculation based on {{

}}2(a),(c)

{{

}}2(a),(c)

{{

}}2(a),(c)

{{

}}2(a),(c)

{{

}}2(a),(c)

Figure 1. {{ }}2(a),(c)

{{

}}2(a),(c)

{{

}}2(a),(c)

{{

}}2(a),(c)

Figure 2. {{ }}2(a),(c)

{{

}}2(a),(c)

{{

}}2(a),(c)

{{

}}2(a),(c)

{{

}}2(a),(c)

Figure 3. {{ }}2(a),(c)

{{

}}2(a),(c)

{{

}}2(a),(c)

{{

}}2(a),(c)

Impact on Topical Report:

Topical Report TR-131981, Methodology for the Determination of the Onset of Density Wave Oscillations (DWO), has been revised as described in the response above and as shown in the markup provided in this response.

RSI-4, RSI-9, RSI-13

10.0 Uncertainty Evaluation and Margin for the NuScale Power Module with ~~r~~Respect to Density Wave Oscillation

RSI-4, RSI-9, RSI-10, RSI-11, RSI-13

This section describes the methodology for uncertainty quantification and margin evaluation applied to the NRELAP5 calculation of DWO onset for the NPM-20 ~~SG~~. The uncertainty methodology ~~used~~ takes into account code input uncertainties stemming from a variety of sources (e.g., initial~~/~~ and boundary conditions, models~~/~~ and correlations~~, etc.~~), as well as output uncertainty associated with the code calculations. ~~Code predictions of both SETs and IETs are used to assess how well important phenomena and processes are predicted, as well as overall system response~~Code predictions of both SETs and IETs assess how well important phenomena and processes are predicted, and a global sensitivity analysis distills the important geometric and operating conditions to be modeled. Margin to DWO onset is calculated for the NPM-20 by evaluating DWO onset with biased inputs at varying nominal power levels.~~SGs by reducing feedwater flow from nominal conditions until onset occurs. The difference between the FW flow rate that requires, automatic control system or operator response, or produces a protective trip, and the FW flow rate at DWO onset taking into consideration NRELAP5 code uncertainty, is the margin to DWO for the NPM.~~

RSI-4, RSI-9, RSI-10, RSI-11, RSI-13

For the NPM-20 ~~SG~~, a ~~best estimate~~deterministic methodology is applied using a combination of conservative and realistic input data and boundary~~/~~ and initial conditions. Uncertainty is assessed using the methodology described as follows.~~in the following section, which considers both code input and output phase uncertainties.~~

RSI-4, RSI-9, RSI-13

10.1 Sensitivity~~Uncertainty~~ Analysis Methodology Development

RSI-4, RSI-9, RSI-10, RSI-13

~~Reference 12.47 provides an integrated methodology for uncertainty quantification wherein uncertainty evaluation is divided into two distinct parts – the input phase and the output phase.~~

RSI-4, RSI-9, RSI-10, RSI-13

~~Input uncertainty quantification focuses on the identification of uncertainties in code input parameters, and those associated with the models and sub-models of the code. Sources of input uncertainty include:~~

RSI-4, RSI-9, RSI-10, RSI-13

- ~~Model parameters,~~
- ~~Boundary/initial conditions, and~~
- ~~Uncertainties in the structure of sub-models.~~

RSI-4, RSI-9, RSI-10, RSI-13

~~Input uncertainty includes the sources of code uncertainties that can be explicitly accounted for and are propagated through code calculations. SET data that is used to assess code models and correlations, is also used for input based uncertainty quantification.~~

RSI-4, RSI-9, RSI-10, RSI-13

~~The output phase of uncertainty accounts for the impact of uncertainties associated with the FoM output. For NRELAP5, applicable experimental data come from IET facilities designed to provide information on system behavior. Output phase uncertainty can be characterized by comparing measured IET data to NRELAP5 calculated values.~~

RSI-4, RSI-9, RSI-11, RSI-13

{{

RSI-4, RSI-9, RSI-11, RSI-13

RSI-4, RSI-9, RSI-13

}}2(a),(c),ECI

RSI-4, RSI-9, RSI-11, RSI-13

Table 10-1 {{ }}2(a),(c),ECI

{{			
			}}2(a),(c),ECI

Table 10-1 {{ }}2(a),(c),ECI (Continued)

	{{		
	}}2(a),(c),ECI		

RSI-4, RSI-9, RSI-13

10.2 NRELAP5 Code Uncertainty

RSI-4, RSI-9, RSI-10, RSI-11, RSI-13

{{

RSI-10

}}2(a),(c)

{{

RSI-10

RSI-10

RSI-10

RSI-10

RSI-10

RSI-10

RSI-10

RSI-4, RSI-9, RSI-10, RSI-13

RSI-4, RSI-9, RSI-10, RSI-13

RSI-10

RSI-10

}}2(a),(c)

RSI-4, RSI-9, RSI-10, RSI-11, RSI-13

2. {{

RSI-4, RSI-9, RSI-10, RSI-11, RSI-13

RSI-4, RSI-9, RSI-10, RSI-11, RSI-13

RSI-4, RSI-9, RSI-10, RSI-11, RSI-13

RSI-4, RSI-9, RSI-10, RSI-11, RSI-13

}}2(a),(c)

{{

RSI-4, RSI-9, RSI-10, RSI-11, RSI-13

Equation 10-1

RSI-4, RSI-9, RSI-10, RSI-11, RSI-13

Equation 10-2

RSI-4, RSI-9, RSI-10, RSI-11, RSI-13

Equation 10-3

RSI-4, RSI-9, RSI-10, RSI-11, RSI-13

}}2(a),(c)

{{

Equation 10-4

RSI-4, RSI-9, RSI-10, RSI-11, RSI-13

RSI-4, RSI-9, RSI-13

RSI-4, RSI-9, RSI-10, RSI-11, RSI-13

Equation 10-5

RSI-4, RSI-9, RSI-11, RSI-13

RSI-4, RSI-9, RSI-13

}}2(a),(c)

RSI-4, RSI-9, RSI-10, RSI-11, RSI-13

{{

Equation 10-6

RSI-4, RSI-9, RSI-10, RSI-11, RSI-13

RSI-4, RSI-9, RSI-10, RSI-11, RSI-13

RSI-4, RSI-9, RSI-10, RSI-11, RSI-13

RSI-4, RSI-9, RSI-13

RSI-4, RSI-9, RSI-10, RSI-11, RSI-13

RSI-4, RSI-9, RSI-10, RSI-11, RSI-13

}}2(a),(c)

{{

Equation 10-7

RSI-4, RSI-9, RSI-10, RSI-11, RSI-13

Equation 10-8

RSI-4, RSI-9, RSI-10, RSI-11, RSI-13

Equation 10-9

RSI-4, RSI-9, RSI-13

RSI-4, RSI-9, RSI-13

RSI-4, RSI-9, RSI-13

RSI-4, RSI-9, RSI-10, RSI-11, RSI-13

}}2(a),(c)

RSI-4, RSI-9, RSI-10, RSI-11, RSI-13

{{

RSI-4, RSI-9, RSI-10, RSI-11, RSI-13

RSI-4, RSI-9, RSI-13

RSI-4, RSI-9, RSI-13

RSI-4, RSI-9, RSI-13

Equation 10-10

RSI-4, RSI-9, RSI-13

}}2(a),(c)

RSI-4, RSI-9, RSI-11, RSI-13

Table 10-2 {{

}}2(a),(c)

{{

}}2(a),(c)

Table 10-2 {{ }}2(a),(c) (Continued)

{{

}}2(a),(c)

Table 10-2 {{ }}2(a),(c) (Continued)

	{{			
	}}2(a),(c)			

RSI-4, RSI-9, RSI-13

{{

}}2(a),(c)

RSI-4, RSI-9, RSI-11, RSI-13

The error in NRELAP5 DWO onset prediction is calculated using Equation 10-11.

$$\varepsilon = \frac{NRELAP5 - Data}{Data} \qquad \text{Equation 10-11}$$

Variable *NRELAP5* is the FW flow rate as predicted by NRELAP5 at DWO onset, and *Data* is the FW flow rate as measured by test facility at DWO onset.

RSI-4, RSI-9, RSI-13

Using the statistical methods described in previous key steps, NRELAP5 average error $\bar{x}$ and standard deviation of mean $\bar{u}$ are calculated. Assuming t-distribution and a 95 percent one-sided distribution and degrees of freedom of 35, the coverage factor is 1.69. The one-sided confidence interval value is calculated using Equation 10-12.

RSI-4, RSI-9, RSI-13

$$95\%\ \mathrm{CI}_t = \bar{x} - 1.69 \times \bar{u} \qquad \text{Equation 10-12}$$

A 95 percent confidence interval method is used for evaluating the NRELAP5 DWO onset prediction uncertainty. A 95 percent confidence interval error estimate (Equation 10-12) indicates that there is a 95 percent probability that the NRELAP5 error in predicting the DWO onset phenomena is within the error span.

RSI-4, RSI-9, RSI-11, RSI-13

5. Overall NRELAP5 Density Wave Oscillation Prediction Uncertainty

{{

RSI-4, RSI-9, RSI-11, RSI-13

RSI-4, RSI-9, RSI-11, RSI-13

}}2(a),(c),ECI

RSI-4, RSI-9, RSI-13

6. {{

RSI-4, RSI-9, RSI-13

RSI-4, RSI-9, RSI-13

}}2(a),(c)

RSI-4, RSI-9, RSI-13

{{

}}2(a),(c)

{{

}}2(a),(c)

RSI-10

10.3 Other High Ranked Phenomena Identification and Ranking Table Phenomena Not Considered in the Uncertainty Evaluation

10.3.1 {{ }}2(a),(c)

RSI-10

{{

RSI-4, RSI-9, RSI-10, RSI-11, RSI-13

}}2(a),(c)

RSI-10

10.3.2 {{ }}2(a),(c),ECI

{{

RSI-4, RSI-9, RSI-11, RSI-13

}}2(a),(c),ECI

RSI-10

Table 10-3 {{ }}2(a),(c),ECI

{{			}}2(a),(c),ECI

RSI-10

{{

}}2(a),(c),ECI

RSI-10

10.3.3 {{ }}2(a),(c),ECI

{{

RSI-10

}}2(a),(c),ECI

RSI-10

Figure 10-1 {{ }}2(a),(c),ECI

	{{	
	}}2(a),(c),ECI	

RSI-4, RSI-9, RSI-10, RSI-11, RSI-13

{{

}}2(a),(c),ECI

RSI-10

Figure 10-2 {{ }}2(a),(c),ECI

{{

}}2(a),(c),ECI

RSI-10

{{

}}2(a),(c),ECI

{{

}}2(a),(c)

RSI-10

10.3.4 {{ }}2(a),(c)

{{

}}2(a),(c)

RSI-10

Figure 10-3 {{ }}2(a),(c),ECI

{{

}}2(a),(c)

RSI-10

{{

}}2(a),(c)

RSI-10

10.3.5 {{ }}2(a),(c)

{{

RSI-10

}}2(a),(c),ECI

RSI-10

10.3.6 {{ }}2(a),(c),ECI

{{

RSI-10

}}2(a),(c),ECI

- {{

}}2(a),(c),ECI

RSI-10

Table 10-4 {{

}}2(a),(c),ECI

	{{				
				}}2(a),(c),ECI	

RSI-10

{{

}}2(a),(c),ECI

RSI-10

Figure 10-4 {{

}}2(a),(c),ECI

{{

}}2(a),(c),ECI

RSI-10

{{

}}2(a),(c),ECI

RSI-10

Figure 10-5 {{

}}2(a),(c),ECI

{{

}}2(a),(c),ECI

RSI-10

{{

}}2(a),(c),ECI

RSI-10

Figure 10-6 {{

}}2(a),(c),ECI

{{

}}2(a),(c),ECI

RSI-10

{{

}}2(a),(c),ECI

RSI-10

Table 10-5 {{

}}2(a),(c),ECI

{{

}}2(a),(c),ECI

RSI-10

Figure 10-7 {{ }}2(a),(c),ECI

{{

}}2(a),(c),ECI

RSI-10

{{

}}2(a),(c),ECI

RSI-10

Figure 10-8 {{ }}2(a),(c),ECI

{{

}}2(a),(c),ECI

RSI-10

Figure 10-9 {{ }}2(a),(c),ECI

	{{	
	}}2(a),(c),ECI	

RSI-10

{{ }}2(a),(c),ECI

{{

}}2(a),(c),ECI

RSI-10

10.3.7 {{ **}}2(a),(c),ECI**

{{

RSI-4, RSI-9, RSI-10, RSI-11, RSI-13

RSI-4, RSI-9, RSI-10, RSI-11, RSI-13

}}2(a),(c),ECI

RSI-4, RSI-9, RSI-10, RSI-11, RSI-13

10.3.8 {{ **}}2(a),(c),ECI**

{{

}}2(a),(c),ECI

RSI-10

10.3.9 {{ **}}2(a),(c)**

{{

}}2(a),(c)

{{

}}2(a),(c)

RSI-4, RSI-9, RSI-13

10.4 ~~NPM Operation Margin~~Methodology for Density Wave Oscillation Analysis~~Onset~~

RSI-4, RSI-9, RSI-11, RSI-13

{{

RSI-4, RSI-9, RSI-13

RSI-4, RSI-9, RSI-11, RSI-13

RSI-4, RSI-9, RSI-11, RSI-13

}}2(a),(c)

{{

}}$^{2(a),(c)}$

RSI-4, RSI-9, RSI-11, RSI-13

Table 10-6 {{ }}$^{2(a),(c)}$

{{

}}$^{2(a),(c)}$

Table 10-6 {{ }}2(a),(c) (Continued)

	{{			
	}}2(a),(c)			

RSI-4, RSI-9, RSI-11, RSI-13

10.4.1 {{ }}2(a),(c)

RSI-4, RSI-9, RSI-11, RSI-13

{{

RSI-4, RSI-9, RSI-11, RSI-13

}}2(a),(c)

{{

RSI-4, RSI-9, RSI-11, RSI-13

RSI-4, RSI-9, RSI-11, RSI-13

Equation 10-13

RSI-4, RSI-9, RSI-11, RSI-13

RSI-4, RSI-9, RSI-11, RSI-13

Equation 10-14

}}2(a),(c)

}}2(a),(c)

}}2(a),(c)

RSI-4, RSI-9, RSI-13

Figure 10-10 {{

{{

RSI-4, RSI-9, RSI-13

~~For evaluating NPM operating margin for DWO onset, sensitivity analysis is used. The sources of uncertainty for the NPM full-plant calculation with respect to DWO are identified. Effects of these uncertainty parameters on DWO are evaluated using IETs/SETs, plant design conditions, operating conditions, design basis safety analysis assumptions/limits, and literature.~~

RSI-4, RSI-9, RSI-13

~~{{~~

RSI-4, RSI-9, RSI-13

~~}}2(a),(c)~~

RSI-4, RSI-9, RSI-13

~~The methodology for calculating margin for DWO involves accounting for uncertainties in different geometric parameters and operating conditions. Sensitivity analysis is carried out accounting for uncertainties in margin calculation.~~

RSI-4, RSI-9, RSI-13

~~The methodology for calculating margin identified important uncertainty contributors for DWO. These contributors are derived from the SG stability PIRT, code validation, NPM~~

~~operating parameters, and safety analysis limits/assumptions. The uncertainty contributors are divided into three categories – analytical uncertainties/T-H model and correlation uncertainties; geometrical uncertainties; and the plant conditions uncertainties. These parameters are varied in a parametric evaluation to ensure that uncertainties are adequately addressed in the evaluation of margin.~~

RSI-4, RSI-9, RSI-13

~~{{~~

RSI-4, RSI-9, RSI-13

RSI-4, RSI-9, RSI-13

RSI-4, RSI-9, RSI-13

~~}}2(a),(c)~~

{{

RSI-4, RSI-9, RSI-13

RSI-4, RSI-9, RSI-13

RSI-4, RSI-9, RSI-13

RSI-4, RSI-9, RSI-13

}}2(a),(c)

RSI-4, RSI-9, RSI-13

Table 10-7 ~~NPM Sensitivity Cases at Off-Normal Conditions for DWO Evaluation~~

	{{							}}~~2(a),(c)~~

RSI-4, RSI-9, RSI-13

~~{{~~

RSI-4, RSI-9, RSI-13

~~}}2(a),(c)~~

{{

}}2(a),(c)

Response to Request for Additional Information
Docket: 99902078

RAI No.: RSI
Date of RAI Issue: 03/27/2023

NRC Question No.: RSI-5

The DWO LTR is missing the rationale for the Phenomenon Identification and Ranking Table (PIRT) rankings. For the knowledge level ranking, the applicant is using a 1-4 relative scale, but a subjective description of the interpretation for each ranking is not provided. The staff cannot conduct a review of the PIRT rankings (either importance or knowledge level) without the rationale supporting the reporting rankings.

NuScale Response:

A markup of TR-131981-P includes tables that define the importance and knowledge level rankings used in the phenomena identification and ranking table (PIRT), similar to those in the loss of coolant accident (LOCA), non-LOCA, and Extended Passive Cooling topical reports. Section 4.3 of TR-131981-P is revised to clarify the basis for the importance and knowledge ranking for the high ranked phenomena.

The following text and tables are added to TR-131981-P in Section 4.1.The remaining tables in Section 4.0 are renumbered accordingly.

Each phenomenon identified in the PIRT was assigned an importance ranking and knowledge level ranking. Table 4-1 and Table 4-2 describe the importance rankings and the knowledge level rankings considered by the PIRT panel.

Table 4-1 Importance Rankings

Importance Ranking	***Definition***
High (H)	*Significant influence on Figures of Merit (FoM)*
Medium (M)	*Moderate influence on FoM*
Low (L)	*Small influence on FoM*

Table 4-2 Knowledge Levels

Knowledge Level	***Definition***
4	*Well-known and small uncertainty*
3	*Known and low uncertainty*
2	*Partially known and moderate uncertainty*
1	*Very limited knowledge or uncertainty cannot be characterized.*

Section 4.3 of TR-131981-P is revised to clarify the basis for the importance and knowledge ranking for the high ranked phenomena. The markup of TR-131981-P is attached to this response.

There was an additional set of clarifying questions on this RSI transmitted on May 11, 2023. The questions are in italics with responses following each question.

- *The draft RSI-5 response is insufficient. The draft RSI-5 response does not appear to address all the PIRT phenomena. {{*

}}$^{2(a),(c)}$

TR-131981-P focuses on high ranked phenomena, following the format and style of the approved LOCA topical report. As advised by the NRC during the post-application meetings, NuScale provided a description of high ranked phenomena, along with the rationale for the knowledge level of each phenomena, following the example in the

LOCA topical report. Low and medium ranked phenomena and associated knowledge levels are described in the steam generator stability PIRT.

- *Section 4.3 of the DWO LTR (original and revised) is titled "Discussion of High Ranked Phenomena," but if one reviews the revisions in RSI-5, there are examples of phenomena in this section that are not ranked high (see Sections 4.3.2 and 4.3.13). Therefore, it is not clear if these phenomena should be discussed in different sections (say one for Medium and another for Low ranked phenomena) or if the section is mistitled. It appears that the report sections intended to include the rationales for the medium and low ranked phenomena have been omitted.*

  TR-131981-P focuses on high ranked phenomena and describes the rationale for specifying the knowledge level. There are some instances where medium ranked phenomena is described. For example, Section 4.3.2 of TR-131981-P describes the {{

  }}2(a),(c)

There was an additional clarifying question on this RSI transmitted on June 23, 2023. The question is in italics with the response following the question.

Remaining half of PIRT table still not provided. Revision to response is not responsive to the initial feedback, and merely mentions that for the LOCA TR these types of justifications were not required, and therefore should not be for the DWO TR. Unlike the LOCA TR, this is a first of a kind review, and what is necessary for the staff's review should not be compared to other reviews.

Additionally, on June 28, 2023, David Drucker sent the following via email to Wren Fowler.

As a follow-up to yesterday's meeting - - our request for NuScale to provide the rationales for all PIRT phenomena (RSI 5) is consistent with Section 4.4 of "Evaluation Methodology for Stability Analysis of the NuScale Power Module," TR-0516-49417-P.

Section 4.4 of TR-0516-49417-P (stability topical report) includes a brief description that is included below as Table 1. Note that Table 1 is equivalent to Table 4-4 of TR-131981-P (density wave oscillation (DWO) topical report) with descriptions or locations of descriptions within TR-13198-P included in the comment column.

Table 1 {{

}}2(a),(c)

{{								}}2(a),(c)
{{								
								}}2(a),(c)

{{								}}2(a),(c)
{{								
								}}2(a),(c)

{{								}}2(a),(c)
{{								}}2(a),(c)

{{								}}[2(a),(c)]
{{								

{{								}}[2(a),(c)]
{{								
								}}[2(a),(c)]

{{								}}2(a),(c)
{{								
								}}2(a),(c)

{{								}}2(a),(c)
}}2(a),(c)								

Impact on Topical Report:

Topical Report TR-131981, Methodology for the Determination of the Onset of Density Wave Oscillations (DWO), has been revised as described in the response above and as shown in the markup provided in this response.

4.0 Phenomena Identification and Ranking and Scaling Analysis

RSI-5

NuScale developed a ~~phenomena identification and ranking table (~~PIRT~~)~~ for DWO in the NPM-20 steam generator ~~SG~~. Reference 12.1 outlines the EMDAP, which is summarized in Appendix A. Developing the PIRT is the first step of the EMDAP process because it provides critical input to the development of the EM, assessment bases, and methodology of its application. This EM utilizes~~d~~ the process as needed to facilitate the PIRT development in a tractable manner.

RSI-5

4.1 Phenomena Identification and Ranking Table Objectives

RSI-5

The objectives of the PIRT are to~~:~~

- ~~E~~establish FoM~~s~~.
- ~~I~~identify phenomena affecting FoM.
- ~~R~~rank phenomena applicable to the appropriate FoM.
- ~~I~~identify the knowledge base associated with the phenomena, and to provide a recommendation for closing the knowledge gap, as applicable.
- ~~D~~determine the high-importance/low knowledge level phenomena to focus the development of the analytical model and to determine additional testing requirements and design improvements.

RSI-5

Traditionally, the PIRT development uses a simplified nine-step process described in Reference 12.2. Those nine steps were followed on an as~~-~~-needed basis~~bases~~ in the development of the NPM-20 ~~SG DWO~~density wave oscillation PIRT. The PIRT supports scaling of ~~separate effects~~SET and prototypical testing, and design and operation of test facilities. The PIRT identifies the most important ~~thermal hydraulic~~T-H phenomena for DWO.

RSI-5

4.2 Phenomena Identification and Ranking Table Phenomena

RSI-5

Each phenomenon identified in the PIRT was assigned an importance ranking and knowledge level ranking. Table 4-1 and Table 4-2 describe the importance rankings and the knowledge level rankings considered by the PIRT panel.

RSI-5

Phenomena are evaluated and ranked on ~~a~~ component bases. For the NPM-20 ~~HC~~helical coil SG, the necessary components are ~~1)~~ the FW line, ~~2)~~ the FW plenum, ~~3)~~ the HCSG tube internal fluid, ~~4)~~ the HCSG tube wall metal, ~~5)~~ the HCSG tube external fluid (i.e., primary side liquid), ~~6)~~ the steam plenum, and ~~7)~~ the steam line. These components are grouped as shown in Table 4-3.

RSI-5

Table 4-1 Importance Rankings

Importance Ranking	Definition
High (H)	Significant influence on FoM
Medium (M)	Moderate influence on FoM
Low (L)	Small influence on FoM
Inactive (I)	Phenomenon not present or negligible

RSI-5

Table 4-2 Knowledge Level Rankings

Knowledge Level	Definition
4	Well-known and low uncertainty
3	Known and low uncertainty
2	Partially known and moderate uncertainty
1	Very limited knowledge or uncertainty cannot be characterized

RSI-5

Table 4-3 Component Designation for Phenomena Identification and Ranking

Component	Description	Identification
Tube inside	HCSG inside evaluated for T-H phenomena	1
Tube geometry	HCSG tube wall thickness, roughness, geometry	2
Tube outside	Primary side T-H condition for heat transfer and boundary conditions	3
FW line and FW plenum	FW line, FW plenum, and other components upstream ~~to~~of HCSG	4
Steam line and steam plenum	Steam line, steam plenum, and other components downstream of HCSG	5

RSI-5

The DWO stability PIRT (Table 4-4)~~PIRT Table~~ is organized as follows.~~:~~

- The first column lists the components identified for the system.
- The second column lists the phenomena likely to occur relevant to that component.

RSI-5

- The FoM columns are split where:
  - ~~"~~1~~"~~ refers to DWO onset.
  - ~~"~~2~~"~~ refers to DWO flow change amplitude.
  - ~~"~~3~~"~~ refers to DWO temperature change amplitude.~~, and~~
  - ~~"~~4~~"~~ refers to DWO frequency.

RSI-5

The four FoM are important to quantifying tube inlet fluid temperature oscillations that can cause stress cycles~~stresses on tube-to-tube sheet welds~~.

RSI-5

- The seventh column identifies the importance ranking ~~column ("H" for high, "M" for medium, and "L" for low)~~.

RSI-5

- The eighth column identifies the knowledge level ranking (where ~~"~~4~~"~~ indicates the highest knowledge level).

RSI-5

The ~~SG~~DWO stability PIRT (Table 4-4) lists a total of 26~~5~~ phenomena or processes for the NPM-20 ~~HC~~helical coil SG related to the following ~~figures of merit (~~FoM~~)~~: DWO onset, DWO flow amplitude, DWO temperature amplitude, and DWO frequency. No phenomena~~on/~~ or processes are ranked with a knowledge level of ~~"1"~~one. Seventeen are importance ranked ~~"~~H~~"~~, and a subset of six are importance ranked ~~"~~H~~"~~ with a knowledge level of ~~"2"~~two. The subset of six H-2 ranked phenomena are emphasized in bold font in Table 4-4, and are discussed in Section 4.3.

RSI-5

Table 4-4 ~~SG DWO stability PIRT~~Density Wave Oscillation Stability Phenomena Identification and Ranking Table

{{

}}2(a),(c)

Table 4-4 ~~SG DWO stability PIRT~~Density Wave Oscillation Stability Phenomena Identification and Ranking Table (Continued)

{{

}}2(a),(c)

4.3 Discussion of High Ranked Phenomena

RSI-5

This section provides a summary of the high (H) ranked~~ing~~ phenomena, bases for phenomena importance ranking, and knowledge level.

RSI-5

4.3.1 {{ }}2(a),(c)

RSI-5

{{

RSI-5

}}2(a),(c)

{{

}}2(a),(c)

RSI-5

4.3.2 {{ }}2(a),(c)

RSI-5

{{

}}2(a),(c)

RSI-5

4.3.3 {{ }}2(a),(c)

RSI-5

{{

RSI-5

}}2(a),(c)

RSI-5

4.3.4 {{ }}2(a),(c)

RSI-5

{{

}}2(a),(c)

4.3.5 {{ }}2(a),(c)

RSI-5

{{

}}2(a),(c)

4.3.6 {{ }}2(a),(c)

RSI-5

{{

RSI-5

}}2(a),(c)

4.3.7 **{{** **}}2(a),(c)**

RSI-5

{{

}}2(a),(c)

4.3.8 **{{** **}}2(a),(c)**

RSI-5

{{

}}2(a),(c)

4.3.9 **{{** **}}2(a),(c)**

RSI-5

{{

}}2(a),(c)

RSI-5

4.3.10 **{{** **}}2(a),(c)**

RSI-5

{{

}}2(a),(c)

4.3.11 **{{** **}}2(a),(c)**

RSI-5

{{

RSI-5

}}2(a),(c)

RSI-5

4.3.12 **{{** **}}2(a),(c)**

RSI-5

{{

}}2(a),(c)

RSI-5

{{

RSI-5

}}2(a),(c)

RSI-5

4.3.13 {{ }}2(a),(c)

RSI-5

{{

}}2(a),(c)

4.3.14 {{ }}2(a),(c)

RSI-5

{{

}}2(a),(c)

Response to Request for Additional Information
Docket: 99902078

RAI No.: RSI
Date of RAI Issue: 03/27/2023

NRC Question No.: RSI-6

In Sections 7.6, 7.7, and 7.8, the DWO LTR is missing specificity with respect to the EM requirements in terms of nodalization. These sections largely include recommendations, but without any descriptions of how the methodology would proceed if the recommendations are deviated from, and what criteria would permit such deviation. This makes it extremely difficult to proceed with a review where the fundamental methodology being reviewed is non-specific as to what is being requested for approval, and the schedule and resources necessary to execute such a review could not be determined with any reliability. Further, it is highly likely that in the absence of this specificity, complex or overly burdensome conditions, limitations, and restrictions would be necessary in the staff's safety evaluation.

NuScale Response:

The attached Section 7.6, Section 7.7, and Section 7.8 markups clarify the use of the nodalization in TR-131981-P.

There was an additional set of clarifying questions on this RSI transmitted on May 11, 2023. The questions are in italics with responses following each question.

The draft RSI-6 response is insufficient. The RSI-6 response does not appear to address all the recommendations in Sections 7.6, 7.7, and 7.8. In reviewing the DWO LTR the staff identified approximately 30 instances of recommendations in these sections. The frequent use of words such as: "should," "encouraged," "advisable," "appropriate," "sufficiently," "recommended," and "optional," (this list is not exhaustive) means that there are many instances in the DWO LTR where the nodalization is described in ambiguous language without a clear indication as to what is required of the nodalization as opposed to what are merely recommendations.

- *The RSI-6 is intended to address all these cases of ambiguity by clarifying which of the descriptions are recommendations and which of the descriptions are requirements. Stability analyses are known for having strict requirements on the model nodalization due to the effect of numerical diffusion on the results. Therefore, the staff suspects that many of these nodalization recommendations actually represent strict requirements on the nodalization to ensure that the results are not distorted due to numerical diffusion effects. However, with few exceptions, they are described as recommendations rather than requirements in the DWO LTR. The RSI-6 response does not remove much of the ambiguous language.*

  Some examples of ambiguous language in the markup:

  Markup page 121 - "Boiling channel node length should increase along the HCSG tube. However, sudden changes in node size by more than 3 times are discouraged." has been changed to "Boiling channel node length increases along the HCSG tube."

  Markup page 122 – "{{ }}$^{2(a),(c)}$" has been changed to "{{ }}$^{2(a),(c)}$"

  Section 7.8 of the topical report has been revised to remove ambiguous language.

- *The RSI-6 response does not seem to provide a discussion of the criteria that are used to determine if a deviation from the recommendations of Section 7.6-7.8 in the Evaluation Model is acceptable for licensing analysis. If the description of the nodalization in these sections is truly intended to reflect recommendations as opposed to requirements, and the DWO LTR does not provide expressed requirements, then the DWO LTR and RSI-6 response must describe the process by which deviations from the recommendations are evaluated and the criteria used to determine acceptability of those deviations.*

  Section 7.8 of the topical report has been revised to clarify what nodalization is required. Optional is used where there are optional components to the NRELAP5 model. Optional components are not required, but a description of use is provided if these optional components are implemented.

Impact on Topical Report:

Topical Report TR-131981, Methodology for the Determination of the Onset of Density Wave Oscillations (DWO), has been revised as described in the response above and as shown in the markup provided in this response.

RSI-6

Figure 7-2 Evaluation Model Input/Output Flow Chart (Simplified)

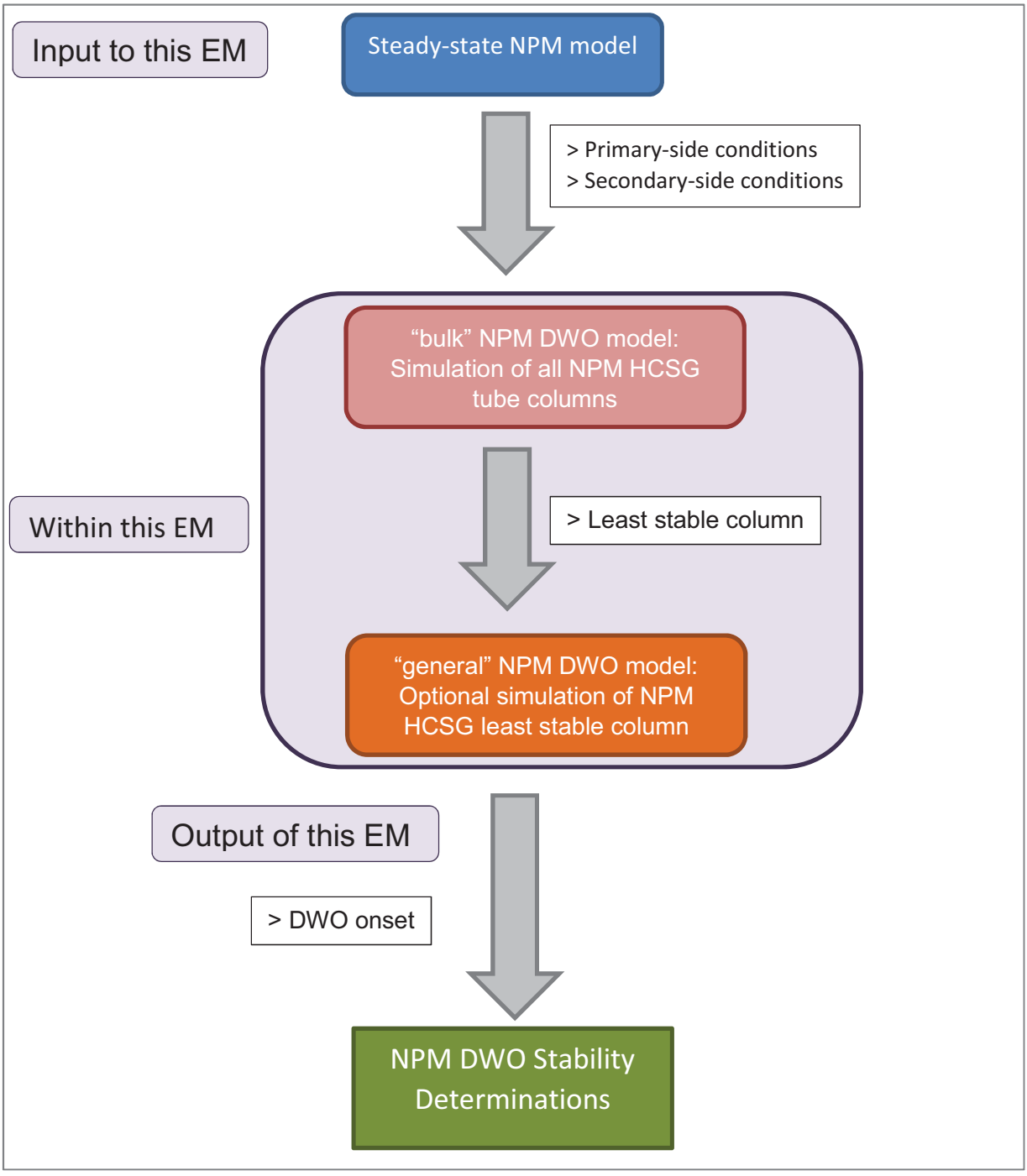

RSI-6

{{

}}2(a),(c)

RSI-6

Because both the primary -side and secondary -side operate in a "once--through" configuration (Section 7.6 and Section 7.7), the system-wide mass error checks may be disabled. Disabling mass error checks only prevents code termination based on cumulative mass error buildup (i.e., at 1 percent of total system mass); it does not prevent time-step controls based on mass error accumulation during the current time step.

7.5.4 Initial Conditions

RSI-6

For the NPM-20 SG DWO analysis model, ICs are set to values whichthat allow for simulation convergence within a reasonable period of time (e.g., ~2,000 seconds) before ramping begins per Section 7.4. Herein, "simulation convergence" refers to behavior wherein BCs are fixed at values and thatwherein conditions within individual components (e.g., HCSG tubes, upper downcomer, etc.) are not noticeably changing as a function of time.

RSI-6

Generally, poorly tailored ICs only lead to the need for extended convergence times. However, sometimes very poor ICs can lead to initial instability. In these cases, it can take some time for convergence to occur. Therefore suggestions for IC tailoring is provided for each relevant component in Section 7.6 through Section 7.8.

RSI-6

7.6 Model Nodalization - Steam Generator Primary- Side

RSI-6

The required components for the SG primary- side are the primary-side inlet, the upper downcomer (i.e., the upper section containing the HCSG tubes), and the primary-side exit.

RSI-6

The optional components for the SG primary- side are the riser, the riser holes, and the upper plenum.

RSI-6

7.6.1 Steam Generator Primary- Side: Inlet

RSI-6

{{

RSI-6

RSI-6

RSI-6

}}2(a),(c)

RSI-6

7.6.1.1 Steam Generator Primary- Side: Inlet Boundary Conditions

{{

}}2(a),(c)

Section 7.3.1 provides more information on BCs.

RSI-6

7.6.2 Steam Generator Primary- Side: Upper Downcomer

{{

RSI-6

RSI-6

}}2(a),(c)

RSI-6

{{

RSI-6

RSI-6

RSI-6

}}2(a),(c)

RSI-6

7.6.2.1 Steam Generator Primary- Side: Upper Downcomer Heat Structures

RSI-6

{{

RSI-6

RSI-6

}}2(a),(c)

RSI-6

7.6.2.2 Steam Generator Primary- Side: Upper Downcomer Initial Conditions

RSI-6

{{

}}2(a),(c)

RSI-6

7.6.3 Steam Generator Primary- Side: Exit

RSI-6

{{

}}2(a),(c)

RSI-6

7.6.3.1 Steam Generator Primary- Side: Exit Boundary Conditions

{{

}}2(a),(c)

RSI-6

7.6.4 Steam Generator Primary- Side: Riser

This component is not required.

RSI-6

{{

}}2(a),(c)

RSI-6

~~{{~~

~~}}2(a),(c)~~

RSI-6

7.6.4.1 Steam Generator Primary- Side: Riser Heat Structures

These heat structures are not required.

RSI-6

{{

}}2(a),(c)

RSI-6

7.6.4.2 Steam Generator Primary- Side: Riser Initial Conditions

Pressure is set to values similar to initial BCs per Section 7.6.3.1. Temperature is set to initial BCs per Section 7.6.1.1. Mass flow rate is set to initial BCs per Section 7.6.1.1.

RSI-6

7.6.5 Steam Generator Primary- Side: Riser Holes

This component is not required.

RSI-6

{{

}}2(a),(c)

If included, the riser holes must include realistic and accurate flow area, hydraulic diameter, and loss coefficient inputs.

RSI-6

7.6.5.1 Steam Generator Primary- Side: Riser Holes Initial Conditions

RSI-6

{{ }}2(a),(c)

RSI-6

7.6.6 Steam Generator Primary- Side: Upper Plenum

This component is not required.

RSI-6

{{

}}2(a),(c)

RSI-6

7.6.6.1 Steam Generator Primary- Side: Upper Plenum Heat Structures

Any HCSG tubes in the upper plenum require heat structures. Other heat structures are not required for this component.

RSI-6

7.6.6.2 Steam Generator Primary- Side: Upper Plenum Initial Conditions

Pressures are set to values similar to initial BCs per Section 7.6.3.1. Temperatures are set to initial BCs per Section 7.6.1.1. Mass flow rates are set to initial BCs per Section 7.6.1.1.

RSI-6

7.7 Model Nodalization - FeedwaterW and SteamTM Plenums

RSI-6

{{

RSI-6

RSI-6

}}2(a),(c)

{{

RSI-6

}}2(a),(c)

RSI-6

7.7.1 Feedwater~~W~~ Source

{{

}}2(a),(c)

RSI-6

7.7.1.1 Feedwater~~W~~ Source: Inlet Boundary Conditions

RSI-6

{{

RSI-6

}}2(a),(c)

Section 7.3.1 provides more information on BCs.

RSI-6

7.7.2 Feedwater~~W~~ Plenum

RSI-6

{{

}}2(a),(c)

RSI-6

7.7.2.1 FeedwaterW Plenum: Heat Structures

RSI-6

{{

}}2(a),(c)

RSI-6

7.7.2.2 FeedwaterW Plenum: Initial Conditions

RSI-6

Pressure is set to values slightly higher than initial steamSTM pressure BCs per Section 7.7.3. Temperature is set to initial FW temperature BCs per Section 7.7.1.1Section 7.7.1.

RSI-6

7.7.3 SteamTM Plenum

RSI-6

~~The STM plenum is a mandatory component for flow-controlled BC methods.~~

RSI-6

{{

}}2(a),(c)

RSI-6

7.7.3.1 SteamTM Plenum: Heat Structures~~:~~

Pending SCP1-3318

RSI-6

{{

}}2(a),(c)

RSI-6

7.7.3.2 Steam~~TM~~ Plenum: Initial Conditions

Pressure is set to the initial values per Section 7.7.3. Temperature is set to T_{hot} initial values per Section 7.6.1.1.

RSI-6

7.7.4 Steam~~TM~~ Exit

RSI-6

{{

RSI-6

}}2(a),(c)

RSI-6

7.7.4.1 Steam~~TM~~ Exit: Exit Boundary Conditions

RSI-6

{{

RSI-6

}}2(a),(c)

Section 7.3.1 provides more information on BCs.

RSI-6

7.8 Model Nodalization - Helical Coil Steam Generator Tubes

The HCSG tubes are composed of the tube inlet(s), the tubes, and the tube exit(s).

RSI-6

~~Different BC methods, which are discussed in more detail in Section 7.4, make use of different numbers of boiling channels.~~

RSI-6

7.8.1 Helical Coil Steam Generator Tube Inlets

RSI-6

{{

RSI-6

}}2(a),(c)

{{

RSI-6

RSI-6

}}2(a),(c)

RSI-6

7.8.1.1 Helical Coil Steam Generator Tube Inlets: Initial Conditions

RSI-6

{{

}}2(a),(c)

RSI-6

7.8.2 Helical Coil Steam Generator Tubes

{{

RSI-6

RSI-6

}}2(a),(c)

RSI-6

7.8.2.1 Helical Coil Steam Generator Tubes: Columns

RSI-6

{{

RSI-6

}}2(a),(c)

RSI-6

7.8.2.1.1 {{

}}2(a),(c)

RSI-6

{{

RSI-6

RSI-6

RSI-6

}}2(a),(c)

RSI-6

- {{

RSI-6

RSI-6

RSI-6

}}2(a),(c)

RSI-6

7.8.2.1.2 **{{**

}}2(a),(c)

{{

RSI-6

RSI-6

}}2(a),(c)

{{

}}2(a),(c)

RSI-6

7.8.2.2 Helical Coil Steam Generator~~HCSG~~ Tubes: Sections

RSI-6

{{

RSI-6

RSI-6

RSI-6

}}2(a),(c)

RSI-6

7.8.2.3 HCSG Helical Coil Steam Generator Tubes: Main Section General Nodalization

RSI-6

{{

RSI-6

}}2(a),(c)

RSI-6

{{

RSI-6

RSI-6

RSI-6

RSI-6

}}2(a),(c)

RSI-6

7.8.2.4 Helical Coil Steam Generator~~HCSG~~ Tubes: Heat Structures

RSI-6

{{

RSI-6

RSI-6

RSI-6

}}2(a),(c)

RSI-6

7.8.2.5 Helical Coil Steam Generator~~HCSG~~ Tubes: Initial Conditions

RSI-6

{{

}}2(a),(c)

{{

}}2(a),(c)

Mass flow rates are set consistent with Section 7.8.1.1.

RSI-6

7.8.3 Helical Coil Steam Generator~~HCSG~~ Tube Exits

RSI-6

{{

RSI-6

}}2(a),(c)

RSI-6

7.8.3.1 Helical Coil Steam Generator~~HCSG~~ Tube Inlets: Initial Conditions

RSI-6

{{

}}2(a),(c)

Response to Request for Additional Information
Docket: 99902078

RAI No.: RSI
Date of RAI Issue: 03/27/2023

NRC Question No.: RSI-7

Section 8 of the DWO LTR is missing information about the tests that form the validation basis, and supports a large part of the justification for the methodology. The only table provided contains a broad overview of the test condition ranges, but does not include the specific conditions for each test and the conditions of the density wave oscillation onset. At a minimum: (1) test matrices that provide the thermal-hydraulic conditions of the tests and (2) high level descriptions of the test procedures are needed for the staff to review the applicability of the experimental campaigns to the requested methodology.

NuScale Response:

The TF-1 test matrix, Table 8-3, is added to Section 8.1 of the Methodology for the Determination of the Onset of Density Wave Oscillations (DWO) topical report, TR-131981-P. The test matrix provides thermal-hydraulic conditions of the tests. A summary of the TF-2 tests are also provided in Section 8.2 and in Table 8-4, which summarizes a high-level description of the test procedures. The markup of TR-131981-P is attached to this response.

There was an additional set of clarifying questions on this RSI transmitted on May 11, 2023. The questions are in italics with responses following each question.

- *The RSI response states that the TF-2 test matrix, summary of the tests and high-level description of the test procedure has been added to the topical report. However, the RSI requested information for all tests that form the validation basis and supports a large portion of the justification for the methodology. The DWO topical report is missing a similar scope of information provided for the SIET-TF2 tests in the topical report markups but for the SIET TF-1 and POLIMI tests.*

In the markups attached to the original request for supplemental information, NuScale provided information about the tests that form the validation bases and that support a large part of the justification for the evaluation methodology in TR-131981-P, Revision 0. {{

}}2(a),(c)

{{

}}2(a),(c)

{{

}}2(a),(c),ECI

Table 1 shows the TF-1 DWO test matrix from DWO tests for information. {{

}}2(a),(c),ECI Table 1 is included in the attached markup to TR-131981-P as Table 8-3.

{{

}}2(a),(c),ECI Table 2 is for information only and is not included in the markup to TR-131981-P.

Table 1 {{ }}[2(a),(c),ECI]

{{

}}[2(a),(c),ECI]

Table 2 {{

}}2(a),(c),ECI

{{

}}2(a),(c),ECI

{{

}}2(a),(c),ECI

Table 3 {{ }}[2(a),(c),ECI]

{{

}}[2(a),(c),ECI]

{{

}}2(a),(c),ECI

Impact on Topical Report:

Topical Report TR-131981, Methodology for the Determination of the Onset of Density Wave Oscillations (DWO), has been revised as described in the response above and as shown in the markup provided in this response.

Figure 8-17 Wall Temperature Comparison for Coil 3

{{

}}2(a),(c)

RSI-7, RSI-8

8.1.5 Performance against TF-1 Density Wave Oscillation Data

RSI-7

{{

}}2(a),(c),ECI

RSI-7

{{

}}2(a),(c),ECI

RSI-7

Table 8-3 {{ }}2(a),(c),ECI

{{							
							}}2(a),(c),ECI

RSI-7, RSI-8

A code-to-data NRELAP5 comparison of DWO onset power is plotted in Figure 8-18.
{{

}}2(a),(c),ECI

RSI-7, RSI-8

The TF-2 facility test section consists of a bundle of 252 HCSG tubes split between five ~~"~~rows~~"~~ as shown in Figure 8-19. The five tube rows are placed in an annulus formed by two cylindrical barrels installed axially within the pressure vessel. Each row of HCSG tubes (i.e., groups of 48 or 52 tubes) is fed by a row-specific FW header, ~~(~~which is mounted inside the vessel~~) that~~ and distributes water to each tube inlet as shown in Figure 8-20. Steam exiting the tubes is collected on a per-row basis by a steam header and driven out through the top nozzle. The five rows of the SG can either operate together or individually (i.e., FW flow is delivered on a per-row basis).

RSI-7, RSI-8

The TF-2 testing was conducted in both ~~"~~single-row~~"~~ and ~~"~~multi-row~~"~~ configurations. TF-2 adiabatic and diabatic tests involve a series of single-row and multi-row tests with conditions designed to analyze primary-side flow behavior. The TF-2 DWO tests involve a series of single-row and multi-row tests with scaled NPM-20 operating conditions and sensitivity parameter variations. ~~r~~Row 3 is the most highly~~-~~instrumented for HCSG tube inlet differential pressure, which is used to calculate SG tube inlet flow.

RSI-7, RSI-8

Geometric information for TF-2 HCSG tubes is provided in Table 8-1. The TF-2 HCSG tubes represent geometries that are similar to the five innermost columns of the NPM-20 helical coil ~~HC~~SG at the time the facility was first commissioned in terms of diameter, length, and helical coil characteristics. Compared to the latest version of the NPM-20 design, the TF-2 HCSG tubes have a very similar inside diameter, a slightly longer tube length, a helical radius within the NPM-20 range, and a tube inclination angle within the NPM-20 range. Therefore, TF-2 provides a valuable assessment base for analyzing DWO in the NPM-20.

TF-2 test condition ranges are provided in Table 8-2.

RSI-7, RSI-8

The overall goal of each test in this experiment is to induce DWO onset. The method to induce DWO was varied along with the operating parameters. The test conditions for each test are shown in Table 8-4. The main conditions varied during testing were:

- {{

RSI-7, RSI-8

RSI-7, RSI-8

}}2(a),(c)

RSI-7, RSI-8

{{

}}2(a),(c)

RSI-7, RSI-8

Table 8-4 Density Wave Oscillation Test Matrix

{{

}}2(a),(c),ECI

Table 8-4 Density Wave Oscillation Test Matrix (Continued)

{{

}}2(a),(c),ECI

RSI-7

Table 8-5 {{ }}2(a),(c),ECI

{{

}}2(a),(c),ECI

Table 8-5 {{ }}2(a),(c),ECI (Continued)

{{

}}2(a),(c),ECI

For DWO flow period and DWO flow amplitude:

RSI-7, RSI-8

- The base model results for DWO flow period show~~ed~~ reasonable agreement.
- The base model results for DWO flow amplitude show~~ed~~ minimal agreement overall, but ~~we~~are mostly conservative and ~~thus~~ considered acceptable per Section 3.2 EM requirements.

RSI-7, RSI-8

8.3 Assessment ~~vs~~of POLIMI ~~d~~Data

RSI-7, RSI-8

This section provides a summary of the testing activities and subsequent code-to-data comparisons for the ~~Polytechnic University of Milan (~~POLIMI~~)~~ data.

RSI-7, RSI-8

The test data presented in this section is from the POLIMI ~~P~~parallel HCSG tests. Because POLIMI data was not developed under NQA-1 2008/2009a, the data was qualified for use in this EM following the NuScale Procedure for the Qualification of Existing Data~~-~~.

8.3.1 Test Description and Experimental Procedure

RSI-7, RSI-8

The POLIMI Parallel HCSG configuration included two electrically~~-~~heated HCSG tubes in parallel fed by a single FW line, as shown in Figure 8-45~~.~~ ~~-~~ ~~b~~Both coils were connected to a shared FW header and steam header.

RSI-7

{{

}}2(a),(c),ECI

RSI-7

Table 8-7 {{ }}2(a),(c),ECI

{{

}}2(a),(c),ECI

Table 8-7 {{ }}2(a),(c),ECI (Continued)

	{{										
											}}2(a),(c),ECI

RSI-7, RSI-8

~~During testing, BCs such as inlet mass flow, pressure, and temperature were kept relatively constant while the electrical power supplied to heat the coils was increased.~~ {{ }}2(a),(c),ECI

Response to Request for Additional Information
Docket: 99902078

RAI No.: RSI
Date of RAI Issue: 03/27/2023

NRC Question No.: RSI-8

Section 8 of the DWO LTR is missing comparisons between NRELAP5 and tube-side data from the SIET-TF2 tests used for validation– such as differential pressures and wall temperatures. If DWOs are to occur, it would occur on the tube-side. The staff cannot review the validation of the method without comparison to the tube-side data.

NuScale Response:

NRELAP5 code-to-data comparisons for select TF-2 helical coil steam generator (HCSG) tube parameters are not in TR-131981-P, Revision 0, but are added in the attached markup. This information added to TR-131981-P includes NRELAP5 code-to-data comparisons for HCSG tube inlet flow, pressure drop, wall temperature, and fluid temperature.

{{

}}2(a),(c),ECI

{{

}}2(a),(c),ECI

{{

}}2(a),(c),ECI

There was an additional set of clarifying questions on this RSI transmitted on May 11, 2023. The questions are in italics with responses following each question.

- *The RSI response states that NRELAP5 code-to-data comparisons for select TF-2 HCSG tube parameters are not in TR-131981-P, Revision 0, but will be added as noted in the attached markup.*

  The RSI response markup states "The code-to-data comparisons included herein are comparisons at steady-state conditions for row 3." in section 8.2.4, Performance against TF-2 SET Data. However, it is unclear if the information provided in the RSI markup is consistent with the data comparisons presented in Section 8.2.5, Performance against TF-2 DWO IET Data, to quantify uncertainty for DWO onset.

  The staff is expecting data comparisons, such as differential pressure and wall temperatures, of steady state conditions before the flowrate ramp down that leads to the onset of DWO. Please clarify that the data comparisons provided in the RSI markup are consistent with the steady state conditions before the flowrate ramp down prior to the onset of DWO.

  {{

}}2(a),(c),ECI

Impact on Topical Report:

Topical Report TR-131981, Methodology for the Determination of the Onset of Density Wave Oscillations (DWO), has been revised as described in the response above and as shown in the markup provided in this response.

RSI-7, RSI 8

Figure 8-25 TF-2 Diabatic Tests, Primary ~~s~~Side Temperature Comparison

{{

}}2(a),(c)

RSI-8

8.2.4.1 TF-2 Tube-Side Data

{{

}}2(a),(c)

RSI-8

{{

RSI-7, RSI-8

RSI-7, RSI-8

RSI-8

RSI-7, RSI-8

}}2(a),(c)

RSI-7, RSI-8

Figure 8-26 {{ }}2(a),(c),ECI

{{ }}2(a),(c),ECI

RSI-8

{{ }}2(a),(c),ECI

{{

}}2(a),(c),ECI

RSI-7, RSI-8

Figure 8-27 {{

}}2(a),(c),ECI

	{{	
	}}2(a),(c),ECI	

RSI-7, RSI-8

Figure 8-28 {{ }}2(a),(c),ECI

{{

}}2(a),(c),ECI

RSI-7, RSI-8

Figure 8-29 {{ }}2(a),(c),ECI

{{

}}2(a),(c),ECI

RSI-8

{{ }}2(a),(c),ECI

RSI-7, RSI-8

Figure 8-30 {{

}}2(a),(c),ECI

{{

}}2(a),(c),ECI

RSI-7, RSI-8

Figure 8-31 {{

}}2(a),(c),ECI

{{

}}2(a),(c),ECI

RSI-7, RSI-8

Figure 8-32 {{

}}2(a),(c),ECI

{{

}}2(a),(c),ECI

RSI-7, RSI-8

{{

RSI-7, RSI-8

}}2(a),(c),ECI

RSI-7, RSI-8

Figure 8-33 {{

}}2(a),(c),ECI

{{

}}2(a),(c),ECI

RSI-7, RSI-8

Figure 8-34 {{

}}2(a),(c),ECI

	{{	
	}}2(a),(c),ECI	

RSI-7, RSI-8

Figure 8-35 {{

}}2(a),(c),ECI

RSI-7, RSI-8

{{

}}2(a),(c),ECI

RSI-8

{{

}}2(a),(c),ECI

RSI-7, RSI-8

Figure 8-36 {{

}}2(a),(c),ECI

	{{	
		}}2(a),(c),ECI

RSI-8

{{

}}2(a),(c),ECI

RSI-7, RSI-8

Figure 8-37 {{ }}2(a),(c),ECI

{{

}}2(a),(c),ECI

RSI-8

{{

}}2(a),(c),ECI

{{

}}2(a),(c),ECI

RSI-7, RSI-8

Figure 8-38 {{ }}2(a),(c),ECI

{{

}}2(a),(c),ECI

RSI-7, RSI-8

Figure 8-39 {{

}}2(a),(c),ECI

{{

}}2(a),(c),ECI

RSI-8

{{

}}2(a),(c),ECI

{{

}}2(a),(c),ECI

RSI-7, RSI-8

Figure 8-40 {{

}}2(a),(c),ECI

	{{	
		}}2(a),(c),ECI

RSI-7, RSI-8

Figure 8-41 {{

}}2(a),(c),ECI

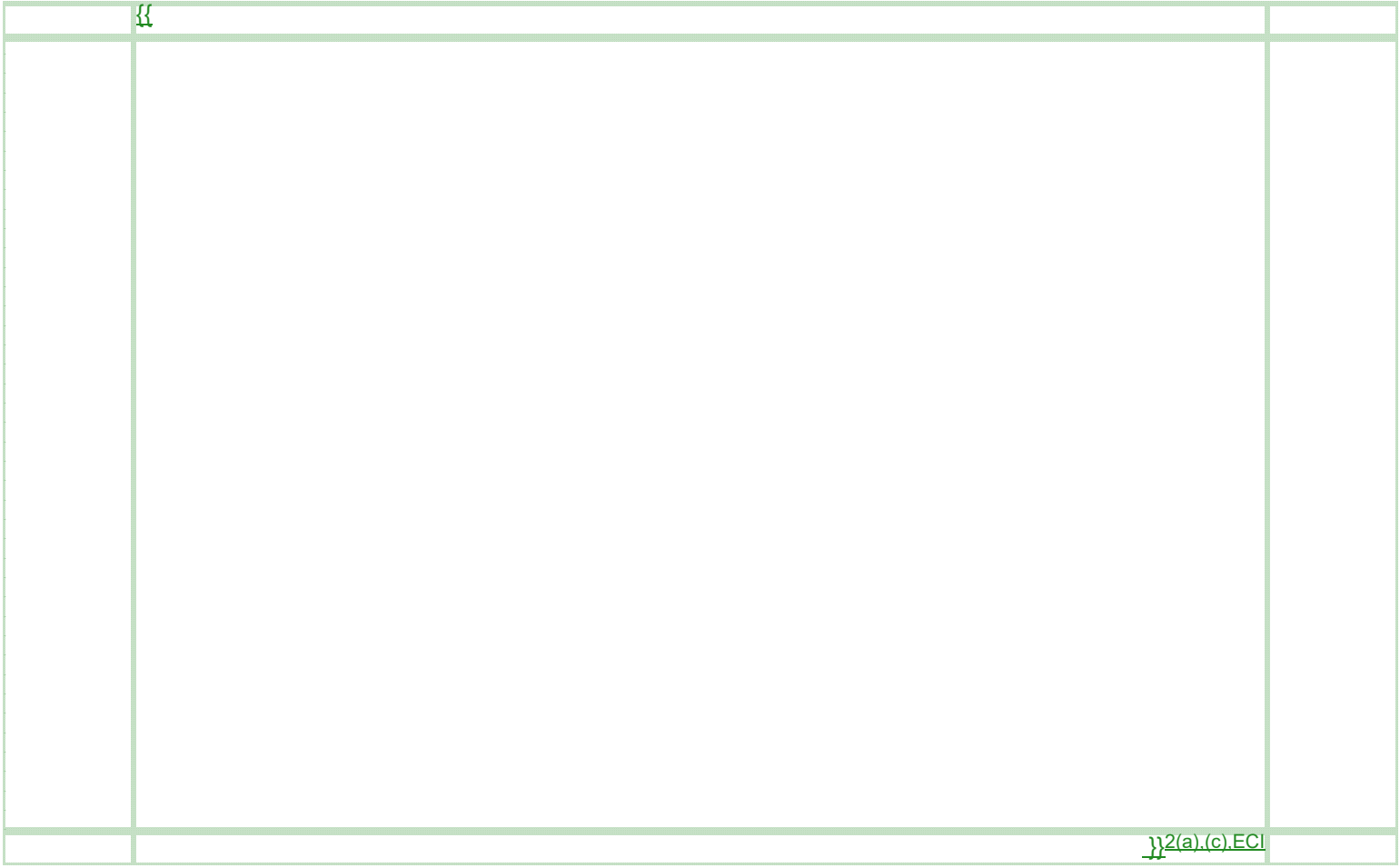

{{

}}2(a),(c),ECI

RSI-7, RSI-8

8.2.5 Performance against TF-2 Density Wave Oscillation Integral Effects Test Data

RSI-7, RSI-8

For TF-2 DWO test simulation, both ~~"~~base~~"~~ and ~~"~~biased~~"~~ NRELAP5 cases were run to quantify uncertainty for DWO onset. The biased cases include conservative values for input parameters with potentially large impacts: ~~(i.e.~~ higher HCSG tube ~~inlet~~ K_{inlet} ~~K loss~~, colder FW temperature, and higher total FW flow~~)~~. The magnitudes of these biases were determined per uncertainty estimates.

RSI-7, RSI-8

Table 8-6 provides a summary for the base and biased results. An NRELAP5 case showing DWO onset at a higher FW flowrate is considered conservative. A positive error denotes a conservative prediction, while a negative error denotes a

Response to Request for Additional Information
Docket: 99902078

RAI No.: RSI
Date of RAI Issue: 03/27/2023

NRC Question No.: RSI-9

The Section 10 uncertainty analysis in the DWO LTR is lacking fundamental descriptions of the methodology procedures. In many cases numerical results are provided without any description of how they are calculated. Sufficient level of detail and justification is missing for how the uncertainty analysis is performed and results in the final value reported. For example, there is no description of what is treated with biasing, what is treated with statistical methods for uncertainty propagation, and how uncertainty propagation of component uncertainties is combined with integral effects test (IET) validation results, and how scaling distortions from IET validation results are applied to the uncertainties and considered in the method. Further, there is conflicting information regarding conservatism in terms of biasing of certain parameters described in Section 10, the approach outlined in Equation 10-5, and discussion in Section 8 such that the staff cannot realistically begin meaningful review of the approach. Similarly, there is not a sufficient description of whether the uncertainties are applied to achieve a 95% probability as well as a 95% confidence interval, or if a deviation from RG 1.203 (which references RG 1.157) is intended (in which case no justification has been provided).

NuScale Response:

Overall Uncertainty Analysis Methodology for Density Wave Oscillation Onset

{{

}}2(a),(c)

{{

}}2(a),(c)

{{

}}2(a),(c)

{{

}}2(a),(c)

{{

}}2(a),(c)

NRELAP5 Density Wave Oscillation Onset Error Prediction Uncertainty

{{

}}2(a),(c)

{{

}}2(a),(c),ECI

{{

}}2(a),(c)

{{

}}2(a),(c)

{{ }}[2(a),(c)]

{{ }}[2(a),(c)]

Table 1 {{

}}2(a),(c),ECI

Parameter	Category Type	Impact Description	Selected Uncertainty

{{

}}2(a),(c)

Parameter	Category Type	Impact Description	Selected Uncertainty
{{			

}}2(a),(c)

Parameter	Category Type	Impact Description	Selected Uncertainty
{{			

}}2(a),(c)

Parameter	Category Type	Impact Description	Selected Uncertainty
{{			
			}}2(a),(c)
{{			
		}}2(a),(c)	
{{			}}2(a),(c)
{{			
			}}2(a),(c)
{{			
	}}2(a),(c)		
{{			
			}}2(a),(c)
{{			
			}}2(a),(c)

{{

}}2(a),(c)

Accounting for Scaling Distortions in NRELAP5 Uncertainty

{{

}}2(a),(c),ECI

{{

}}2(a),(c),ECI

{{

}}2(a),(c),ECI

{{

}}2(a),(c),ECI

Table 2 {{

}}2(a),(c)

{{				}}2(a),(c)

{{

}}2(a),(c)

{{				}}[2(a),(c)]

{{

8.36 }}[2(a),(c)]

{{				}}2(a),(c)
{{				}}2(a),(c)

Table 3. {{

}}2(a),(c)

{{				}}2(a),(c)

{{

}}2(a),(c)

{{				}}2(a),(c)

{{

15 }}2(a),(c)

{{				}}2(a),(c)
{{				}}2(a),(c)

{{

}}2(a),(c),ECI

{{

}}2(a),(c)

- {{

}}2(a),(c)

There was an additional clarifying question on this RSI transmitted on June 16, 2023. The question is in italics below.

NuScale made significant modifications to the uncertainty analysis section. The response included some of the information that was requested. {{

}}2(a),(c) There remains an incomplete description of how the scaling distortions from IET validation results are applied to the uncertainties and considered in the method. Further, the response to RSI-9 impacted the prior changed pages in response to RSI-10 and the staff will need to go back and revisit its determination for RSI-10 as some information was overwritten.

Then, there was another additional clarifying question on this RSI transmitted on June 23, 2023. The question is in italics below with the response immediately after.

NuScale made significant modifications to the uncertainty analysis section. The response included some of the information that was requested. {{

}}2(a),(c) There remains an incomplete description of how the scaling distortions from IET validation results are applied to the uncertainties and considered in the method. Further, the response to RSI-9 impacted the prior changed pages in response to RSI-10 and the staff will need to go back and revisit its determination for RSI-10 as some information was overwritten.

The RSI-9 response contains scaling analysis information that provides the distortions (see Tables 2 and 3 in RSI-9 response). However, the response is lacking the description requested in RSI-9 regarding how these distortions are applied to the uncertainties and considered in the method. {{

}}2(a),(c)

{{

}}2(a),(c)

{{

}}2(a),(c)

Finally, the response is not consistent with the LTR revisions. The written response refers to the uncertainty in single-phase and two-phase heat transfer uncertainties calculated from SETs and IETs, but this does not agree with Table 10-2 in the change pages. Therefore, the disposition even of the highlighted distortions in the written response is not consistent with the revised LTR. This is addressed in more detail in additional feedback on the RSI-10 response.

Therefore, the response is lacking a description of how the distortions are treated in the uncertainty analysis.

Distortions for important Π groups between TF-2 and the NPM-20 at 100 percent and 15 percent power are shown in Table 4-12 and Table 4-13 of TR-131981-P. {{

}}2(a),(c)

The original RSI-9 response provides the reason for excluding distortions in Π groups with the highest distortions at 100 percent and 15 percent conditions. Explanations for distortions in the remaining Π groups is provided below.

The criteria for preserving the Π groups between the model (M) and prototype (P) or accounting for distortions in the uncertainty are as follows; all criteria are not required to be fulfilled in order to account for or neglect the distortions.

1. {{

}}2(a),(c)

{{

}}2(a),(c)

100 Percent Power Condition Distortions

Single-Phase Liquid Region Π Groups

{{

}}2(a),(c)

{{

}}2(a),(c)

Two-Phase Region Π Groups

{{

}}2(a),(c)

{{

}}2(a),(c)

{{

}}2(a),(c)

Single-Phase Vapor Region Π Groups

{{

}}2(a),(c)

{{

}}2(a),(c)

Other Π Groups

{{

}}2(a),(c)

15 Percent Power Conditions Distortions

While TR-131981-P only applies to the nominal power range from 20 percent to 100 percent, the scaling analysis was conducted at low power to allow for operation of the TF-2 facility with all rows active.

Single-Phase Liquid Region Π Groups

{{

}}2(a),(c)

{{

}}2(a),(c)

{{

}}2(a),(c)

Two-Phase Region Π Groups

{{

}}2(a),(c)

Single-Phase Vapor Region Π Groups

{{

}}2(a),(c)

{{

}}2(a),(c)

Other Π Groups

{{

}}2(a),(c)

The response to the clarification question on uncertainties corresponding to SETs and IETs and how it aligns with Table 10-2 is in the additional response to RSI-10.

Impact on Topical Report:

Topical Report TR-131981, Methodology for the Determination of the Onset of Density Wave Oscillations (DWO), has been revised as described in the response above and as shown in the markup provided in this response.

RSI-4, RSI-9, RSI-13

10.0 Uncertainty Evaluation and Margin for the NuScale Power Module with ~~r~~Respect to Density Wave Oscillation

RSI-4, RSI-9, RSI-10, RSI-11, RSI-13

This section describes the methodology for uncertainty quantification and margin evaluation applied to the NRELAP5 calculation of DWO onset for the NPM-20 ~~SG~~. The uncertainty methodology ~~used~~ takes into account code input uncertainties stemming from a variety of sources (e.g., initial~~/~~ and boundary conditions, models~~/~~ and correlations~~, etc.~~), as well as output uncertainty associated with the code calculations. ~~Code predictions of both SETs and IETs are used to assess how well important phenomena and processes are predicted, as well as overall system response~~Code predictions of both SETs and IETs assess how well important phenomena and processes are predicted, and a global sensitivity analysis distills the important geometric and operating conditions to be modeled. Margin to DWO onset is calculated for the NPM-20 by evaluating DWO onset with biased inputs at varying nominal power levels.~~SGs by reducing feedwater flow from nominal conditions until onset occurs. The difference between the FW flow rate that requires, automatic control system or operator response, or produces a protective trip, and the FW flow rate at DWO onset taking into consideration NRELAP5 code uncertainty, is the margin to DWO for the NPM.~~

RSI-4, RSI-9, RSI-10, RSI-11, RSI-13

For the NPM-20 ~~SG~~, a ~~best estimate~~deterministic methodology is applied using a combination of conservative and realistic input data and boundary~~/~~ and initial conditions. Uncertainty is assessed using the methodology described as follows.~~in the following section, which considers both code input and output phase uncertainties.~~

RSI-4, RSI-9, RSI-13

10.1 Sensitivity~~Uncertainty~~ Analysis Methodology Development

RSI-4, RSI-9, RSI-10, RSI-13

~~Reference 12.47 provides an integrated methodology for uncertainty quantification wherein uncertainty evaluation is divided into two distinct parts – the input phase and the output phase.~~

RSI-4, RSI-9, RSI-10, RSI-13

~~Input uncertainty quantification focuses on the identification of uncertainties in code input parameters, and those associated with the models and sub-models of the code. Sources of input uncertainty include:~~

RSI-4, RSI-9, RSI-10, RSI-13

- ~~Model parameters,~~
- ~~Boundary/initial conditions, and~~
- ~~Uncertainties in the structure of sub-models.~~

RSI-4, RSI-9, RSI-10, RSI-13

~~Input uncertainty includes the sources of code uncertainties that can be explicitly accounted for and are propagated through code calculations. SET data that is used to assess code models and correlations, is also used for input based uncertainty quantification.~~

RSI-4, RSI-9, RSI-10, RSI-13

~~The output phase of uncertainty accounts for the impact of uncertainties associated with the FoM output. For NRELAP5, applicable experimental data come from IET facilities designed to provide information on system behavior. Output phase uncertainty can be characterized by comparing measured IET data to NRELAP5 calculated values.~~

RSI-4, RSI-9, RSI-11, RSI-13

{{

RSI-4, RSI-9, RSI-11, RSI-13

RSI-4, RSI-9, RSI-13

}}2(a),(c),ECI

RSI-4, RSI-9, RSI-11, RSI-13

Table 10-1 {{ }}2(a),(c),ECI

{{			
			}}2(a),(c),ECI

Table 10-1 {{ }}2(a),(c),ECI (Continued)

	{{		
	}}2(a),(c),ECI		

RSI-4, RSI-9, RSI-13

10.2 NRELAP5 Code Uncertainty

RSI-4, RSI-9, RSI-10, RSI-11, RSI-13

{{

RSI-10

}}2(a),(c)

{{

RSI-10

RSI-10

RSI-10

RSI-10

RSI-10

RSI-10

RSI-10

RSI-4, RSI-9, RSI-10, RSI-13

RSI-4, RSI-9, RSI-10, RSI-13

RSI-10

RSI-10

}}2(a),(c)

RSI-4, RSI-9, RSI-10, RSI-11, RSI-13

2. {{

RSI-4, RSI-9, RSI-10, RSI-11, RSI-13

RSI-4, RSI-9, RSI-10, RSI-11, RSI-13

RSI-4, RSI-9, RSI-10, RSI-11, RSI-13

RSI-4, RSI-9, RSI-10, RSI-11, RSI-13

}}2(a),(c)

{{

RSI-4, RSI-9, RSI-10, RSI-11, RSI-13

Equation 10-1

RSI-4, RSI-9, RSI-10, RSI-11, RSI-13

Equation 10-2

RSI-4, RSI-9, RSI-10, RSI-11, RSI-13

Equation 10-3

RSI-4, RSI-9, RSI-10, RSI-11, RSI-13

}}2(a),(c)

{{

Equation 10-4

RSI-4, RSI-9, RSI-10, RSI-11, RSI-13

RSI-4, RSI-9, RSI-13

RSI-4, RSI-9, RSI-10, RSI-11, RSI-13

Equation 10-5

RSI-4, RSI-9, RSI-11, RSI-13

RSI-4, RSI-9, RSI-13

}}2(a),(c)

RSI-4, RSI-9, RSI-10, RSI-11, RSI-13

{{

Equation 10-6

RSI-4, RSI-9, RSI-10, RSI-11, RSI-13

RSI-4, RSI-9, RSI-10, RSI-11, RSI-13

RSI-4, RSI-9, RSI-10, RSI-11, RSI-13

RSI-4, RSI-9, RSI-13

RSI-4, RSI-9, RSI-10, RSI-11, RSI-13

RSI-4, RSI-9, RSI-10, RSI-11, RSI-13

}}2(a),(c)

{{

Equation 10-7

RSI-4, RSI-9, RSI-10, RSI-11, RSI-13

Equation 10-8

RSI-4, RSI-9, RSI-10, RSI-11, RSI-13

Equation 10-9

RSI-4, RSI-9, RSI-13

RSI-4, RSI-9, RSI-13

RSI-4, RSI-9, RSI-13

RSI-4, RSI-9, RSI-10, RSI-11, RSI-13

}}2(a),(c)

RSI-4, RSI-9, RSI-10, RSI-11, RSI-13

{{

RSI-4, RSI-9, RSI-10, RSI-11, RSI-13

RSI-4, RSI-9, RSI-13

RSI-4, RSI-9, RSI-13

RSI-4, RSI-9, RSI-13

Equation 10-10

RSI-4, RSI-9, RSI-13

}}2(a),(c)

RSI-4, RSI-9, RSI-11, RSI-13

Table 10-2 {{

}}2(a),(c)

{{

}}2(a),(c)

Table 10-2 {{ }}2(a),(c) (Continued)

{{

}}2(a),(c)

Table 10-2 {{ }}2(a),(c) (Continued)

	{{			
	}}2(a),(c)			

RSI-4, RSI-9, RSI-13

{{

}}2(a),(c)

RSI-4, RSI-9, RSI-11, RSI-13

The error in NRELAP5 DWO onset prediction is calculated using Equation 10-11.

$$\varepsilon = \frac{NRELAP5 - Data}{Data} \qquad \text{Equation 10-11}$$

Variable *NRELAP5* is the FW flow rate as predicted by NRELAP5 at DWO onset, and *Data* is the FW flow rate as measured by test facility at DWO onset.

RSI-4, RSI-9, RSI-13

Using the statistical methods described in previous key steps, NRELAP5 average error $\bar{x}$ and standard deviation of mean $\bar{u}$ are calculated. Assuming t-distribution and a 95 percent one-sided distribution and degrees of freedom of 35, the coverage factor is 1.69. The one-sided confidence interval value is calculated using Equation 10-12.

RSI-4, RSI-9, RSI-13

$$95\%\ \mathrm{CI}_t = \bar{x} - 1.69 \times \bar{u} \qquad \text{Equation 10-12}$$

A 95 percent confidence interval method is used for evaluating the NRELAP5 DWO onset prediction uncertainty. A 95 percent confidence interval error estimate (Equation 10-12) indicates that there is a 95 percent probability that the NRELAP5 error in predicting the DWO onset phenomena is within the error span.

RSI-4, RSI-9, RSI-11, RSI-13

5. Overall NRELAP5 Density Wave Oscillation Prediction Uncertainty

{{

RSI-4, RSI-9, RSI-11, RSI-13

RSI-4, RSI-9, RSI-11, RSI-13

}}2(a),(c),ECI

RSI-4, RSI-9, RSI-13

6. {{

RSI-4, RSI-9, RSI-13

RSI-4, RSI-9, RSI-13

}}2(a),(c)

RSI-4, RSI-9, RSI-13

{{

}}2(a),(c)

{{

}}2(a),(c)

RSI-10

10.3 Other High Ranked Phenomena Identification and Ranking Table Phenomena Not Considered in the Uncertainty Evaluation

10.3.1 {{ }}2(a),(c)

RSI-10

{{

RSI-4, RSI-9, RSI-10, RSI-11, RSI-13

}}2(a),(c)

RSI-10

10.3.2 {{ }}2(a),(c),ECI

{{

RSI-4, RSI-9, RSI-11, RSI-13

}}2(a),(c),ECI

RSI-10

Table 10-3 {{ }}2(a),(c),ECI

{{			}}2(a),(c),ECI

RSI-10

{{

}}2(a),(c),ECI

RSI-10

10.3.3 {{ }}2(a),(c),ECI

{{

RSI-10

}}2(a),(c),ECI

RSI-10

Figure 10-1 {{ }}2(a),(c),ECI

	{{	
	}}2(a),(c),ECI	

RSI-4, RSI-9, RSI-10, RSI-11, RSI-13

{{

}}2(a),(c),ECI

RSI-10

Figure 10-2 {{ }}2(a),(c),ECI

{{

}}2(a),(c),ECI

RSI-10

{{

}}2(a),(c),ECI

{{

}}2(a),(c)

RSI-10

10.3.4 {{ }}2(a),(c)

{{

}}2(a),(c)

RSI-10

Figure 10-3 {{ }}2(a),(c),ECI

{{

}}2(a),(c)

RSI-10

{{

}}2(a),(c)

RSI-10

10.3.5 {{ }}2(a),(c)

{{

RSI-10

}}2(a),(c),ECI

RSI-10

10.3.6 {{ }}2(a),(c),ECI

{{

RSI-10

}}2(a),(c),ECI

- {{

}}2(a),(c),ECI

RSI-10

Table 10-4 {{

}}2(a),(c),ECI

	{{				
				}}2(a),(c),ECI	

RSI-10

{{

}}2(a),(c),ECI

RSI-10

Figure 10-4 {{

}}2(a),(c),ECI

{{

}}2(a),(c),ECI

RSI-10

{{

}}2(a),(c),ECI

RSI-10

Figure 10-5 {{

}}2(a),(c),ECI

{{

}}2(a),(c),ECI

RSI-10

{{

}}2(a),(c),ECI

RSI-10

Figure 10-6 {{

}}2(a),(c),ECI

{{

}}2(a),(c),ECI

RSI-10

{{

}}2(a),(c),ECI

RSI-10

Table 10-5 {{

}}2(a),(c),ECI

{{

}}2(a),(c),ECI

RSI-10

Figure 10-7 {{ }}2(a),(c),ECI

{{

}}2(a),(c),ECI

RSI-10

{{

}}2(a),(c),ECI

RSI-10

Figure 10-8 {{ }}2(a),(c),ECI

{{

}}2(a),(c),ECI

RSI-10

Figure 10-9 {{ }}2(a),(c),ECI

	{{	
	}}2(a),(c),ECI	

RSI-10

{{ }}2(a),(c),ECI

{{

}}2(a),(c),ECI

RSI-10

10.3.7 {{ **}}2(a),(c),ECI**

{{

RSI-4, RSI-9, RSI-10, RSI-11, RSI-13

RSI-4, RSI-9, RSI-10, RSI-11, RSI-13

}}2(a),(c),ECI

RSI-4, RSI-9, RSI-10, RSI-11, RSI-13

10.3.8 {{ **}}2(a),(c),ECI**

{{

}}2(a),(c),ECI

RSI-10

10.3.9 {{ **}}2(a),(c)**

{{

}}2(a),(c)

{{

}}2(a),(c)

RSI-4, RSI-9, RSI-13

10.4 ~~NPM Operation Margin~~Methodology for Density Wave Oscillation Analysis~~Onset~~

RSI-4, RSI-9, RSI-11, RSI-13

{{

RSI-4, RSI-9, RSI-13

RSI-4, RSI-9, RSI-11, RSI-13

RSI-4, RSI-9, RSI-11, RSI-13

}}2(a),(c)

{{

}}$^{2(a),(c)}$

RSI-4, RSI-9, RSI-11, RSI-13

Table 10-6 {{ }}$^{2(a),(c)}$

{{

}}$^{2(a),(c)}$

Table 10-6 {{ }}2(a),(c) (Continued)

	{{			
	}}2(a),(c)			

RSI-4, RSI-9, RSI-11, RSI-13

10.4.1 {{ }}2(a),(c)

RSI-4, RSI-9, RSI-11, RSI-13

{{

RSI-4, RSI-9, RSI-11, RSI-13

}}2(a),(c)

{{

RSI-4, RSI-9, RSI-11, RSI-13

RSI-4, RSI-9, RSI-11, RSI-13

Equation 10-13

RSI-4, RSI-9, RSI-11, RSI-13

RSI-4, RSI-9, RSI-11, RSI-13

Equation 10-14

}}2(a),(c)

}}2(a),(c)

}}2(a),(c)

RSI-4, RSI-9, RSI-13

Figure 10-10 {{

{{

RSI-4, RSI-9, RSI-13

~~For evaluating NPM operating margin for DWO onset, sensitivity analysis is used. The sources of uncertainty for the NPM full-plant calculation with respect to DWO are identified. Effects of these uncertainty parameters on DWO are evaluated using IETs/SETs, plant design conditions, operating conditions, design basis safety analysis assumptions/limits, and literature.~~

RSI-4, RSI-9, RSI-13

~~{{~~

RSI-4, RSI-9, RSI-13

~~}}2(a),(c)~~

RSI-4, RSI-9, RSI-13

~~The methodology for calculating margin for DWO involves accounting for uncertainties in different geometric parameters and operating conditions. Sensitivity analysis is carried out accounting for uncertainties in margin calculation.~~

RSI-4, RSI-9, RSI-13

~~The methodology for calculating margin identified important uncertainty contributors for DWO. These contributors are derived from the SG stability PIRT, code validation, NPM~~

~~operating parameters, and safety analysis limits/assumptions. The uncertainty contributors are divided into three categories – analytical uncertainties/T-H model and correlation uncertainties; geometrical uncertainties; and the plant conditions uncertainties. These parameters are varied in a parametric evaluation to ensure that uncertainties are adequately addressed in the evaluation of margin.~~

RSI-4, RSI-9, RSI-13

~~{{~~

RSI-4, RSI-9, RSI-13

RSI-4, RSI-9, RSI-13

RSI-4, RSI-9, RSI-13

~~}}2(a),(c)~~

{{

RSI-4, RSI-9, RSI-13

RSI-4, RSI-9, RSI-13

RSI-4, RSI-9, RSI-13

RSI-4, RSI-9, RSI-13

}}2(a),(c)

RSI-4, RSI-9, RSI-13

Table 10-7 ~~NPM Sensitivity Cases at Off-Normal Conditions for DWO Evaluation~~

	{{							}}~~2(a),(c)~~

RSI-4, RSI-9, RSI-13

~~{{~~

RSI-4, RSI-9, RSI-13

~~}}2(a),(c)~~

{{

}}2(a),(c)

Response to Request for Additional Information
Docket: 99902078

RAI No.: RSI
Date of RAI Issue: 03/27/2023

NRC Question No.: RSI-10

Section 10 of the DWO LTR is missing the inclusion of the contribution of multiple highly important phenomena listed in PIRT results Table 7-1, or a justification for why these phenomena can be excluded.

NuScale Response:

NuScale evaluated all of the high ranked phenomena from the steam generator (SG) stability phenomena identification and ranking table (PIRT) (Table 4-4 from request for supplemental information (RSI) 5 response) . All of the high ranked phenomena were evaluated based on the TF-1, TF-2, and POLIMI test programs. During the test data validation from these programs, the effects of high ranked phenomena on density wave oscillation (DWO) were evaluated. NuScale directly included most of the high ranked phenomena in the uncertainty by direct biasing, modeling, or analysis. {{

}}2(a),(c)

Section 4.1 through Section 4.3 of TR-131981-P describe and discuss the high ranked PIRT phenomena. Table 7-1 of TR-131981-P shows the link between the EM and PIRT phenomena; all phenomena are either covered or excluded with justification for the EM development. Section 10.2 describes the uncertainty analysis methodology, which includes identifying important phenomena that have a significant impact on DWO. Section 10.2 also provides the

method of transforming important PIRT phenomena into appropriate correlations and uncertainty calculations that can be applied to the NuScale Power Module (NPM-20) via the EM.

The purpose of the uncertainty methodology is to evaluate NRELAP5-specific model uncertainties, geometric uncertainties, and overall NRELAP5 uncertainty in predicting DWO onset so that these uncertainties can be applied to the NPM-20 stability analysis. For this purpose, test data and code validation from the TF-1, TF-2, and POLIMI test programs are used.

{{

}}2(a),(c)

There was an additional clarifying question on this RSI transmitted on June 23, 2023. The question is in italics below.

In RSI-10, the response states:

{{

}}2(a),(c)

But this is contradicted by the RSI-9 response, which makes numerous revisions to Section 10 of the LTR, including the removal of Bullet 6 on Page 280 of the original submittal. This is replaced by Table 10-2 in the RSI-9 response. The first entry in Table 10-2 of the RSI-9 response indicates that: {{

}}2(a),(c)

{{

}}2(a),(c)

Therefore, when RSI-10 includes justifications in Section 10.2, the list of phenomena is no longer complete because it should include: {{

}}2(a),(c)

The staff had previously determined that the RSI-10 response was sufficient, but because RSI-9 changed Section 10, there is now a conflict between the RSI-9 and RSI-10 responses.

So if RSI-9 response is accurate, then the RSI-10 response is no longer complete in the scope of the additional justification provided in Section 10.2.

{{

}}2(a),(c)

{{

}}2(a),(c)

{{

}}2(a),(c)

{{

}}2(a),(c)

- {{

}}2(a),(c)

{{

}}2(a),(c)

{{

}}2(a),(c)

Impact on Topical Report:

Topical Report TR-131981, Methodology for the Determination of the Onset of Density Wave Oscillations (DWO), has been revised as described in the response above and as shown in the markup provided in this response.

Table 10-1 {{ }}2(a),(c),ECI (Continued)

	{{		
	}}2(a),(c),ECI		

RSI-4, RSI-9, RSI-13

10.2 NRELAP5 Code Uncertainty

RSI-4, RSI-9, RSI-10, RSI-11, RSI-13

{{

RSI-10

}}2(a),(c)

{{

RSI-10

RSI-10

RSI-10

RSI-10

RSI-10

RSI-10

RSI-10

RSI-4, RSI-9, RSI-10, RSI-13

RSI-4, RSI-9, RSI-10, RSI-13

RSI-10

RSI-10

}}2(a),(c)

{{

}}2(a),(c)

RSI-10

10.3 Other High Ranked Phenomena Identification and Ranking Table Phenomena Not Considered in the Uncertainty Evaluation

10.3.1 {{ }}2(a),(c)

RSI-10

{{

RSI-4, RSI-9, RSI-10, RSI-11, RSI-13

}}2(a),(c)

RSI-10

10.3.2 {{ }}2(a),(c),ECI

{{

RSI-4, RSI-9, RSI-11, RSI-13

}}2(a),(c),ECI

RSI-10

Table 10-3 {{ }}2(a),(c),ECI

{{			}}2(a),(c),ECI

RSI-10

{{

}}2(a),(c),ECI

RSI-10

10.3.3 {{ }}2(a),(c),ECI

{{

RSI-10

}}2(a),(c),ECI

RSI-10

Figure 10-1 {{ }}2(a),(c),ECI

	{{	
	}}2(a),(c),ECI	

RSI-4, RSI-9, RSI-10, RSI-11, RSI-13

{{

}}2(a),(c),ECI

RSI-10

Figure 10-2 {{ }}2(a),(c),ECI

{{

}}2(a),(c),ECI

RSI-10

{{

}}2(a),(c),ECI

{{

}}2(a),(c)

RSI-10

10.3.4 {{ }}2(a),(c)

{{

}}2(a),(c)

RSI-10

Figure 10-3 {{ }}2(a),(c),ECI

{{

}}2(a),(c)

RSI-10

{{

}}2(a),(c)

RSI-10

10.3.5 {{ }}2(a),(c)

{{

RSI-10

}}2(a),(c),ECI

RSI-10

10.3.6 {{ }}2(a),(c),ECI

{{

RSI-10

}}2(a),(c),ECI

- {{

}}2(a),(c),ECI

RSI-10

Table 10-4 {{

}}2(a),(c),ECI

	{{				
				}}2(a),(c),ECI	

RSI-10

{{

}}2(a),(c),ECI

RSI-10

Figure 10-4 {{

}}2(a),(c),ECI

{{

}}2(a),(c),ECI

RSI-10

{{

}}2(a),(c),ECI

RSI-10

Figure 10-5 {{

}}2(a),(c),ECI

{{

}}2(a),(c),ECI

RSI-10

{{

}}2(a),(c),ECI

RSI-10

Figure 10-6 {{

}}2(a),(c),ECI

{{

}}2(a),(c),ECI

RSI-10

{{

}}2(a),(c),ECI

RSI-10

Table 10-5 {{

}}2(a),(c),ECI

{{

}}2(a),(c),ECI

RSI-10

Figure 10-7 {{ }}2(a),(c),ECI

{{

}}2(a),(c),ECI

RSI-10

{{

}}2(a),(c),ECI

RSI-10

Figure 10-8 {{ }}2(a),(c),ECI

{{

}}2(a),(c),ECI

RSI-10

Figure 10-9 {{ }}2(a),(c),ECI

	{{	
	}}2(a),(c),ECI	

RSI-10

{{ }}2(a),(c),ECI

{{

}}2(a),(c),ECI

RSI-10

10.3.7 {{ **}}2(a),(c),ECI**

{{

RSI-4, RSI-9, RSI-10, RSI-11, RSI-13

RSI-4, RSI-9, RSI-10, RSI-11, RSI-13

}}2(a),(c),ECI

RSI-4, RSI-9, RSI-10, RSI-11, RSI-13

10.3.8 {{ **}}2(a),(c),ECI**

{{

}}2(a),(c),ECI

RSI-10

10.3.9 {{ **}}2(a),(c)**

{{

}}2(a),(c)

{{

}}2(a),(c)

RSI-4, RSI-9, RSI-13

10.4 ~~NPM Operation Margin~~Methodology for Density Wave Oscillation Analysis~~Onset~~

RSI-4, RSI-9, RSI-11, RSI-13

{{

RSI-4, RSI-9, RSI-13

RSI-4, RSI-9, RSI-11, RSI-13

RSI-4, RSI-9, RSI-11, RSI-13

}}2(a),(c)

Response to Request for Additional Information
Docket: 99902078

RAI No.: RSI
Date of RAI Issue: 03/27/2023

NRC Question No.: RSI-11

The DWO LTR is missing a justification related to how the scaling analysis accounts for SIET-TF2 test setup limitations in representing the actual NPM configuration (SIET-TF2 only uses a few banks of tubes to represent 21 banks in the actual NPM design).

NuScale Response:

{{

}}2(a),(c)

{{

}}2(a),(c)

{{

}}2(a),(c)

Table 1 {{

}}2(a),(c)

{{

}}2(a),(c)

{{

}}2(a),(c),ECI

{{

}}2(a),(c),ECI

{{

}}2(a),(c),ECI

{{

}}2(a),(c),ECI

{{

}}2(a),(c),ECI

{{

}}2(a),(c)

{{

}}2(a),(c),ECI

{{

}}2(a),(c),ECI

{{

}}2(a),(c)

{{

}}2(a),(c),ECI

{{

}}2(a),(c),ECI

{{

}}2(a),(c)

Table 2 {{

}}2(a),(c)

{{

}}2(a),(c),ECI

{{

}}2(a),(c),ECI

{{

}}2(a),(c),ECI

{{

}}2(a),(c),ECI

Table 3 {{

}}2(a),(c),ECI

{{

}}2(a),(c),ECI

{{

}}2(a),(c),ECI

There was an additional clarifying question on this RSI transmitted on June 16, 2023. The question is in italics.

The response quantifies the test setup limitations, but the response remains lacking in a justification or rationale for the applicability of the uncertainty derived from comparisons to the test (for example, the scaling analysis was not incorporated into the LTR in a manner where it could be used to potentially justify that the impact is adequately reflected).

There was another additional clarifying question on this RSI transmitted on June 23, 2023. The question is in italics with the response following the question.

The response quantifies the test setup limitations, but the response remains lacking in a justification or rationale for the applicability of the uncertainty derived from comparisons to the test (for example, the scaling analysis was not incorporated into the LTR in a manner where it could be used to potentially justify that the impact is adequately reflected).

The RSI-11 response contains scaling analysis information that provides the distortions (see Tables 2 and 3 in the RSI-9 response and Table 3 in the RSI-11 response). However, the response is lacking the justification requested in RSI-11. The RSI-11 response includes two necessary pieces of information {{

}}2(a),(c)

{{ }}2(a),(c),ECI

{{ }}2(a),(c),ECI

{{ }}2(a),(c),ECI

{{ }}2(a),(c),ECI

{{ }}2(a),(c),ECI

{{ }}2(a),(c),ECI

{{ }}2(a),(c),ECI

{{ }}2(a),(c),ECI

{{ }}2(a),(c),ECI

{{

}}2(a),(c),ECI

{{

}}2(a),(c),ECI

{{

}}2(a),(c),ECI

{{

}}2(a),(c),ECI

{{

}}2(a),(c),ECI

{{

}}2(a),(c),ECI

{{

}}2(a),(c),ECI

{{ }}2(a),(c),ECI

The criteria for preserving the Π groups between the model (M) and prototype (P) or accounting for distortions in the uncertainty are as follows; all criteria are not required to be fulfilled in order to account for or neglect the distortions.

1. {{

}}2(a),(c)

{{

}}2(a),(c),ECI

{{

}}2(a),(c),ECI

{{

}}2(a),(c),ECI

{{

}}2(a),(c),ECI

{{ }}2(a),(c),ECI

{{

}}2(a),(c),ECI

{{ }}2(a),(c),ECI

{{

}}2(a),(c),ECI

{{ }}2(a),(c),ECI

{{

}}2(a),(c),ECI

Impact on Topical Report:

Topical Report TR-131981, Methodology for the Determination of the Onset of Density Wave Oscillations (DWO), has been revised as described in the response above and as shown in the markup provided in this response.

RSI-4, RSI-9, RSI-13

10.0 Uncertainty Evaluation and Margin for the NuScale Power Module with ~~r~~Respect to Density Wave Oscillation

RSI-4, RSI-9, RSI-10, RSI-11, RSI-13

This section describes the methodology for uncertainty quantification and margin evaluation applied to the NRELAP5 calculation of DWO onset for the NPM-20 ~~SG~~. The uncertainty methodology ~~used~~ takes into account code input uncertainties stemming from a variety of sources (e.g., initial~~/~~ and boundary conditions, models~~/~~ and correlations~~, etc.~~), as well as output uncertainty associated with the code calculations. ~~Code predictions of both SETs and IETs are used to assess how well important phenomena and processes are predicted, as well as overall system response~~Code predictions of both SETs and IETs assess how well important phenomena and processes are predicted, and a global sensitivity analysis distills the important geometric and operating conditions to be modeled. Margin to DWO onset is calculated for the NPM-20 by evaluating DWO onset with biased inputs at varying nominal power levels.~~SGs by reducing feedwater flow from nominal conditions until onset occurs. The difference between the FW flow rate that requires, automatic control system or operator response, or produces a protective trip, and the FW flow rate at DWO onset taking into consideration NRELAP5 code uncertainty, is the margin to DWO for the NPM.~~

RSI-4, RSI-9, RSI-10, RSI-11, RSI-13

For the NPM-20 ~~SG~~, a ~~best estimate~~deterministic methodology is applied using a combination of conservative and realistic input data and boundary~~/~~ and initial conditions. Uncertainty is assessed using the methodology described as follows.~~in the following section, which considers both code input and output phase uncertainties.~~

RSI-4, RSI-9, RSI-13

10.1 Sensitivity~~Uncertainty~~ Analysis Methodology Development

RSI-4, RSI-9, RSI-10, RSI-13

~~Reference 12.47 provides an integrated methodology for uncertainty quantification wherein uncertainty evaluation is divided into two distinct parts – the input phase and the output phase.~~

RSI-4, RSI-9, RSI-10, RSI-13

~~Input uncertainty quantification focuses on the identification of uncertainties in code input parameters, and those associated with the models and sub-models of the code. Sources of input uncertainty include:~~

RSI-4, RSI-9, RSI-10, RSI-13

- ~~Model parameters,~~
- ~~Boundary/initial conditions, and~~
- ~~Uncertainties in the structure of sub-models.~~

RSI-4, RSI-9, RSI-10, RSI-13

~~Input uncertainty includes the sources of code uncertainties that can be explicitly accounted for and are propagated through code calculations. SET data that is used to assess code models and correlations, is also used for input based uncertainty quantification.~~

RSI-4, RSI-9, RSI-10, RSI-13

~~The output phase of uncertainty accounts for the impact of uncertainties associated with the FoM output. For NRELAP5, applicable experimental data come from IET facilities designed to provide information on system behavior. Output phase uncertainty can be characterized by comparing measured IET data to NRELAP5 calculated values.~~

RSI-4, RSI-9, RSI-11, RSI-13

{{

RSI-4, RSI-9, RSI-11, RSI-13

RSI-4, RSI-9, RSI-13

}}2(a),(c),ECI

RSI-4, RSI-9, RSI-11, RSI-13

Table 10-1 {{ }}2(a),(c),ECI

{{			
			}}2(a),(c),ECI

Table 10-1 {{ }}2(a),(c),ECI (Continued)

	{{		
	}}2(a),(c),ECI		

RSI-4, RSI-9, RSI-13

10.2 NRELAP5 Code Uncertainty

RSI-4, RSI-9, RSI-10, RSI-11, RSI-13

{{

RSI-10

}}2(a),(c)

{{

RSI-10

RSI-10

RSI-10

RSI-10

RSI-10

RSI-10

RSI-10

RSI-4, RSI-9, RSI-10, RSI-13

RSI-4, RSI-9, RSI-10, RSI-13

RSI-10

RSI-10

}}2(a),(c)

RSI-4, RSI-9, RSI-10, RSI-11, RSI-13

2. {{

RSI-4, RSI-9, RSI-10, RSI-11, RSI-13

RSI-4, RSI-9, RSI-10, RSI-11, RSI-13

RSI-4, RSI-9, RSI-10, RSI-11, RSI-13

RSI-4, RSI-9, RSI-10, RSI-11, RSI-13

}}2(a),(c)

{{

RSI-4, RSI-9, RSI-10, RSI-11, RSI-13

Equation 10-1

RSI-4, RSI-9, RSI-10, RSI-11, RSI-13

Equation 10-2

RSI-4, RSI-9, RSI-10, RSI-11, RSI-13

Equation 10-3

RSI-4, RSI-9, RSI-10, RSI-11, RSI-13

}}2(a),(c)

{{

Equation 10-4

RSI-4, RSI-9, RSI-10, RSI-11, RSI-13

RSI-4, RSI-9, RSI-13

RSI-4, RSI-9, RSI-10, RSI-11, RSI-13

Equation 10-5

RSI-4, RSI-9, RSI-11, RSI-13

RSI-4, RSI-9, RSI-13

}}2(a),(c)

RSI-4, RSI-9, RSI-10, RSI-11, RSI-13

{{

Equation 10-6

RSI-4, RSI-9, RSI-10, RSI-11, RSI-13

RSI-4, RSI-9, RSI-10, RSI-11, RSI-13

RSI-4, RSI-9, RSI-10, RSI-11, RSI-13

RSI-4, RSI-9, RSI-13

RSI-4, RSI-9, RSI-10, RSI-11, RSI-13

RSI-4, RSI-9, RSI-10, RSI-11, RSI-13

}}2(a),(c)

{{

Equation 10-7

RSI-4, RSI-9, RSI-10, RSI-11, RSI-13

Equation 10-8

RSI-4, RSI-9, RSI-10, RSI-11, RSI-13

Equation 10-9

RSI-4, RSI-9, RSI-13

RSI-4, RSI-9, RSI-13

RSI-4, RSI-9, RSI-13

RSI-4, RSI-9, RSI-10, RSI-11, RSI-13

}}2(a),(c)

RSI-4, RSI-9, RSI-10, RSI-11, RSI-13

{{

RSI-4, RSI-9, RSI-10, RSI-11, RSI-13

RSI-4, RSI-9, RSI-13

RSI-4, RSI-9, RSI-13

RSI-4, RSI-9, RSI-13

Equation 10-10

RSI-4, RSI-9, RSI-13

}}2(a),(c)

RSI-4, RSI-9, RSI-11, RSI-13

Table 10-2 {{

}}2(a),(c)

{{

}}2(a),(c)

Table 10-2 {{ }}2(a),(c) (Continued)

{{

}}2(a),(c)

Table 10-2 {{ }}2(a),(c) (Continued)

	{{			
	}}2(a),(c)			

RSI-4, RSI-9, RSI-13

{{

}}2(a),(c)

RSI-4, RSI-9, RSI-11, RSI-13

The error in NRELAP5 DWO onset prediction is calculated using Equation 10-11.

$$\varepsilon = \frac{NRELAP5 - Data}{Data} \qquad \text{Equation 10-11}$$

Variable *NRELAP5* is the FW flow rate as predicted by NRELAP5 at DWO onset, and *Data* is the FW flow rate as measured by test facility at DWO onset.

RSI-4, RSI-9, RSI-13

Using the statistical methods described in previous key steps, NRELAP5 average error $\bar{x}$ and standard deviation of mean $\bar{u}$ are calculated. Assuming t-distribution and a 95 percent one-sided distribution and degrees of freedom of 35, the coverage factor is 1.69. The one-sided confidence interval value is calculated using Equation 10-12.

RSI-4, RSI-9, RSI-13

$$95\%\ \mathrm{CI}_t = \bar{x} - 1.69 \times \bar{u} \qquad \text{Equation 10-12}$$

A 95 percent confidence interval method is used for evaluating the NRELAP5 DWO onset prediction uncertainty. A 95 percent confidence interval error estimate (Equation 10-12) indicates that there is a 95 percent probability that the NRELAP5 error in predicting the DWO onset phenomena is within the error span.

RSI-4, RSI-9, RSI-11, RSI-13

5. Overall NRELAP5 Density Wave Oscillation Prediction Uncertainty

{{

RSI-4, RSI-9, RSI-11, RSI-13

RSI-4, RSI-9, RSI-11, RSI-13

}}2(a),(c),ECI

RSI-4, RSI-9, RSI-13

6. {{

RSI-4, RSI-9, RSI-13

RSI-4, RSI-9, RSI-13

}}2(a),(c)

RSI-4, RSI-9, RSI-13

{{

}}2(a),(c)

{{

}}2(a),(c)

RSI-10

10.3 Other High Ranked Phenomena Identification and Ranking Table Phenomena Not Considered in the Uncertainty Evaluation

10.3.1 {{ }}2(a),(c)

RSI-10

{{

RSI-4, RSI-9, RSI-10, RSI-11, RSI-13

}}2(a),(c)

RSI-10

10.3.2 {{ }}2(a),(c),ECI

{{

RSI-4, RSI-9, RSI-11, RSI-13

}}2(a),(c),ECI

RSI-10

Table 10-3 {{ }}2(a),(c),ECI

{{			}}2(a),(c),ECI

RSI-10

{{

}}2(a),(c),ECI

RSI-10

10.3.3 {{ }}2(a),(c),ECI

{{

RSI-10

}}2(a),(c),ECI

RSI-10

Figure 10-1 {{ }}2(a),(c),ECI

	{{	
	}}2(a),(c),ECI	

RSI-4, RSI-9, RSI-10, RSI-11, RSI-13

{{

}}2(a),(c),ECI

RSI-10

Figure 10-2 {{ }}2(a),(c),ECI

{{

}}2(a),(c),ECI

RSI-10

{{

}}2(a),(c),ECI

{{

}}2(a),(c)

RSI-10

10.3.4 {{ }}2(a),(c)

{{

}}2(a),(c)

RSI-10

Figure 10-3 {{ }}2(a),(c),ECI

{{

}}2(a),(c)

RSI-10

{{

}}2(a),(c)

RSI-10

10.3.5 {{ }}2(a),(c)

{{

RSI-10

}}2(a),(c),ECI

RSI-10

10.3.6 {{ }}2(a),(c),ECI

{{

RSI-10

}}2(a),(c),ECI

- {{

}}2(a),(c),ECI

RSI-10

Table 10-4 {{

}}2(a),(c),ECI

	{{				
				}}2(a),(c),ECI	

RSI-10

{{

}}2(a),(c),ECI

RSI-10

Figure 10-4 {{

}}2(a),(c),ECI

{{

}}2(a),(c),ECI

RSI-10

{{

}}2(a),(c),ECI

RSI-10

Figure 10-5 {{

}}2(a),(c),ECI

{{

}}2(a),(c),ECI

RSI-10

{{

}}2(a),(c),ECI

RSI-10

Figure 10-6 {{

}}2(a),(c),ECI

{{

}}2(a),(c),ECI

RSI-10

{{

}}2(a),(c),ECI

RSI-10

Table 10-5 {{

}}2(a),(c),ECI

{{

}}2(a),(c),ECI

RSI-10

Figure 10-7 {{ }}2(a),(c),ECI

{{

}}2(a),(c),ECI

RSI-10

{{

}}2(a),(c),ECI

RSI-10

Figure 10-8 {{ }}2(a),(c),ECI

{{

}}2(a),(c),ECI

RSI-10

Figure 10-9 {{ }}2(a),(c),ECI

	{{	
	}}2(a),(c),ECI	

RSI-10

{{ }}2(a),(c),ECI

{{

}}2(a),(c),ECI

RSI-10

10.3.7 {{ **}}2(a),(c),ECI**

{{

RSI-4, RSI-9, RSI-10, RSI-11, RSI-13

RSI-4, RSI-9, RSI-10, RSI-11, RSI-13

}}2(a),(c),ECI

RSI-4, RSI-9, RSI-10, RSI-11, RSI-13

10.3.8 {{ **}}2(a),(c),ECI**

{{

}}2(a),(c),ECI

RSI-10

10.3.9 {{ **}}2(a),(c)**

{{

}}2(a),(c)

{{

}}2(a),(c)

RSI-4, RSI-9, RSI-13

10.4 ~~NPM Operation Margin~~Methodology for Density Wave Oscillation Analysis~~Onset~~

RSI-4, RSI-9, RSI-11, RSI-13

{{

RSI-4, RSI-9, RSI-13

RSI-4, RSI-9, RSI-11, RSI-13

RSI-4, RSI-9, RSI-11, RSI-13

}}2(a),(c)

{{

}}$^{2(a),(c)}$

RSI-4, RSI-9, RSI-11, RSI-13

Table 10-6 {{ }}$^{2(a),(c)}$

{{

}}$^{2(a),(c)}$

Table 10-6 {{ }}2(a),(c) (Continued)

	{{			
	}}2(a),(c)			

RSI-4, RSI-9, RSI-11, RSI-13

10.4.1 {{ }}2(a),(c)

RSI-4, RSI-9, RSI-11, RSI-13

{{

RSI-4, RSI-9, RSI-11, RSI-13

}}2(a),(c)

{{

RSI-4, RSI-9, RSI-11, RSI-13

RSI-4, RSI-9, RSI-11, RSI-13

Equation 10-13

RSI-4, RSI-9, RSI-11, RSI-13

RSI-4, RSI-9, RSI-11, RSI-13

Equation 10-14

}}2(a),(c)

}}2(a),(c)

}}2(a),(c)

RSI-4, RSI-9, RSI-13

Figure 10-10 {{

{{

RSI-4, RSI-9, RSI-13

~~For evaluating NPM operating margin for DWO onset, sensitivity analysis is used. The sources of uncertainty for the NPM full-plant calculation with respect to DWO are identified. Effects of these uncertainty parameters on DWO are evaluated using IETs/SETs, plant design conditions, operating conditions, design basis safety analysis assumptions/limits, and literature.~~

RSI-4, RSI-9, RSI-13

~~{{~~

RSI-4, RSI-9, RSI-13

~~}}2(a),(c)~~

RSI-4, RSI-9, RSI-13

~~The methodology for calculating margin for DWO involves accounting for uncertainties in different geometric parameters and operating conditions. Sensitivity analysis is carried out accounting for uncertainties in margin calculation.~~

RSI-4, RSI-9, RSI-13

~~The methodology for calculating margin identified important uncertainty contributors for DWO. These contributors are derived from the SG stability PIRT, code validation, NPM~~

~~operating parameters, and safety analysis limits/assumptions. The uncertainty contributors are divided into three categories – analytical uncertainties/T-H model and correlation uncertainties; geometrical uncertainties; and the plant conditions uncertainties. These parameters are varied in a parametric evaluation to ensure that uncertainties are adequately addressed in the evaluation of margin.~~

RSI-4, RSI-9, RSI-13

~~{{~~

RSI-4, RSI-9, RSI-13

RSI-4, RSI-9, RSI-13

RSI-4, RSI-9, RSI-13

~~}}2(a),(c)~~

{{

RSI-4, RSI-9, RSI-13

RSI-4, RSI-9, RSI-13

RSI-4, RSI-9, RSI-13

RSI-4, RSI-9, RSI-13

}}2(a),(c)

RSI-4, RSI-9, RSI-13

Table 10-7 ~~NPM Sensitivity Cases at Off-Normal Conditions for DWO Evaluation~~

	{{							}}~~2(a),(c)~~

RSI-4, RSI-9, RSI-13

~~{{~~

RSI-4, RSI-9, RSI-13

~~}}2(a),(c)~~

{{

}}2(a),(c)

Response to Request for Additional Information
Docket: 99902078

RAI No.: RSI
Date of RAI Issue: 03/27/2023

NRC Question No.: RSI-12

The steam generator tube-side two-phase flow instability may be significantly impacted by the dynamic feedback of the secondary side controllers; namely those that control the steam line pressure, the individual steam generator feed flow rates, and the feedwater temperature. The DWO on-set prediction methodology in the DWO LTR is missing a description of the impact of these secondary side control systems on stability margin and how they are considered in the analysis.

NuScale Response:

{{

}}2(a),(c),ECI

{{

}}2(a),(c),ECI

{{

}}2(a),(c),ECI

{{

}}2(a),(c),ECI

COL Item 7.0-1: An applicant that references the NuScale Power Plant US460 standard design will demonstrate the stability of the NuScale Power Module during normal and power maneuvering operations for closed-loop module control system subsystems that use reactor power as a control input.

{{

}}2(a),(c),ECI

Figure 1 {{ }}2(a),(c),ECI

{{

}}2(a),(c),ECI

{{

}}2(a),(c),ECI

{{

}}2(a),(c),ECI

{{

}}2(a),(c),ECI

Table 1 {{

}}2(a),(c),ECI

Parameter	Control Mechanism	Controller Effect on DWO Onset

{{

}}2(a),(c),ECI

Parameter	Control Mechanism	Controller Effect on DWO Onset
{{		

}}2(a),(c),ECI

Parameter	Control Mechanism	Controller Effect on DWO Onset

{{

}}2(a),(c),ECI

{{

}}2(a),(c),ECI

{{

}}2(a),(c),ECI

Figure 2 {{

}}2(a),(c),ECI

{{

}}2(a),(c),ECI

{{

}}2(a),(c),ECI

Table 2 {{

}}2(a),(c),ECI

{{

}}2(a),(c),ECI

Table 3 {{

}}2(a),(c),ECI

{{

}}2(a),(c),ECI

{{

}}2(a),(c),ECI

There was an additional clarifying question on this RSI transmitted on June 16, 2023. The question is in italics with the response following the question. Note that the clarifying questions on RSI-4 and RSI-13 contain this same response and that the responses to RSI-4, RSI-12, and RSI-13 should be considered together to address the operating band considered for DWO.

The response is largely qualitative. The staff understands the secondary side controllers are not yet designed, yet the response still is missing how they are considered in the analysis (in other words, the quantitative approach and numerical tools that will be used once the design is finished). Further, the qualitative description of the control strategy implies that a very

open-ended approach is being employed to secondary side operation, yet the response to RSI-4 implies that there would be a very narrow operating window. These 2 responses appear to be inconsistent.

The objective of this additional information is to clarify the systematic construction of the global sensitivity analysis for DWO onset, which represents the full range of the anticipated NPM-20 operating domain using the following combination of inputs:

- {{

}}2(a),(c),ECI

Table 10-6 of TR-131981-P provides the summary of significant system parameter biases necessary to ensure a conservative DWO onset calculation based on {{

}}2(a),(c),ECI

{{

}}2(a),(c),ECI

{{

}}2(a),(c),ECI

{{

}}2(a),(c),ECI

{{

}}2(a),(c),ECI

Figure 3. {{ }}2(a),(c),ECI

{{

}}2(a),(c),ECI

{{

}}2(a),(c),ECI

{{

}}2(a),(c),ECI

Figure 4. {{ }}2(a),(c),ECI

{{

}}2(a),(c),ECI

{{

}}2(a),(c),ECI

{{

}}2(a),(c),ECI

Figure 5. {{ }}2(a),(c),ECI

{{

}}2(a),(c),ECI

{{

}}2(a),(c),ECI

{{

}}2(a),(c),ECI

Impact on Topical Report:

There are no impacts to Topical Report TR-131981, Methodology for the Determination of the Onset of Density Wave Oscillations (DWO), as a result of this response.

Response to Request for Additional Information
Docket: 99902078

RAI No.: RSI
Date of RAI Issue: 03/27/2023

NRC Question No.: RSI-13

The DWO LTR is missing a description of a systematic approach in the evaluation model to characterize and quantify the stability margin over the full range of conditions on the secondary side consistent with the applicability range of the method (i.e., 20-100% power).

NuScale Response:

{{

}}2(a),(c)

{{

}}2(a),(c)

{{

}}2(a),(c)

{{

}}2(a),(c)

{{

}}2(a),(c)

{{

}}2(a),(c)

{{

}}2(a),(c)

{{

}}2(a),(c)

{{

}}2(a),(c)

{{

}}2(a),(c)

{{

}}2(a),(c)

{{

}}2(a),(c)

{{

}}2(a),(c)

There was an additional clarifying question on this RSI transmitted on June 16, 2023. The question is in italics with the response following the question. Note that the clarifying questions on RSI-4 and RSI-12 contain this same response, except for some additional text addressing feedwater flow ramping, and that the responses to RSI-4, RSI-12, and RSI-13 should be considered together to address the operating band considered for DWO.

A description of an approach is provided but remains largely incomplete because it does not consider the full range of conditions, considering that the RSI-13 response map provided (Figure 10-10) conflicts with the RSI-12 response (the qualitative description of the control strategy). Further, the proposed approach is not systematic in nature in that it varies merely a single parameter, feedwater flow, in performing the assessments, rather than the full range of parameters.

The objective of this additional information is to clarify the systematic construction of the global sensitivity analysis for DWO onset, which represents the full range of the anticipated NPM-20 operating domain using the following combination of inputs:

- {{

}}2(a),(c)

Table 10-6 of TR-131981-P provides the summary of significant system parameter biases necessary to ensure a conservative DWO onset calculation based on {{

}}2(a),(c)

{{

}}2(a),(c)

{{

}}2(a),(c)

{{

}}2(a),(c)

{{

}}2(a),(c)

Figure 1. {{ }}2(a),(c)

{{

}}2(a),(c)

{{

}}2(a),(c)

{{

}}2(a),(c)

Figure 2. {{ }}2(a),(c)

{{

}}2(a),(c)

{{

}}2(a),(c)

{{

}}2(a),(c)

{{

}}2(a),(c)

Figure 3. {{ }}2(a),(c)

{{

}}2(a),(c)

{{

}}2(a),(c)

{{

}}2(a),(c)

{{

}}2(a),(c)

{{

}}2(a),(c)

{{

}}2(a),(c)

Impact on Topical Report:

Topical Report TR-131981, Methodology for the Determination of the Onset of Density Wave Oscillations (DWO), has been revised as described in the response above and as shown in the markup provided in this response.

RSI-4, RSI-9, RSI-13

10.0 Uncertainty Evaluation and Margin for the NuScale Power Module with ~~r~~Respect to Density Wave Oscillation

RSI-4, RSI-9, RSI-10, RSI-11, RSI-13

This section describes the methodology for uncertainty quantification and margin evaluation applied to the NRELAP5 calculation of DWO onset for the NPM-20 ~~SG~~. The uncertainty methodology ~~used~~ takes into account code input uncertainties stemming from a variety of sources (e.g., initial~~/~~ and boundary conditions, models~~/~~ and correlations~~, etc.~~), as well as output uncertainty associated with the code calculations. ~~Code predictions of both SETs and IETs are used to assess how well important phenomena and processes are predicted, as well as overall system response~~Code predictions of both SETs and IETs assess how well important phenomena and processes are predicted, and a global sensitivity analysis distills the important geometric and operating conditions to be modeled. Margin to DWO onset is calculated for the NPM-20 by evaluating DWO onset with biased inputs at varying nominal power levels.~~SGs by reducing feedwater flow from nominal conditions until onset occurs. The difference between the FW flow rate that requires, automatic control system or operator response, or produces a protective trip, and the FW flow rate at DWO onset taking into consideration NRELAP5 code uncertainty, is the margin to DWO for the NPM.~~

RSI-4, RSI-9, RSI-10, RSI-11, RSI-13

For the NPM-20 ~~SG~~, a ~~best estimate~~deterministic methodology is applied using a combination of conservative and realistic input data and boundary~~/~~ and initial conditions. Uncertainty is assessed using the methodology described as follows.~~in the following section, which considers both code input and output phase uncertainties.~~

RSI-4, RSI-9, RSI-13

10.1 Sensitivity~~Uncertainty~~ Analysis Methodology Development

RSI-4, RSI-9, RSI-10, RSI-13

~~Reference 12.47 provides an integrated methodology for uncertainty quantification wherein uncertainty evaluation is divided into two distinct parts – the input phase and the output phase.~~

RSI-4, RSI-9, RSI-10, RSI-13

~~Input uncertainty quantification focuses on the identification of uncertainties in code input parameters, and those associated with the models and sub-models of the code. Sources of input uncertainty include:~~

RSI-4, RSI-9, RSI-10, RSI-13

- ~~Model parameters,~~
- ~~Boundary/initial conditions, and~~
- ~~Uncertainties in the structure of sub-models.~~

RSI-4, RSI-9, RSI-10, RSI-13

~~Input uncertainty includes the sources of code uncertainties that can be explicitly accounted for and are propagated through code calculations. SET data that is used to assess code models and correlations, is also used for input based uncertainty quantification.~~

RSI-4, RSI-9, RSI-10, RSI-13

~~The output phase of uncertainty accounts for the impact of uncertainties associated with the FoM output. For NRELAP5, applicable experimental data come from IET facilities designed to provide information on system behavior. Output phase uncertainty can be characterized by comparing measured IET data to NRELAP5 calculated values.~~

RSI-4, RSI-9, RSI-11, RSI-13

{{

RSI-4, RSI-9, RSI-11, RSI-13

RSI-4, RSI-9, RSI-13

}}2(a),(c),ECI

RSI-4, RSI-9, RSI-11, RSI-13

Table 10-1 {{ }}2(a),(c),ECI

{{			
			}}2(a),(c),ECI

Table 10-1 {{ }}2(a),(c),ECI (Continued)

	{{		
	}}2(a),(c),ECI		

RSI-4, RSI-9, RSI-13

10.2 NRELAP5 Code Uncertainty

RSI-4, RSI-9, RSI-10, RSI-11, RSI-13

{{

RSI-10

}}2(a),(c)

{{

RSI-10

RSI-10

RSI-10

RSI-10

RSI-10

RSI-10

RSI-10

RSI-4, RSI-9, RSI-10, RSI-13

RSI-4, RSI-9, RSI-10, RSI-13

RSI-10

RSI-10

}}2(a),(c)

RSI-4, RSI-9, RSI-10, RSI-11, RSI-13

2. {{

RSI-4, RSI-9, RSI-10, RSI-11, RSI-13

RSI-4, RSI-9, RSI-10, RSI-11, RSI-13

RSI-4, RSI-9, RSI-10, RSI-11, RSI-13

RSI-4, RSI-9, RSI-10, RSI-11, RSI-13

}}2(a),(c)

{{

RSI-4, RSI-9, RSI-10, RSI-11, RSI-13

Equation 10-1

RSI-4, RSI-9, RSI-10, RSI-11, RSI-13

Equation 10-2

RSI-4, RSI-9, RSI-10, RSI-11, RSI-13

Equation 10-3

RSI-4, RSI-9, RSI-10, RSI-11, RSI-13

}}2(a),(c)

{{

Equation 10-4

RSI-4, RSI-9, RSI-10, RSI-11, RSI-13

RSI-4, RSI-9, RSI-13

RSI-4, RSI-9, RSI-10, RSI-11, RSI-13

Equation 10-5

RSI-4, RSI-9, RSI-11, RSI-13

RSI-4, RSI-9, RSI-13

}}2(a),(c)

RSI-4, RSI-9, RSI-10, RSI-11, RSI-13

{{

Equation 10-6

RSI-4, RSI-9, RSI-10, RSI-11, RSI-13

RSI-4, RSI-9, RSI-10, RSI-11, RSI-13

RSI-4, RSI-9, RSI-10, RSI-11, RSI-13

RSI-4, RSI-9, RSI-13

RSI-4, RSI-9, RSI-10, RSI-11, RSI-13

RSI-4, RSI-9, RSI-10, RSI-11, RSI-13

}}2(a),(c)

{{

Equation 10-7

RSI-4, RSI-9, RSI-10, RSI-11, RSI-13

Equation 10-8

RSI-4, RSI-9, RSI-10, RSI-11, RSI-13

Equation 10-9

RSI-4, RSI-9, RSI-13

RSI-4, RSI-9, RSI-13

RSI-4, RSI-9, RSI-13

RSI-4, RSI-9, RSI-10, RSI-11, RSI-13

}}2(a),(c)

RSI-4, RSI-9, RSI-10, RSI-11, RSI-13

{{

RSI-4, RSI-9, RSI-10, RSI-11, RSI-13

RSI-4, RSI-9, RSI-13

RSI-4, RSI-9, RSI-13

RSI-4, RSI-9, RSI-13

Equation 10-10

RSI-4, RSI-9, RSI-13

}}2(a),(c)

RSI-4, RSI-9, RSI-11, RSI-13

Table 10-2 {{

}}2(a),(c)

{{

}}2(a),(c)

Table 10-2 {{ }}2(a),(c) (Continued)

{{

}}2(a),(c)

Table 10-2 {{ }}2(a),(c) (Continued)

	{{			
	}}2(a),(c)			

RSI-4, RSI-9, RSI-13

{{

}}2(a),(c)

RSI-4, RSI-9, RSI-11, RSI-13

The error in NRELAP5 DWO onset prediction is calculated using Equation 10-11.

$$\varepsilon = \frac{NRELAP5 - Data}{Data} \qquad \text{Equation 10-11}$$

Variable *NRELAP5* is the FW flow rate as predicted by NRELAP5 at DWO onset, and *Data* is the FW flow rate as measured by test facility at DWO onset.

RSI-4, RSI-9, RSI-13

Using the statistical methods described in previous key steps, NRELAP5 average error $\bar{x}$ and standard deviation of mean $\bar{u}$ are calculated. Assuming t-distribution and a 95 percent one-sided distribution and degrees of freedom of 35, the coverage factor is 1.69. The one-sided confidence interval value is calculated using Equation 10-12.

RSI-4, RSI-9, RSI-13

$$95\%\ \mathrm{CI}_t = \bar{x} - 1.69 \times \bar{u} \qquad \text{Equation 10-12}$$

A 95 percent confidence interval method is used for evaluating the NRELAP5 DWO onset prediction uncertainty. A 95 percent confidence interval error estimate (Equation 10-12) indicates that there is a 95 percent probability that the NRELAP5 error in predicting the DWO onset phenomena is within the error span.

RSI-4, RSI-9, RSI-11, RSI-13

5. Overall NRELAP5 Density Wave Oscillation Prediction Uncertainty

{{

RSI-4, RSI-9, RSI-11, RSI-13

RSI-4, RSI-9, RSI-11, RSI-13

}}2(a),(c),ECI

RSI-4, RSI-9, RSI-13

6. {{

RSI-4, RSI-9, RSI-13

RSI-4, RSI-9, RSI-13

}}2(a),(c)

RSI-4, RSI-9, RSI-13

{{

}}2(a),(c)

{{

}}2(a),(c)

RSI-10

10.3 Other High Ranked Phenomena Identification and Ranking Table Phenomena Not Considered in the Uncertainty Evaluation

10.3.1 {{ }}2(a),(c)

RSI-10

{{

RSI-4, RSI-9, RSI-10, RSI-11, RSI-13

}}2(a),(c)

RSI-10

10.3.2 {{ }}2(a),(c),ECI

{{

RSI-4, RSI-9, RSI-11, RSI-13

}}2(a),(c),ECI

RSI-10

Table 10-3 {{ }}2(a),(c),ECI

{{			}}2(a),(c),ECI

RSI-10

{{

}}2(a),(c),ECI

RSI-10

10.3.3 {{ }}2(a),(c),ECI

{{

RSI-10

}}2(a),(c),ECI

RSI-10

Figure 10-1 {{ }}2(a),(c),ECI

	{{	
	}}2(a),(c),ECI	

RSI-4, RSI-9, RSI-10, RSI-11, RSI-13

{{

}}2(a),(c),ECI

RSI-10

Figure 10-2 {{ }}2(a),(c),ECI

{{

}}2(a),(c),ECI

RSI-10

{{

}}2(a),(c),ECI

{{

}}2(a),(c)

RSI-10

10.3.4 {{ }}2(a),(c)

{{

}}2(a),(c)

RSI-10

Figure 10-3 {{ }}2(a),(c),ECI

{{

}}2(a),(c)

RSI-10

{{

}}2(a),(c)

RSI-10

10.3.5 {{ }}2(a),(c)

{{

RSI-10

}}2(a),(c),ECI

RSI-10

10.3.6 {{ }}2(a),(c),ECI

{{

RSI-10

}}2(a),(c),ECI

- {{

}}2(a),(c),ECI

RSI-10

Table 10-4 {{

}}2(a),(c),ECI

	{{				
				}}2(a),(c),ECI	

RSI-10

{{

}}2(a),(c),ECI

RSI-10

Figure 10-4 {{

}}2(a),(c),ECI

{{

}}2(a),(c),ECI

RSI-10

{{

}}2(a),(c),ECI

RSI-10

Figure 10-5 {{

}}2(a),(c),ECI

{{

}}2(a),(c),ECI

RSI-10

{{

}}2(a),(c),ECI

RSI-10

Figure 10-6 {{

}}2(a),(c),ECI

{{

}}2(a),(c),ECI

RSI-10

{{

}}2(a),(c),ECI

RSI-10

Table 10-5 {{

}}2(a),(c),ECI

{{

}}2(a),(c),ECI

RSI-10

Figure 10-7 {{ }}2(a),(c),ECI

{{

}}2(a),(c),ECI

RSI-10

{{

}}2(a),(c),ECI

RSI-10

Figure 10-8 {{ }}2(a),(c),ECI

{{

}}2(a),(c),ECI

RSI-10

Figure 10-9 {{ }}2(a),(c),ECI

{{ }}2(a),(c),ECI

RSI-10

{{ }}2(a),(c),ECI

{{

}}2(a),(c),ECI

RSI-10

10.3.7 {{ **}}2(a),(c),ECI**

{{

RSI-4, RSI-9, RSI-10, RSI-11, RSI-13

RSI-4, RSI-9, RSI-10, RSI-11, RSI-13

}}2(a),(c),ECI

RSI-4, RSI-9, RSI-10, RSI-11, RSI-13

10.3.8 {{ **}}2(a),(c),ECI**

{{

}}2(a),(c),ECI

RSI-10

10.3.9 {{ **}}2(a),(c)**

{{

}}2(a),(c)

{{

}}2(a),(c)

RSI-4, RSI-9, RSI-13

10.4 ~~NPM Operation Margin~~Methodology for Density Wave Oscillation Analysis~~Onset~~

RSI-4, RSI-9, RSI-11, RSI-13

{{

RSI-4, RSI-9, RSI-13

RSI-4, RSI-9, RSI-11, RSI-13

RSI-4, RSI-9, RSI-11, RSI-13

}}2(a),(c)

{{

}}2(a),(c)

RSI-4, RSI-9, RSI-11, RSI-13

Table 10-6 {{ }}2(a),(c)

{{

}}2(a),(c)

Table 10-6 {{ }}2(a),(c) (Continued)

	{{			
	}}2(a),(c)			

RSI-4, RSI-9, RSI-11, RSI-13

10.4.1 {{ }}2(a),(c)

RSI-4, RSI-9, RSI-11, RSI-13

{{

RSI-4, RSI-9, RSI-11, RSI-13

}}2(a),(c)

{{

RSI-4, RSI-9, RSI-11, RSI-13

RSI-4, RSI-9, RSI-11, RSI-13

Equation 10-13

RSI-4, RSI-9, RSI-11, RSI-13

RSI-4, RSI-9, RSI-11, RSI-13

Equation 10-14

}}2(a),(c)

}}2(a),(c)

}}2(a),(c)

RSI-4, RSI-9, RSI-13

Figure 10-10 {{

{{

RSI-4, RSI-9, RSI-13

~~For evaluating NPM operating margin for DWO onset, sensitivity analysis is used. The sources of uncertainty for the NPM full-plant calculation with respect to DWO are identified. Effects of these uncertainty parameters on DWO are evaluated using IETs/SETs, plant design conditions, operating conditions, design basis safety analysis assumptions/limits, and literature.~~

RSI-4, RSI-9, RSI-13

~~{{~~

RSI-4, RSI-9, RSI-13

~~}}2(a),(c)~~

RSI-4, RSI-9, RSI-13

~~The methodology for calculating margin for DWO involves accounting for uncertainties in different geometric parameters and operating conditions. Sensitivity analysis is carried out accounting for uncertainties in margin calculation.~~

RSI-4, RSI-9, RSI-13

~~The methodology for calculating margin identified important uncertainty contributors for DWO. These contributors are derived from the SG stability PIRT, code validation, NPM~~

~~operating parameters, and safety analysis limits/assumptions. The uncertainty contributors are divided into three categories – analytical uncertainties/T-H model and correlation uncertainties; geometrical uncertainties; and the plant conditions uncertainties. These parameters are varied in a parametric evaluation to ensure that uncertainties are adequately addressed in the evaluation of margin.~~

RSI-4, RSI-9, RSI-13

~~{{~~

RSI-4, RSI-9, RSI-13

RSI-4, RSI-9, RSI-13

RSI-4, RSI-9, RSI-13

~~}}2(a),(c)~~

{{

RSI-4, RSI-9, RSI-13

RSI-4, RSI-9, RSI-13

RSI-4, RSI-9, RSI-13

RSI-4, RSI-9, RSI-13

}}2(a),(c)

RSI-4, RSI-9, RSI-13

Table 10-7 ~~NPM Sensitivity Cases at Off-Normal Conditions for DWO Evaluation~~

	{{							}}~~2(a),(c)~~

RSI-4, RSI-9, RSI-13

~~{{~~

RSI-4, RSI-9, RSI-13

~~}}2(a),(c)~~

{{

}}2(a),(c)

Response to Request for Additional Information
Docket: 99902078

RAI No.: RSI
Date of RAI Issue: 03/27/2023

NRC Question No.: RSI-14

The Chapter 15 transient and accident analyses do not reflect all the design changes for the SDAA. Based on the input decks provided via optical storage media, the updated IFR design loss coefficient is not reflected in the NRELAP input files used to calculate the plant response. The IFR impacts onset of DWO, initial conditions, natural circulation, heat transfer, and response to the design basis events analyzed.

NuScale Response:

Response Summary:

The NRELAP5 basemodel for the Chapter 15 analyses uses a loss coefficient (K_{inlet}) of {{ }}$^{2(a),(c),ECI}$ for the steam generator (SG) tube inlet flow restrictor (IFR). The topical report "Methodology for the Determination of the Onset of Density Wave Oscillations (DWO)," TR-131981-P, describes evaluation of a minimum IFR K_{inlet} of {{ }}$^{2(a),(c),ECI}$, but does not establish a specific nominal value. The value of K_{inlet} used in the Chapter 15 input files is appropriate because:

- the value is greater than the expected minimum design value,
- the value is a reasonable estimate of the nominal value based on available design information, and
- the value has a negligible impact on Chapter 15 design-basis event initial conditions and event progressions.

Detailed Response:

Topical report "Methodology for the Determination of the Onset of Density Wave Oscillations (DWO)," TR-131981-P, Section 3.1 identifies that an SG tube IFR is a design feature that can be used to mitigate DWO. The topical report provides a methodology by which the onset of DWO can be predicted. This methodology then allows for verification of the adequacy of an SG tube IFR design to perform its intended function.

An IFR creates a single-phase liquid pressure drop in an SG tube. {{

}}2(a),(c)

Appendix B of the topical report provides sample calculations using the topical report methodology. Section B.4 studies the impact of the IFR K_{inlet} on DWO stability calculations. {{

}}2(a),(c),ECI Section B.4 is revised to clarify the discussion regarding the value of IFR K_{inlet}. Based on the sensitivity and other supporting work during development of the DWO topical report, the K_{inlet} of {{

}}2(a),(c),ECI

As indicated in this question, the IFR K_{inlet} may also impact initial conditions and the transient response to design-basis events analyzed in Chapter 15. The NRELAP5 calculations associated with Chapter 15 use a K_{inlet} of {{ }}2(a),(c),ECI. A detailed value for the nominal IFR K_{inlet} has not been established. The NRELAP5 input files are consistent with the currently available design information on the IFR. However, this request for supplemental information (RSI) raises the question of whether the selection of the IFR K_{inlet} input value based on DWO considerations (described above) is appropriate for the Chapter 15 analyses. For example, {{

}}2(a),(c),ECI The remainder of this response demonstrates that the impact of the IFR K_{inlet} on Chapter 15 analyses is negligible.

Qualitative Assessment of Impact of IFR K_{inlet}

As described previously, an IFR creates a single-phase liquid pressure drop in an SG tube. {{

}}$^{2(a),(c)}$ The qualitative explanation of the minimal impact of the IFR K_{inlet} value is supplemented by quantitative sensitivity studies in the following sections.

Quantitative Assessment of Impact of IFR K_{inlet} on Steady-State Conditions

Initial conditions and transient progression of a representative Chapter 15 design-basis event, the loss of normal feedwater flow in final safety analysis report (FSAR) Section 15.2.7, are examined for a range of IFR K_{inlet} values from {{

}}$^{2(a),(c),ECI}$

A loss of normal feedwater flow case that does not result in immediate reactor trip is selected as the base case to allow for differences, if any, to be observed in the period prior to reactor trip. The sensitivity results are examined for impact on the steady-state conditions achieved as part of initialization and for the transient response.

Table 1 shows the cases analyzed and the IFR K_{inlet} value applied for each case. {{

}}$^{2(a),(c)}$ The primary and secondary steady-state conditions achieved during initialization of the cases are shown in Figure 1 through Figure 10. {{

}}$^{2(a),(c)}$ The sensitivity study results confirm that, even over a wide range, the IFR K_{inlet} value has no impact on steady-state initial conditions, {{

}}$^{2(a),(c)}$

Table 1:
Steam Generator Inlet Flow Restrictor Steady-State Sensitivity Cases
and Initialized Feedwater Pressure Results

{{

}}2(a),(c),ECI

{{

}}2(a),(c)

Figure 1:
Steam Generator Tube Inlet Flow Restrictor Sensitivity Study for Loss of Feedwater Event
Steady-State Initialization Results – Core Power

{{

}}2(a),(c)

Figure 2:
Steam Generator Tube Inlet Flow Restrictor Sensitivity Study for Loss of Feedwater Event
Steady-State Initialization Results – Reactor Coolant System Flow

{{

}}2(a),(c)

Figure 3:
Steam Generator Tube Inlet Flow Restrictor Sensitivity Study for Loss of Feedwater Event
Steady-State Initialization Results – Reactor Coolant System Average Temperature

{{

}}2(a),(c)

Figure 4:
Steam Generator Tube Inlet Flow Restrictor Sensitivity Study for Loss of Feedwater Event
Steady-State Initialization Results – Pressurizer Pressure

{{

}}2(a),(c)

Figure 5:
Steam Generator Tube Inlet Flow Restrictor Sensitivity Study for Loss of Feedwater Event
Steady-State Initialization Results – Pressurizer Level

{{

}}2(a),(c)

Figure 6:
Steam Generator Tube Inlet Flow Restrictor Sensitivity Study for Loss of Feedwater Event
Steady-State Initialization Results – Steam Generator Pressure (one of two SGs)

{{

}}2(a),(c)

Figure 7:
Steam Generator Tube Inlet Flow Restrictor Sensitivity Study for Loss of Feedwater Event
Steady-State Initialization Results – Feedwater Flow

{{

}}2(a),(c)

Figure 8:
Steam Generator Tube Inlet Flow Restrictor Sensitivity Study for Loss of Feedwater Event
Steady-State Initialization Results – Feedwater Plenum Pressure (one of two SGs)

{{

}}2(a),(c)

Figure 9:
Steam Generator Tube Inlet Flow Restrictor Sensitivity Study for Loss of Feedwater Event
Steady-State Initialization Results – Steam Generator Level (one of two SGs)

{{

}}2(a),(c)

Figure 10:
Steam Generator Tube Inlet Flow Restrictor Sensitivity Study for Loss of Feedwater Event
Steady-State Initialization Results – Steam Generator Superheat (one of two SGs)

Quantitative Assessment of Impact of IFR K_{inlet} on Transient Conditions

The sensitivity results are also examined for impact on the transient response to a loss of feedwater flow. The range of IFR K_{inlet} values considered is the same as in the steady-state initialization described above. For the transient cases, {{

}}[2(a),(c)] Table 2 provides the cases analyzed and the IFR K_{inlet} values applied for each case. Table 2 also provides key transient results for each case. {{

}}[2(a),(c)]

Transient plots for primary and secondary conditions are shown in Figure 11 through Figure 21. {{

}}[2(a),(c)] The effects of the IFR K_{inlet} value on longer-term DHRS operation and conditions is further analyzed in separate sensitivity studies described later in this response. Overall, the sensitivity study results shown here confirm that,

even over a wide range, IFR K_{inlet} value has no impact on the transient response to a representative design-basis event.

Table 2:
Steam Generator Inlet Flow Restrictor Loss of Feedwater Event Transient Sensitivity Cases and Results

{{

}}2(a),(c),ECI

{{

}}2(a),(c)

Figure 11:
Steam Generator Tube Inlet Flow Restrictor Sensitivity Study for Loss of Feedwater Event
Transient Results – Core Power

{{

}}2(a),(c)

Figure 12:
Steam Generator Tube Inlet Flow Restrictor Sensitivity Study for Loss of Feedwater Event
Transient Results – Reactor Coolant System Flow

{{

}}2(a),(c)

Figure 13:
Steam Generator Tube Inlet Flow Restrictor Sensitivity Study for Loss of Feedwater Event Transient Results – Reactor Coolant System Average Temperature

{{

}}2(a),(c)

Figure 14:
Steam Generator Tube Inlet Flow Restrictor Sensitivity Study for Loss of Feedwater Event
Transient Results – Pressurizer Pressure

{{

}}2(a),(c)

Figure 15:
Steam Generator Tube Inlet Flow Restrictor Sensitivity Study for Loss of Feedwater Event Transient Results – Pressurizer Level

{{

}}2(a),(c)

Figure 16:
Steam Generator Tube Inlet Flow Restrictor Sensitivity Study for Loss of Feedwater Event
Transient Results – Steam Generator Pressure (one of two SGs)

{{

}}2(a),(c)

Figure 17:
Steam Generator Tube Inlet Flow Restrictor Sensitivity Study for Loss of Feedwater Event
Transient Results – Feedwater Flow

{{

}}2(a),(c)

Figure 18:
Steam Generator Tube Inlet Flow Restrictor Sensitivity Study for Loss of Feedwater Event
Transient Results – Feedwater Plenum Pressure (one of two SGs)

{{

}}2(a),(c)

Figure 19:
Steam Generator Tube Inlet Flow Restrictor Sensitivity Study for Loss of Feedwater Event
Transient Results – Steam Generator Level (one of two SGs)

{{

}}2(a),(c)

Figure 20:
Steam Generator Tube Inlet Flow Restrictor Sensitivity Study for Loss of Feedwater Event Transient Results – Steam Generator Superheat (one of two SGs)

{{

}}2(a),(c)

Figure 21:
Steam Generator Tube Inlet Flow Restrictor Sensitivity Study for Loss of Feedwater Event Transient Results – Decay Heat Removal System Flow (one of two trains)

Quantitative Assessments of Impact of IFR K_{inlet} on Decay Heat Removal System Operation

The sensitivity results demonstrate that the IFR K_{inlet} value does not affect the steady-state conditions or NuScale Power Module (NPM) response to a transient. After reactor trip, power decreases rapidly to decay heat levels which then gradually decrease over time. If normal heat removal through the secondary side is not available, the DHRS is actuated to remove heat from the NPM to the ultimate heat sink. The effect of the IFR K_{inlet} value on the transient progression after the actuation of DHRS is considered further here.

First, the differences between normal operating conditions and SG/DHRS operating conditions relevant to the IFR K_{inlet} value impact are discussed. During normal operating conditions, feedwater pumps supply feedwater to the SGs under forced flow conditions. Steam is transferred to the main steam piping and to the turbine generator before it is condensed in the feedwater system and recirculated. The IFRs provide a high resistance orifice at the inlet to the SG tubes, {{ }}$^{2(a),(c)}$ In contrast, during SG/DHRS operation, the secondary side loop operates in a boiling/condensing natural circulation mode. The driving force for the loop is the hydrostatic head of liquid in the DHRS condenser tubes. Liquid mass flow rates are low compared to normal operating conditions, and will decrease as decay heat levels decrease during the transient progression. {{

}}$^{2(a),(c)}$

- {{

}}$^{2(a),(c),ECI}$

As part of the non-LOCA evaluation model development, scaling analyses are performed for the NPM and NIST-2 SG/DHRS loops. The scaling analysis, ER-126485, is provided in the electronic reading room (eRR) as part of the response to Standard Design Approval Application (SDAA) audit question A-NonLOCA.LTR-3. Figure 4-17 of ER-126485, which is reproduced as Figure 22 in this response, {{

}}$^{2(a),(c),ECI}$

{{

}}2(a),(c),ECI

{{

}}2(a),(c),ECI

Figure 22:
Normalized Time-Averaged Π Groups for DHRS Momentum Balance

{{ }}2(a),(c),ECI

where: {{

}}2(a),(c),ECI

Sensitivity calculations are also performed to assess the effect of the IFR K_{inlet} value on the long-term DHRS heat transfer capacity. A set of sensitivity calculations is performed {{

}}$^{2(a),(c)}$ to assess the steady-state DHRS heat transfer rate in response to varying parameters of interest. The IFR K_{inlet} values are varied {{

}}$^{2(a),(c),ECI}$

Another set of sensitivity calculations is performed {{ }}$^{2(a),(c)}$ to assess DHRS performance, as in FSAR Figures 5.4-9 and 5.4-10. The response to a turbine trip without bypass transient is assessed for 36 hours, with nominal DHRS operating conditions, two active DHRS trains, and a range of IFR K_{inlet} values from {{ }}$^{2(a),(c),ECI}$ The results are shown in Figure 23 through Figure 34. {{

}}$^{2(a),(c)}$

These sensitivity results to the long-term DHRS response, along with the earlier sensitivity results to the transient response, demonstrate that overall transient behavior is not affected by a wide range of IFR K_{inlet} values.

{{

}}2(a),(c),ECI

Figure 23:
Effect of Inlet Flow Restrictor K_{inlet} on Decay Heat Removal System Performance
Primary Temperature

{{

}}2(a),(c),ECI

Figure 24:
Effect of Inlet Flow Restrictor K_{inlet} on Decay Heat Removal System Performance
Primary Temperature – zoomed-in

{{

}}2(a),(c),ECI

Figure 25:
Effect of Inlet Flow Restrictor K_{inlet} on Decay Heat Removal System Performance
Primary Flow Rate

{{

}}2(a),(c),ECI

Figure 26:
Effect of Inlet Flow Restrictor K_{inlet} on Decay Heat Removal System Performance
Primary Flow Rate – zoomed-in

{{

}}2(a),(c),ECI

Figure 27:
Effect of Inlet Flow Restrictor K_{inlet} on Decay Heat Removal System Performance
Pressurizer Level

{{

}}2(a),(c),ECI

Figure 28:
Effect of Inlet Flow Restrictor K_{inlet} on Decay Heat Removal System Performance
Pressurizer Level – zoomed-in

{{

}}2(a),(c),ECI

Figure 29:
Effect of Inlet Flow Restrictor K_{inlet} on Decay Heat Removal System Performance
Main Steam Pressure

{{

}}2(a),(c),ECI

Figure 30:
Effect of Inlet Flow Restrictor K_{inlet} on Decay Heat Removal System Performance
Feedwater Pressure

{{

}}2(a),(c),ECI

Figure 31:
Effect of Inlet Flow Restrictor K_{inlet} on Decay Heat Removal System Performance
Decay Heat Removal System Power (one train)

{{

}}2(a),(c),ECI

Figure 32:
Effect of Inlet Flow Restrictor K_{inlet} on Decay Heat Removal System Performance
Pressurizer Pressure

{{

}}2(a),(c),ECI

Figure 33:
Effect of Inlet Flow Restrictor K_{inlet} on Decay Heat Removal System Performance
Pressurizer Pressure – zoomed-in

{{

}}2(a),(c),ECI

Figure 34:
Effect of Inlet Flow Restrictor K_{inlet} on Decay Heat Removal System Performance
Level Above Top of Active Fuel

Summary of Technical Justification

Based on the qualitative discussions, the scaling analyses, and the results of various sensitivity studies, the IFR K_{inlet} value is not a parameter that measurably affects Chapter 15 safety analysis initial conditions, natural circulation, heat transfer, DHRS performance, or the overall response to design-basis events. Similar to other input parameters whose impact is negligible, the specific value selected in the NRELAP5 may be a nominal value without bias. Considering these factors, the K_{inlet} of {{ }}$^{2(a),(c),ECI}$ used in the NRELAP5 basemodel for the Chapter 15 analyses is reasonable. Therefore, the NRELAP5 files for the Chapter 15 analyses do adequately consider the IFR design. No changes to the SDAA FSAR are required.

Consistent with the above response, the topical reports associated with Chapter 15 are revised to describe the modeling of the IFR loss as follows:

- Non-loss-of-coolant accident (LOCA) topical report TR-0516-49416-P – Section 6.1.4.2 is revised as shown in the attached markups.
- LOCA topical report TR-0516-49422-P – Section 5.1.3 is revised as shown in the attached markups.
- Extended passive cooling (XPC) topical report TR-124587-P – Section 5.2.1 describes that the emergency core cooling system (ECCS) long-term cooling model is based on the LOCA basemodel and then only identifies changes to the basemodel. The treatment of the IFR K_{inlet} value in the ECCS long-term cooling model is not changed from the LOCA basemodel treatment of the IFR loss. Therefore, the changes to Section 5.1.3 of the LOCA topical report are adequate to address the topic without further explicit discussion in the XPC topical report. Similarly, Section 5.2.1 describes that extended DHRS calculations use the non-LOCA model. Therefore, the changes to Section 6.1.4.2 of the non-LOCA topical report are adequate to address the topic without further explicit discussion in the XPC topical report.

The DWO topical report TR-131981-P Section B.4 discussion of the IFR K_{inlet} values is also revised for clarity as previously described.

Impact on US460 SDA:

There are no impacts to US460 SDA as a result of this response.

Additional Information:

Topical reports TR-0516-49416, Non-Loss-of-Coolant Accident Analysis Methodology, TR-131981, Methodology for the Determination of the Onset of Density Wave Oscillations (DWO), and TR-0516-49422, Loss-of-Coolant Accident Evaluation Model, are revised as described in the response above and as shown in the markups provided in this response.

B.3 Boundary Conditions

RSI-14

The primary-side fluid boundary conditions applied to the NPM-20 ~~SG~~ DWO model includes the primary-side hot temperature, the primary-side pressure, and the primary mass flow rate. {{

}}2(a),(c)

RSI-14

The secondary-side fluid boundary conditions applied to the NPM-20 ~~SG~~ DWO model includes the FW temperature, the FW mass flow rate, and the steam pressure. {{

}}2(a),(c)

RSI-14

Table B-1 lists the steady-state boundary and initial conditions applied to the DWO model.

RSI-14

Table B-1 {{

}}2(a),(c)

{{

}}2(a),(c)

RSI-14

B.4 ~~IFR K_{inlet} Loss~~Inlet Flow Restrictor Loss Coefficient Selection

RSI-14

The ~~SG~~ IFR is a restricting orifice designed to induce a large pressure drop as the subcooled fluid enters the HCSG tube from the FW plenum. If the IFR pressure drop is

sufficiently sized, DWO is prevented and secondary-side stability is maintained. The K_{inlet} ~~loss~~ of the IFR is ~~therefore~~ a crucial component of secondary-side stability.

RSI 14

The NPM-20 ~~SG~~ IFR is a thick orifice, with a {{

RSI 14

RSI 14

RSI-14

RSI 14

}}2(a),(c),ECI

phase change process in the lower region of the tubes. For non-LOCA transient calculations, finer nodalization is not needed near the tube exits due to the state of the fluid being single phase vapor. Section 5.3.5.4 summarizes SG nodalization sensitivity calculations. Based on these studies, modeling the helical coil SG with {{ }}2(a),(c) nodes is expected to produce reasonably accurate results for the non-LOCA transients. Should additional detail be needed in the future, the relevant benchmarks, sensitivity studies, and transient analyses will be reviewed for continued applicability and updated as necessary to demonstrate the higher level of detail for the component is applicable to an NPM.

{{

}}2(a),(c)

RSI 14

For an NPM design that includes an SG tube inlet flow restrictor, {{

}}2(a),(c)

The tube-to-coil diameter ratio is specific to the SG geometry. {{

}}2(a),(c)

RSI 14

For an NPM design that includes an SG tube inlet flow restrictor, {{

}}2(a),(c)

5.1.4 Containment Vessel and Reactor Pool

{{

}}2(a),(c)

Response to Request for Additional Information
Docket: 99902078

RAI No.: RSI
Date of RAI Issue: 03/27/2023

NRC Question No.: RSI-15

Impact of steam generator density wave oscillations and potential flow instability in DHRS loop: Sections 5.4.3, nearly all Chapter 15 sections, and the LOCA, non-LOCA and XPC LTRs are missing analyses and methodologies for the potential impact of steam generator density wave oscillations on DHRS performance when power is below 20% full power. These sections and LTRs are also missing evaluations of the potential impact on DHRS performance from potential flow instability in the loop from multiple phenomena (due to density wave oscillations or other phenomena such as Ledinegg instability, geysering, manometer oscillations, etc) when reactor power is below 20% (such as during the 72 hours following a design basis event). The DWO LTR only covers the methodology to detect the on-set of DWO for steady state and off-normal power levels between 20-100% power. The DWO LTR recognizes that two-phase flow oscillation can occur in the steam generator tube side when the reactor power is below 20% of the rated power, but does not include an evaluation of the potential impacts on DHRS performance. The proposed SDA design relies on the decay heat removal system (DHRS) to remove the heat from the primary system during anticipated operational occurrences. When the steam generator and the coupled DHRS are activated during an event, the steam generator secondary side fluid flow is potentially subject to two-phase instability. The new IFR design increases the flow loss coefficient and is expected to impact the DHRS recirculation flow rate and heat removal capacity. Further, flow instability due to other phenomena are also not evaluated. The heat transferred by DHRS is dependent on whether oscillations occur. The characterization of the DHRS heat transfer (as described in the non-LOCA LTR) is based on a single NIST-2 test that was not specifically designed or setup to measure oscillations in the SG nor cover all the conditions that may experience SG oscillations. The non-LOCA topical report acknowledges some instability phenomena, but is missing PIRT analysis. {{

}}$^{2(a),(c)}$

{{

}}[2(a),(c)] Further, no methodology has been included to evaluate the potential impact of flow instability on the DHRS gravity driven discharge line flow.

NuScale Response:

Response Summary:

This request for supplemental information (RSI) is focused on the impacts on transient analyses from potential secondary side component-level and system-level instabilities when reactor power is below 20 percent. The premise of the RSI is that the impacts are significant. This response demonstrates that the impacts of potential secondary side instabilities are not significant on key safety analysis figures of merit addressed in the final safety analysis report (FSAR) Chapter 15 sections, and the loss of coolant accident (LOCA), non-LOCA and extended passive cooling (XPC) topical reports. The technical justification for this conclusion is based on comparison of test data for different secondary side conditions, comparison of test data to code (NRELAP5) simulations, and NRELAP5 sensitivity studies. Oscillatory behavior that may occur in the secondary side does not meaningfully impact the plant conditions that are used to assess relevant acceptance criteria. Additional modeling or special treatment of oscillatory behavior beyond that already included in the safety analysis methodology topical reports is not required to ensure the adequacy of the safety analyses.

Detailed Response:

The focus of this RSI is on the impacts on transient analyses from potential secondary side component-level and system-level instabilities, from phenomena such as density wave oscillation (DWO), when reactor power is below 20 percent. The response to RSI 16 addresses a similar concern, but for higher power levels. There are two types of transient behavior that occur below 20 percent power: (1) the behavior of transients that are initiated from at or below 20 percent power and (2) the behavior of transients following reactor trip where power levels are driven by decay heat and are less than 20 percent. Each of these types of transient behavior below 20 percent power are addressed as follows.

Assessment of Behavior of Events Initiated from Low Power Levels

The US460 standard design approval application (SDAA) FSAR Section 15.0.0.1 states that "Design-basis analyses consider the range of power operation because events from a low-power or zero-power state could be more limiting than from full-power conditions." Most of the transient and accident analyses in Chapter 15 are initiated from high power levels. For example, many Chapter 15 analyses use an initial power of 102 percent, corresponding to the rated thermal power level plus measurement uncertainty. The reason that the analyses are initiated from high power levels is that those cases typically result in the limiting values for comparison to the acceptance criteria used in Chapter 15. There is a small subset of Chapter 15 design-basis events that have the potential to be limiting for acceptance criteria when initiated from lower power levels and are therefore explicitly analyzed at lower power levels:

- Section 15.1.5 – steam piping failures inside and outside containment
- Section 15.4.1 – uncontrolled control rod assembly withdrawal from a subcritical or lower power startup condition
- Section 15.4.2 – uncontrolled control rod assembly withdrawal at power
- Section 15.4.3 – withdrawal of a single control rod assembly
- Section 15.4.6 – inadvertent decrease in boron concentration in the reactor coolant system
- Section 15.4.8 – spectrum of rod ejection accidents
- Section 15.6.2 – failure of small lines carrying primary coolant outside containment

For non-LOCA transient events, {{

}}[2(a),(c)] The following event-specific descriptions are provided to add context as to the possibility of instabilities to decrease MCHFR or reduce margin to other acceptance criteria specifically for the events evaluated at or below 20 percent initial power level.

As described in FSAR Section 15.1.5.1, a spectrum of steam line break (SLB) locations with varied core and plant conditions are analyzed to determine the scenarios with the most severe results. However, the SLB analyses, described in Section 15.1.5.3.2, identify that the limiting reactor coolant system (RCS) pressure, limiting SG pressure, and limiting MCHFR occur when

initiated from 102 percent power. An SLB results in a large increase in steam flow until the main steam isolation valves close or the affected SG is completely depressurized. The increased steam flow increases primary-to-secondary heat transfer and results in overcooling. A potential secondary side instability will tend to decrease steam generator efficiency resulting in a small decrease in heat transfer and a negligible or beneficial impact on the transient, regardless of initial power level. {{

}}2(a),(c),ECI

Similarly, NPM sensitivity calculation results presented in RSI 16 demonstrate the negligible or beneficial effect of such a heat transfer reduction on transients initiated at full power conditions.

Consideration of secondary side instabilities would therefore not alter the fact that high power cases are limiting for RCS pressure, SG pressure, and MCHFR. Section 15.1.5.1 also identifies that the containment pressure is evaluated in FSAR Section 6.2, including consideration of SLBs that occur inside containment. The containment analyses supporting Section 6.2 show that: (1) SLBs inside containment are bounded by other events for maximum containment pressure and temperature results and (2) initiation from higher powers maximizes the mass and energy release from the primary side and results in a limiting containment response. For example, Figure 1 provides representative containment pressure results comparing the containment response at hot full power to hot zero power for a LOCA. {{

}}2(a),(c) secondary line breaks from low power conditions do not challenge containment pressure and temperature limits. In conclusion, it is not necessary to explicitly address secondary side instabilities for SLBs initiating from powers at or below 20 percent.

{{

}}2(a),(c)

Figure 1:
Containment Pressure Response Sensitivity for Initial Power Level
Loss of Coolant Accident, 100% and 10% Discharge Line Breaks

where:
{{

}}2(a),(c)

As described in FSAR Section 15.4.1.3.2, the uncontrolled control rod assembly withdrawal from a subcritical or lower power startup condition analyses consider a range of initial powers below 15 percent. The methodology associated with the analysis of this event is provided in Section 7.2.13 of the non-LOCA topical report (TR-0516-49416-P, Rev. 4). Tables 7-58 and 7-59 of the non-LOCA topical report identify that the acceptance criteria for this event are MCHFR and fuel centerline temperature. Table 7-60 identifies that secondary side parameters for nominal SG pressure and nominal SG heat transfer are modeled {{

}}[2(a),(c)] Therefore, changes to the heat transfer performance of the SG, caused by potential instabilities, have no impact on the margin to acceptance criteria. In addition, the results for this event, shown in FSAR Table 15.4-3, are less limiting than the results for the same event initiated from higher powers, shown in FSAR Table 15.4-7. In conclusion, it is not necessary to explicitly address secondary side instabilities for uncontrolled control rod assembly withdrawals initiating from powers at or below 20 percent.

As described in FSAR Section 15.4.2.3.2, the uncontrolled control rod assembly withdrawal at power analyses consider a range of initial powers above 15 percent (i.e., it includes some cases below 20 percent power). The methodology associated with the analysis of this event is provided in Section 7.2.14 of the non-LOCA topical report. Tables 7-62 and 7-63 of the non-LOCA topical report identify that the acceptance criteria for this event are MCHFR and fuel centerline temperature. Table 7-64 identifies that secondary side parameters for nominal SG pressure and nominal SG heat transfer are modeled {{

}}[2(a),(c)] Therefore, changes to the heat transfer performance of the SG, caused by potential instabilities, have no impact on the margin to acceptance criteria. In addition, the results for this event identify that the cases below 20 percent power are less limiting than the results for higher powers. The limiting results, shown in FSAR Table 15.4-7, occur for cases initiated from full power. In conclusion, it is not necessary to explicitly address secondary side instabilities for uncontrolled control rod assembly withdrawals initiating from powers at or below 20 percent.

As described in FSAR Section 15.4.3.4.2, the single control rod assembly withdrawal analyses consider a range of initial powers including 20 percent. The methodology associated with the analysis of this event is provided in Section 7.2.15 of the non-LOCA topical report. Tables 7-66 and 7-67 of the non-LOCA topical report identify that the acceptance criteria for this event are MCHFR and fuel centerline temperature. Table 7-68 identifies that secondary side parameters for nominal SG pressure and nominal SG heat transfer are modeled {{

}}[2(a),(c)] Therefore, changes to the heat transfer performance of the SG, caused by potential instabilities, have no impact on the margin to acceptance criteria. In addition, the results for this event identify that the cases at 20 percent power are less limiting than the results for higher powers. The limiting results, shown in FSAR Table 15.4-11, occur for cases initiated from above 20 percent power. In conclusion, it is not necessary to explicitly address secondary side instabilities for single control rod assembly withdrawals initiating from powers at or below 20 percent.

As described in FSAR Section 15.4.6.3.2, the inadvertent decrease in boron concentration in the reactor coolant system analyses consider a range of initial powers including hot zero power. The analyses are performed using hand calculations to determine the time for shutdown margin to be lost. In these hand calculations, the secondary side is not modeled and there is no direct impact of potential secondary side instabilities. Hand calculations are performed with two different mixing models: perfect mixing and wavefront transport. Equation 7-1 of the non-LOCA topical report shows that the perfect mixing model is not affected by the secondary side. Equation 7-3 of the non-LOCA topical report shows that the wavefront model is a function of the RCS primary flow rate. As discussed in the response to RSI 16, {{

}}[2(a),(c)] Because the average flow rate remains constant, the time calculated for shutdown margin to be lost in the wavefront model calculation is not affected. NRELAP5 calculations evaluate the reactor trip timing due to the reactivity insertion from the boron dilution. As discussed in the response to RSI 16, sensitivity calculations show that {{

}}[2(a),(c)] predicted by NRELAP5 would result in additional shutdown margin compared to the FSAR results. Other acceptance criteria, such as MCHFR and fuel centerline temperature are bounded by the uncontrolled control rod assembly withdrawal events in FSAR Sections 15.4.1 and 15.4.2. The impact of potential secondary side instabilities for those events at

powers at or below 20 percent is dispositioned above. In conclusion, it is not necessary to explicitly address secondary side instabilities for inadvertent decreases in boron concentration in the reactor coolant system initiating from powers at or below 20 percent.

As described in FSAR Section 15.4.8.3.2, the spectrum of rod ejection accident analyses consider a range of initial powers including hot zero power and 20 percent power. For high rod worths and end of cycle conditions at these low powers, the rod ejection results in a significant power increase (i.e., a power pulse). The power pulse is mitigated primarily by Doppler feedback and subsequently by reactor trip. The duration of the event prior to reactor trip is a few seconds (FSAR Figure 15.4-18). This short duration of the accident does not allow the secondary side to influence the transient response. For low rod worths or early in cycle conditions at these low powers, the rod ejection may result in only a small increase in power that does not result in reactor trip. Doppler feedback mitigates the small increase and power subsequently remains low. For example, FSAR Table 15.4-20 identifies that the rod ejection from zero power at middle of cycle remains below the high power trip setpoint relevant to this initial power. Because of the initial low power and only minor transient increase in power, these cases are not limiting for any acceptance criteria. In conclusion, it is not necessary to explicitly address secondary side instabilities for rod ejection accidents initiating from powers at or below 20 percent.

As described in FSAR Section 15.6.2.1, the failure of small lines carrying primary coolant outside containment analyses consider a spectrum of break sizes and locations, but not powers. The cases described in FSAR Section 15.6.2 are all full power cases. {{

}}[2(a),(c)] In conclusion, it is not necessary to explicitly address secondary side instabilities for small line breaks initiating from powers at or below 20 percent.

The majority of Chapter 15 events are initiated from high power levels because the higher power levels result in limiting margin to acceptance criteria. Effects of SG oscillations on such events initiated at low power would not challenge margin to acceptance criteria. Effects of SG oscillations on events at high power levels is addressed in the response to RSI 16. For each of the events that are initiated from low power, discussed separately above, secondary side

instability is not a significant consideration. Therefore, the remainder of this response will address the behavior of transients following reactor trip where power levels are driven by decay heat and are less than 20 percent.

Qualitative Assessments of Behavior of Events Post-Trip at Decay Heat Power Levels

The US460 design includes a variety of module protection system (MPS) setpoints to actuate reactor trip and other features, such as decay heat removal system (DHRS). Analytical limits used for FSAR Chapter 15 analyses are provided in Table 15.0-7. After reactor trip, core power quickly decreases to decay heat levels that are below 20 percent power and then gradually decreases over time. The DHRS is designed to remove this decay heat and maintain safe, stable conditions following reactor trip. Many of the MPS signals that result in reactor trip also actuate DHRS. In other cases, DHRS is actuated later by a different MPS signal than caused reactor trip. In some cases, DHRS actuation setpoints are not reached following reactor trip. Transients that result in reactor trip without DHRS actuation do not challenge specified acceptable fuel design limits or design pressure limits after reactor trip, and have ample cooling capability through the SG via the normal condensers. If cooling capability is lost or degraded, DHRS actuation will occur. Therefore, the potential impact of secondary side instability on post-trip behavior when DHRS is not in operation is not considered further. The remainder of this discussion will focus on the potential impact of secondary side instability during DHRS operation following reactor trip.

{{

}}2(a),(c)

During non-LOCA events, the maximum secondary side pressure occurs after DHRS actuation, but while the SG is isolated and before DHRS heat removal is effective. During DHRS

operation, provided there is no SG tube failure, the secondary side pressure is limited to the saturation pressure at the primary side temperature. For an SG tube failure, maximum pressure occurs in the broken loop after pressure equalization between the primary side and secondary side. The spectrum of non-LOCA events evaluated result in secondary side isolation over a wide range of secondary side loop inventories and RCS temperature conditions. Lower inventory conditions occur in loss of feedwater or feedwater line break events, and higher inventory conditions occur in increase in feedwater flow events. The RCS temperature depends on the event progression (i.e., heatup event, reactivity insertion event, or cooldown event) and the timing of secondary side isolation and DHRS actuation relative to reactor trip. Secondary side isolation or DHRS actuation may be concurrent with reactor trip or later in the event sequence, depending on the first signal to reach a reactor trip. Therefore, the entirety of the design-basis event analysis in Chapter 15 results in secondary side isolation over a wide range of conditions. This wide range of conditions encompasses secondary side conditions that may arise from potential secondary side oscillations, such as DWO. The FSAR Chapter 15 analyses demonstrate that there is significant margin between the maximum secondary pressure and its associated limit. For example, excluding the SG tube failure event, the limiting secondary pressure result reported in FSAR Chapter 15 is less than 1600 psia (Table 15.2-12) compared to the acceptance criteria limit of 2420 psia (i.e., over 800 psia of margin). {{

}}[2(a),(c)] Therefore, potential secondary side instabilities, such as DWO, have no effect on peak secondary side pressure margin.

With respect to LOCA events, the MCHFR, minimum level above the top of the core, and containment pressure acceptance criteria are considered. Limiting MCHFR conditions occur during the initial blowdown prior to reactor trip. The effect of secondary side oscillations on limiting conditions during the blowdown are discussed in the response to RSI 16. The short-term collapsed liquid level is a function of the RCS inventory and emergency core cooling system (ECCS) actuation time and is not affected by secondary side oscillations. The limiting containment pressure and temperature conditions occur shortly after ECCS actuation due to the mass and energy release into containment. During small LOCA events, DHRS heat removal prior to ECCS actuation removes decay heat to reduce primary fluid pressure and temperature, thus reducing containment pressure and temperature response after ECCS actuation. Following ECCS actuation and establishment of long-term ECCS recirculation, the DHRS continues to remove energy from the RCS to the reactor pool in parallel with the containment wall heat removal. During long-term ECCS cooling, SG/DHRS cooling provides a means of condensing some vapor on the outside of the steam generator tubes. This condensation due to SG/DHRS heat transfer reduces the vapor flow through the reactor vent valves, thereby reducing the

pressure drop over the reactor vent valves that drives the long-term minimum collapsed liquid level.

{{

}}2(a),(c)

This RSI contains the statement that “The DWO LTR recognizes that two-phase flow oscillation can occur in the steam generator tube side when the reactor power is below 20% of the rated power, but does not include an evaluation of the potential impacts on DHRS performance.” It is important to distinguish between the two operational regimes equated in this statement. In the DWO topical report, the discussion of the potential for DWO below 20 percent power is in reference to normal power operational conditions where there is forced feedwater flow and where DHRS is isolated. In contrast, when DHRS is in operation following a transient, the SG/DHRS operates as a natural circulation system. As a closed-loop boiling-condensing natural circulation system, the SG/DHRS operation includes feedback mechanisms to the loop energy balance and loop momentum balance that affect the overall system behavior. These feedback mechanisms are not present during normal power SG operation with forced feedwater flow. Conclusions about SG component stability drawn from normal operating conditions should not be directly applied to SG/DHRS operation without additional justification. During SG/DHRS operation small, bounded oscillations are possible in the following manner:

- {{

}}2(a),(c)

- {{

}}2(a),(c)

The physical SG wall temperature axial distribution effect on boiling/condensation instability is discussed further. The NPM steam generator is a counter-current flow heat exchanger. Liquid from the DHRS condensate line enters the bottom of the steam generator tubes, where primary side temperature is coolest, and there is convective heat transfer from the primary. Heat transfer raises the condensate temperature to saturation and there is a two-phase boiling region followed by a single-phase vapor region as the secondary fluid rises inside the SG tubes. Vapor temperature is limited to the primary side liquid temperature at the top of the SG. During DHRS operation for decay heat removal, {{

}}2(a),(c) Therefore, boiling/condensation oscillations as described above can result in natural limit cycle oscillations in condensate flow and liquid levels for both the SG and DHRS condenser without significantly affecting the overall phase change rates or total heat removal as long as loop inventory remains in the band where there is both liquid in the SG and condensation area available in the DHRS.

Additional Decay Heat Removal System NIST-2 Testing

This RSI contains the statement that “The characterization of the DHRS heat transfer (as described in the non-LOCA LTR) is based on a single NIST-2 test that was not specifically designed or setup to measure oscillations in the SG nor cover all the conditions that may experience SG oscillations.” This statement is partially correct. {{

}}2(a),(c),ECI

{{ }}[2(a),(c),ECI] Although the non-LOCA topical report only includes results from a single run of the NIST-2 DHRS testing, other test runs were performed. Data from other test runs were not finalized in time to support inclusion in the non-LOCA topical report (TR-0516-49416-P, Rev. 4), but are described in this response. The non-LOCA topical report is revised to include additional test data as part of this RSI response.

Table 1 summarizes three non-LOCA SG/DHRS tests performed at the NIST-2 facility. Run 1 is the test that is currently summarized in Section 5.3.7 of the non-LOCA topical report. Runs 2 and 3 represent variations from Run 1 that study the impact of different DHRS steam line orifice resistance. As described in the response to RSI 14, {{ }}[2(a),(c)] The response to RSI 14 also demonstrates that the loss associated with the inlet flow restrictor (IFR) does not have a significant impact on DHRS behavior.

Table 1:
NIST-2 Integral Effects SG/DHRS Testing for NRELAP5 Code Validation

{{

}}2(a),(c),ECI

{{

}}2(a),(c),ECI

NRELAP5 is assessed against the Run 2 and Run 3 test data. {{

}}2(a),(c),ECI

Figure 10 provides code-to-data comparisons for Run 2 SG and DHRS heat exchanger power. Figure 11 provides code-to-data comparisons for the DHRS power as a function of RCS (core outlet) temperature for Runs 1, 2, and 3. {{

}}2(a),(c),ECI Figure 12 provides code-to-data comparisons for the SG primary side inlet and outlet temperatures, demonstrating RCS cooldown, for Runs 1, 2, and 3. {{

}}2(a),(c),ECI

{{

}}2(a),(c),ECI results from a representative ECCS long-term cooling case are shown in Figure 13 and Figure 14. {{

}}2(a),(c) Therefore, the oscillations are expected to have minimal impact on the overall SG/DHRS heat transfer performance. This conclusion of minimal impact is consistent with the results of the NIST-2 SG/DHRS testing. The testing results for Run 2 show that measured heat transfer is reasonably predicted by NRELAP5 {{

}}2(a),(c),ECI

{{

}}2(a),(b),(c),ECI

Figure 2:
NIST-2 Integral Effects SG/DHRS Testing for NRELAP5 Code Validation

{{

}}2(a),(b),(c),ECI

{{

}}2(a),(b),(c),ECI

Figure 3:
NIST-2 Integral Effects SG/DHRS Testing for NRELAP5 Code Validation
Core Power Comparison for Runs 1, 2, and 3

{{

}}2(a),(b),(c),ECI

Figure 4:
NIST-2 Integral Effects SG/DHRS Testing for NRELAP5 Code Validation
SG/DHRS Active Loop Inventory Comparison for Runs 1, 2, and 3

{{

}}2(a),(b),(c),ECI

Figure 5:
NIST-2 Integral Effects SG/DHRS Testing for NRELAP5 Code Validation
SG and DHRS Heat Exchanger Power for Runs 1, 2, and 3

{{

}}2(a),(b),(c),ECI

Figure 6:
NIST-2 Integral Effects SG/DHRS Testing for NRELAP5 Code Validation
DHRS Condensate Line Flow for Runs 1, 2, and 3

{{

}}2(a),(b),(c),ECI

Figure 7:
NIST-2 Integral Effects SG/DHRS Testing for NRELAP5 Code Validation
DHRS Steam Line Pressure Drop for Runs 1, 2, and 3

{{

}}2(a),(b),(c),ECI

Figure 8:
NIST-2 Integral Effects SG/DHRS Testing for NRELAP5 Code Validation
DHRS Condensate Line Flow for Run 2 – Code to Data Comparison

{{

}}2(a),(b),(c),ECI

Figure 9:
NIST-2 Integral Effects SG/DHRS Testing for NRELAP5 Code Validation
DHRS Steam Line Pressure Drop for Run 2 – Code to Data Comparison

{{

}}2(a),(b),(c),ECI

Figure 10:
NIST-2 Integral Effects SG/DHRS Testing for NRELAP5 Code Validation
SG and DHRS Heat Exchanger Power for Run 2 – Code to Data Comparison

{{

}}2(a),(b),(c),ECI

Figure 11:
NIST-2 Integral Effects SG/DHRS Testing for NRELAP5 Code Validation
DHRS Heat Exchanger Power versus Core Outlet Temperature – Code to Data Comparison

{{

}}2(a),(b),(c),ECI

Figure 12:
NIST-2 Integral Effects SG/DHRS Testing for NRELAP5 Code Validation
Steam Generator Primary Side Inlet and Outlet Temperatures – Code to Data Comparison

{{

}}2(a),(c)

Figure 13:
NRELAP5 Representative Results of Emergency Core Cooling System Cooldown
Decay Heat Removal System Train 1 Liquid Flow

{{

}}2(a),(c)

Figure 14:
NRELAP5 Representative Results of Emergency Core Cooling System Cooldown
Decay Heat Removal System Train 1 Vapor Flow

Quantitative Assessments of Behavior of Events Post-Trip at Decay Heat Power Levels

To further investigate the effect of oscillations on DHRS heat removal, sensitivity calculations are performed for a loss of normal feedwater event. The sensitivity calculation cases are shown in Table 2. {{

}}2(a),(c)

Transient results of the sensitivity calculations are shown in Figure 15 through Figure 43. The decrease in feedwater flow, which is the initiating event, is shown in Figure 15. {{

}}2(a),(c) For transient parameters other than feedwater flow, two different figures are shown: a figure with the full transient results and a figure zoomed-in {{

}}2(a),(c)

The primary system parameters shown are the core power (Figures 16 and 17), RCS flow (Figures 18 and 19), RCS average temperature (Figures 20 and 21), pressurizer pressure (Figures 22 and 23), pressurizer level (Figures 24 and 25), and riser level above the top of the active fuel (Figures 26 and 27). {{

}}2(a),(c)

The secondary system parameters shown are the feedwater flow (Figure 15), SG pressure (Figures 28 and 29), SG superheat (Figures 30 and 31), SG level (Figures 32 and 33), SG inlet flow (Figures 34 and 35), SG outlet flow (Figures 36 and 37), DHRS steam flow (Figures 38 and 39), DHRS inlet vapor velocity (Figures 40 and 41), and DHRS level (Figures 42 and 43).

{{

}}2(a),(c)

Overall, these sensitivity calculations demonstrate that {{ }}2(a),(c) do not substantively affect the ability of the SG/DHRS to remove decay heat. {{

}}2(a),(c),ECI This result is consistent with the expected minimal impact of condensate flow oscillations based on scaling analysis insights discussed in the response to RSI 17.

Table 2:
Decay Heat Removal System Cooling Oscillation Sensitivity Calculations

{{

}}2(a),(c)

{{

}}2(a),(c)

Figure 15:
Decay Heat Removal System Oscillation Sensitivity Study for Loss of Feedwater Event
Transient Results – Feedwater Flow

{{

}}2(a),(c)

Figure 16:
Decay Heat Removal System Oscillation Sensitivity Study for Loss of Feedwater Event
Transient Results – Core Power

{{

}}2(a),(c)

Figure 17:
Decay Heat Removal System Oscillation Sensitivity Study for Loss of Feedwater Event
Transient Results – Core Power
(zoomed-in {{ }}2(a),(c)

{{

}}2(a),(c)

Figure 18:
Decay Heat Removal System Oscillation Sensitivity Study for Loss of Feedwater Event
Transient Results – Reactor Coolant System Flow

{{

}}2(a),(c)

Figure 19:
Decay Heat Removal System Oscillation Sensitivity Study for Loss of Feedwater Event
Transient Results – Reactor Coolant System Flow
(zoomed-in {{ }}2(a),(c)

{{

}}2(a),(c)

Figure 20:
Decay Heat Removal System Oscillation Sensitivity Study for Loss of Feedwater Event
Transient Results – Reactor Coolant System Average Temperature

{{

}}2(a),(c)

Figure 21:
Decay Heat Removal System Oscillation Sensitivity Study for Loss of Feedwater Event
Transient Results – Reactor Coolant System Average Temperature
(zoomed-in {{ }}2(a),(c)

{{

}}2(a),(c)

Figure 22:
Decay Heat Removal System Oscillation Sensitivity Study for Loss of Feedwater Event
Transient Results – Pressurizer Pressure

{{

}}2(a),(c)

Figure 23:
Decay Heat Removal System Oscillation Sensitivity Study for Loss of Feedwater Event
Transient Results – Pressurizer Pressure
(zoomed-in {{ }}2(a),(c)

{{

}}2(a),(c)

Figure 24:
Decay Heat Removal System Oscillation Sensitivity Study for Loss of Feedwater Event
Transient Results – Pressurizer Level

{{

}}2(a),(c)

Figure 25:
Decay Heat Removal System Oscillation Sensitivity Study for Loss of Feedwater Event Transient Results – Pressurizer Level
(zoomed-in {{ }}2(a),(c)

{{

}}2(a),(c)

Figure 26:
Decay Heat Removal System Oscillation Sensitivity Study for Loss of Feedwater Event
Transient Results – Riser Level above Top of Active Fuel

{{

}}2(a),(c)

Figure 27:
Decay Heat Removal System Oscillation Sensitivity Study for Loss of Feedwater Event Transient Results – Riser Level Above Top of Active Fuel
(zoomed-in {{ }}2(a),(c)

{{

}}2(a),(c)

Figure 28:
Decay Heat Removal System Oscillation Sensitivity Study for Loss of Feedwater Event
Transient Results – Steam Generator Pressure (one of two SGs)

{{

}}2(a),(c)

Figure 29:
Decay Heat Removal System Oscillation Sensitivity Study for Loss of Feedwater Event
Transient Results – Steam Generator Pressure (one of two SGs)
(zoomed-in {{ }}2(a),(c)

{{

}}2(a),(c)

Figure 30:
Decay Heat Removal System Oscillation Sensitivity Study for Loss of Feedwater Event
Transient Results – Steam Generator Superheat (one of two SGs)

{{

}}2(a),(c)

Figure 31:
Decay Heat Removal System Oscillation Sensitivity Study for Loss of Feedwater Event
Transient Results – Steam Generator Superheat (one of two SGs)
(zoomed-in {{ }}2(a),(c)

{{

}}2(a),(c)

Figure 32:
Decay Heat Removal System Oscillation Sensitivity Study for Loss of Feedwater Event
Transient Results – Steam Generator Level (one of two SGs)

{{

}}2(a),(c)

Figure 33:
Decay Heat Removal System Oscillation Sensitivity Study for Loss of Feedwater Event
Transient Results – Steam Generator Level (one of two SGs)
(zoomed-in {{ }}2(a),(c)

{{

}}2(a),(c)

Figure 34:
Decay Heat Removal System Oscillation Sensitivity Study for Loss of Feedwater Event
Transient Results – Steam Generator Inlet Flow (one of two SGs)

{{

}}2(a),(c)

Figure 35:
Decay Heat Removal System Oscillation Sensitivity Study for Loss of Feedwater Event
Transient Results – Steam Generator Inlet Flow (one of two SGs)
(zoomed-in {{ }}2(a),(c)

{{

}}2(a),(c)

Figure 36:
Decay Heat Removal System Oscillation Sensitivity Study for Loss of Feedwater Event
Transient Results – Steam Generator Outlet Flow (one of two SGs)

{{

}}2(a),(c)

Figure 37:
Decay Heat Removal System Oscillation Sensitivity Study for Loss of Feedwater Event
Transient Results – Steam Generator Outlet Flow (one of two SGs)
(zoomed-in {{ }}2(a),(c)

{{

}}2(a),(c)

Figure 38:
Decay Heat Removal System Oscillation Sensitivity Study for Loss of Feedwater Event
Transient Results – Decay Heat Removal System Steam Flow (one of two DHRS trains)

{{

}}2(a),(c)

Figure 39:
Decay Heat Removal System Oscillation Sensitivity Study for Loss of Feedwater Event Transient Results – Decay Heat Removal System Steam Flow (one of two DHRS trains) (zoomed-in {{ }}2(a),(c)

{{

}}2(a),(c)

Figure 40:
Decay Heat Removal System Oscillation Sensitivity Study for Loss of Feedwater Event
Transient Results – Decay Heat Removal System Inlet Vapor Velocity (one of two DHRS trains)

{{

}}2(a),(c)

Figure 41:
Decay Heat Removal System Oscillation Sensitivity Study for Loss of Feedwater Event Transient Results – Decay Heat Removal System Inlet Vapor Velocity (one of two DHRS trains) (zoomed-in {{ }}2(a),(c)

{{

}}2(a),(c)

Figure 42:
Decay Heat Removal System Oscillation Sensitivity Study for Loss of Feedwater Event
Transient Results – Decay Heat Removal System Level (one of two DHRS trains)

{{

}}2(a),(c)

Figure 43:
Decay Heat Removal System Oscillation Sensitivity Study for Loss of Feedwater Event Transient Results – Decay Heat Removal System Level (one of two DHRS trains) (zoomed-in {{ }}2(a),(c)

Finally, other factors affecting DHRS heat transfer capacity are considered: the SG/DHRS loop inventory and the temperature difference between the RCS and the ultimate heat sink. Figure 44 shows the effect of SG/DHRS loop inventory on the DHRS performance. {{

}}$^{2(a),(c)}$ Figure 45 shows results from a steam line break sensitivity calculation with high loop inventory {{

}}$^{2(a),(c)}$ {{

}}$^{2(a),(c),ECI}$

With respect to LOCA events and containment pressurization, during small LOCAs the break flow is not sufficient to remove decay heat. However, during a LOCA event, both DHRS trains will operate after containment is isolated; there is no single failure in the short-term event progression that disables an entire DHRS train. Sensitivity calculations show that {{ }}$^{2(a),(c)}$ nominal DHRS heat transfer capacity is sufficient to remove decay heat prior to ECCS actuation for small LOCAs such that they are non-limiting compared to large LOCAs for containment pressure and temperature response. Representative results for the LOCA break spectrum of the injection line liquid space break are shown in Figure 46.

The Chapter 15 non-LOCA safety analyses already consider the effects of loop inventory and ultimate heat sink temperature on DHRS performance. In small LOCA events, the two DHRS trains provide redundant and therefore ample heat transfer capability. {{

}}$^{2(a),(c}$

{{ }}[2(a),(c)] The range of DHRS performance considered thus allows for potential impacts on transient response to be identified.

{{

}}2(a),(c)

Figure 44:
Decay Heat Removal System Performance Sensitivity to Loop Inventory

{{

}}2(a),(c)

Figure 45:
Decay Heat Removal System Performance Sensitivity to Ultimate Heat Sink Temperature

{{

}}2(a),(c)

Figure 46:
Decay Heat Removal System Performance Sensitivity for Containment Pressure
Loss of Coolant Accident, Injection Line Break Spectra

{{ }}2(a),(c)

Summary of Technical Justification

In summary, considering: (1) the characteristic behavior of the DHRS to reach quasi-steady-state conditions where the SG/DHRS heat removal balances the core decay heat levels, (2) the range of DHRS maximum capacity considered in the safety analysis due to factors such as inventory and pool temperature, (3) the NRELAP5 sensitivity calculations {{ }}$^{2(a),(c)}$ (4) the NRELAP5 capability {{ }}$^{2(a),(c),ECI}$ (5) the minor impact of {{ }}$^{2(a),(c),ECI}$ and (6) the scaling insights described in the response to RSI 17, it is concluded that oscillatory behavior that may occur in the SG/DHRS loop does not impact the ability of the DHRS system to remove decay and residual heat. Nominal modeling of the SG/DHRS loop behavior {{ }}$^{2(a),(c)}$ is appropriate for non-LOCA, LOCA, and long-term cooling analyses.

This RSI contains many statements or questions. To ensure that each is addressed, the text of the RSI is repeated in italicized text below, with summary responses to each statement or question provided based on the technical justification provided above.

Impact of steam generator density wave oscillations and potential flow instability in DHRS loop: Sections 5.4.3, nearly all Chapter 15 sections, and the LOCA, non-LOCA and XPC LTRs are missing analyses and methodologies for the potential impact of steam generator density wave oscillations on DHRS performance when power is below 20% full power.

- No analysis is missing from the Chapter 15 safety analysis. The impacts of potential secondary side oscillations are dispositioned for Chapter 15 events that are initiated from 20 percent power or below. The impacts of potential secondary side oscillations during DHRS operation when power is below 20 percent after reactor trip are also dispositioned. The FSAR Section 5.4.3 analysis, and methodologies in the LOCA, non-LOCA, and XPC topical reports are adequate. The non-LOCA and XPC topical reports are updated consistent with this response. No required changes to the LOCA topical report are identified.

These sections and LTRs are also missing evaluations of the potential impact on DHRS performance from potential flow instability in the loop from multiple phenomena (due to density wave oscillations or other phenomena such as Ledinegg instability, geysering, manometer oscillations, etc) when reactor power is below 20% (such as during the 72 hours following a design basis event).

- In the development of non-LOCA and XPC PIRTs, and in review of phenomena for DHRS operation during LOCAs, {{

}}2(a),(c)

The DWO LTR only covers the methodology to detect the on-set of DWO for steady state and off-normal power levels between 20-100% power.

- This statement is correct. The purpose of the DWO topical report is to provide a methodology to predict the onset of DWO.

The DWO LTR recognizes that two-phase flow oscillation can occur in the steam generator tube side when the reactor power is below 20% of the rated power, but does not include an evaluation of the potential impacts on DHRS performance.

- This statement is correct. The purpose of the DWO topical report is to provide a methodology to predict the onset of DWO. The DWO topical report is not intended to evaluate the consequences of potential DWO. The consequence of potential DWO on DHRS performance as it pertains to the safety analysis is considered in this response. The consequence of potential DWO as it pertains to SG tube integrity is assessed separately.

The proposed SDA design relies on the decay heat removal system (DHRS) to remove the heat from the primary system during anticipated operational occurrences.

- This statement is correct.

When the steam generator and the coupled DHRS are activated during an event, the steam generator secondary side fluid flow is potentially subject to two-phase instability.

- This statement is correct. {{

}}2(a),(c) {{

}}2(a),(c),ECI {{

}}2(a),(c)

The new IFR design increases the flow loss coefficient and is expected to impact the DHRS recirculation flow rate and heat removal capacity.

- As identified in the response to RSI 14, the loss coefficient associated with the IFR has minimal impact on DHRS recirculation flow rate and heat removal capacity.

Further, flow instability due to other phenomena are also not evaluated.

- {{

}}2(a),(c)

The heat transferred by DHRS is dependent on whether oscillations occur.

- Time-dependent local heat transfer rates may be affected by oscillatory behavior. {{

}}2(a),(c),ECI

The characterization of the DHRS heat transfer (as described in the non-LOCA LTR) is based on a single NIST-2 test that was not specifically designed or setup to measure oscillations in the SG nor cover all the conditions that may experience SG oscillations.

- This statement is partially correct. Although only a single run of the NIST-2 testing was previously included in the non-LOCA topical report, additional runs were performed. The additional test runs are added to the non-LOCA topical report as part of this response. {{

}}2(a),(c),ECI The tests specifically covered a range of SG conditions (steam line losses) intended to generate a measurable impact on DHRS performance.

The non-LOCA topical report acknowledges some instability phenomena, but is missing PIRT analysis.

- Additional discussions of the PIRT phenomena are provided in this RSI response. The non-LOCA topical report is revised as described in this RSI response {{

}}2(a),(c)

{{

}}2(a),(c)

- As clarified in the body of this RSI response, the non-LOCA topical report {{

}}2(a),(c)

Further, no methodology has been included to evaluate the potential impact of flow instability on the DHRS gravity driven discharge line flow.

- No specific methodology is required because the justifications provided in this response demonstrate that the potential for flow instability has minimal impact on DHRS performance.

The non-LOCA topical report is revised as shown in the attached markups to enhance the discussion of phenomena related to oscillatory behavior in the PIRT in Section 5.1, include the description and results for NIST-2 SG/DHRS testing Runs 2 and 3 in Section 5.3.7, and {{

}}2(a),(c)

Similarly, the XPC topical report is revised as shown in the attached markups to {{

}}2(a),(c) Section 4.4.

There are no changes to the SDAA FSAR, LOCA topical report, or DWO topical report associated with this response.

Impact on US460 SDA:

There are no impacts to US460 SDA as a result of this response.

Additional Information:

Topical reports TR-0516-49416, Non-Loss-of-Coolant Accident Analysis Methodology, and TR-124587, Extended Passive Cooling and Reactivity Control Methodology, are revised as described in the response above and as shown in the markups provided in this response.

5.1.4.41 {{ }}2(a),(c)

RSI 15, RSI 16

{{

}}2(a),(c)

5.1.4.50 {{ }}2(a),(c)

RSI 15, RSI 16

{{

}}2(a),(c)

Figure 5-197 NIST-2 decay heat removal system configuration

{{

}}2(a),(c),ECI

RSI 17

5.3.7.2 NIST-2 Steam Generator - Decay Heat Removal System Integral Effects Test Objectives and Scaling

RSI 17

5.3.7.2.1 Test Objectives

Initial assessment and validation of NRELAP5 for prediction of SG-DHRS phenomena during non-LOCA event sequences was provided in Section 5.3.1, Section 5.3.2, Section 5.3.3, and Section 5.3.5. NuScale identified that additional testing and analysis was needed to reduce the uncertainty associated with heat removal by the DHRS during non-LOCA event sequences.

Section 3.0 provides general discussion of NPM designs, including the DHRS. Changes between NPM designs have resulted in changes to the DHRS geometry, such as the DHRS steam piping configuration, and detailed

condenser design. The PIRT in Section 5.1 identifies several high ranked phenomena associated with DHRS operation in Phase 3. NuScale identified that additional testing and analysis was needed to understand the impact of potential DHRS design changes on the relevant high ranked phenomena.

The NIST-2 SG-DHRS integral effects testing is designed to enhance the DHRS validation database to address the above considerations. The NIST-2 facility permits test conditions that are significantly closer to the prototypical NPM operation conditions than was achieved in prior testing.

RSI 17

5.3.7.2.2 Scaling Analysis

As part of the assessment of EM adequacy, a top-down scaling analysis was performed. The scaling analysis compared dimensionless π groups for the governing field equations of liquid mass, total energy, and total momentum balances in the DHRS loop. Comparisons were made between {{

}}2(a),(c),ECI

RSI 17

The SG/DHRS loop is a boiling/condensation-driven natural circulation system. {{

}}2(a),(c),ECI

{{

}}2(a),(c),ECI

RSI 17

The instantaneous π group balance equations for the total liquid mass in the SG and DHRS loop are given by Equations 5-1 and 5-2, respectively. {{

RSI 17

}}2(a),(c),ECI

The instantaneous π group balance equation for the total two-phase mixture fluid momentum conservation in the SG/DHRS loop is given in Equation 5-4. {{

RSI 17

}}2(a),(c),ECI

{{

}}2(a),(c),ECI

{{

}}2(a),(c),ECI

For each π group, distortion factors were defined as shown in Equation 5:

{{

}}2(a),(c),ECI

RSI 17

Time-dependent and normalized time-averaged π groups were compared. Normalized, time-averaged results of the scaling and distortion analyses are shown in the following plots. The normalized time-averaged π groups and distortion factors are shown for the NPM-20 design, the ISD-20 model, and NIST-2. Table 5-17 provides the π group definitions and figure legend information.

The normalized time-averaged π groups for the liquid mass balance in the SG and DHRS heat exchanger are compared in Figure 5-198 while the significances and distortions of the π groups are compared in Figure 5-199.
{{

}}2(a),(c),ECI

RSI 17

Normalized time-averaged π groups for the energy balance are compared in Figure 5-200. Significances and distortions of the π groups are compared in Figure 5-201. {{

}}2(a),(c),ECI

RSI 17

{{

}}2(a),(c),ECI

Normalized time-averaged π groups for the momentum balance are compared in Figure 5-202. Significances and distortions of the π groups are compared in Figure 5-203. {{

}}2(a),(c),ECI

The top-down scaling and distortion analysis demonstrates similarity in dimensionless π groups, and supports the conclusion that the NRELAP5 mathematical models (field equations) are applicable for NPM integral effects non-LOCA analysis with SG/DHRS heat removal.

RSI 17

Table 5-17 π groups in dimensionless control volume balance equations for decay heat removal system

{{

}}2(a),(c),ECI

Table 5-17 π groups in dimensionless control volume balance equations for decay heat removal system (Continued)

{{

}}2(a),(c),ECI

RSI 17

Figure 5-198 Normalized time-averaged π groups for decay heat removal system liquid mass balance in {{ }}2(a),(c),ECI

{{

}}2(a),(c),ECI

RSI 17

Figure 5-199 Significances vs. distortions of π groups for decay heat removal system liquid mass balance in {{ }}2(a),(c),ECI

	{{	
	}}2(a),(c),ECI	

RSI 17

Figure 5-200 Normalized time-averaged π groups for decay heat removal system energy balance in {{ }}2(a),(c),ECI

	{{	
	}}2(a),(c),ECI	

RSI 17

Figure 5-201 Significances vs. distortions of π groups for decay heat removal system energy balance in {{ }}2(a),(c),ECI

	{{	
	}}2(a),(c),ECI	

RSI 17

Figure 5-202 Normalized time-averaged π groups for decay heat removal system momentum balance in {{ }}2(a),(c),ECI

{{

}}2(a),(c),ECI

RSI 17

Figure 5-203 Significances vs. distortions of π groups for decay heat removal system momentum balance in {{ }}2(a),(c),ECI

{{

}}2(a),(c),ECI

5.3.7.3 Applicability of Decay Heat Removal System Operation to Small Break Loss-of-Coolant Accident Sequences

The assessment and validation of NRELAP5 for prediction of SG-DHRS phenomena provided in Section 5.3.1, Section 5.3.2, and Section 5.3.3 was focused on application during non-LOCA event sequences. DHRS actuation is also expected to occur during LOCA event sequences. For smaller LOCA break sizes, there may be an extended period where DHRS is in operation but ECCS is not yet actuated. In a small break LOCA sequence where there is such an extended period, the phenomena associated with DHRS performance are applicable.

Figure 5-219 NIST-2 modified feedwater system model

{{

}}2(a),(c),ECI

RSI 15

5.3.7.5 NIST-2 Steam Generator - Decay Heat Removal System Integral Effects Test Matrix

Based on the acceptance criteria described in Section 4.2, figures of merit in the non-LOCA events include CHFR, RCS pressure, SG pressure, and CNV pressure. These figures of merit are affected by the DHRS heat removal performance during Phase 3. In addition, Section 5.3.7.3 concludes that DHRS heat removal performance is also applicable during small break LOCA events prior to ECCS performance (corresponding to Phase 3). The high-ranked phenomena identified in the NPM non-LOCA PIRT focusing on the DHRS and its interfacing systems (i.e., RCS and reactor pool) during Phase 3 can be summarized as follows.

- {{

}}2(a),(c)

- {{

}}2(a),(c) Therefore, the SG and DHRS heat exchanger are the primary focus for the NIST-2 DHRS testing. Table 5-18 identifies SG/DHRS testing performed at the NIST-2 facility and assessed with NRELAP5 as part of the non-LOCA EM development.

RSI 15, RSI 17

Table 5-18 NIST-2 integral effects SG/DHRS testing for NRELAP5 code validation

Test Identifier	DHRS Steam Line Orifice Resistance	Initial DHRS Inventory	Test Description
Run 1	Base	Base	This is the base configuration for the testing.
Run 2	Larger	Base	Smaller orifice size to provide larger steam line resistance.
Run 3	Smaller	Base	Larger orifice size to provide smaller steam line resistance.

5.3.7.6 Run 1 Test Description

The NIST-2 facility had the following initial conditions at the start of the Run 1 test:

{{

}}2(a),(b),(c),ECI

- {{

}}2(a),(b),(c),ECI

The NIST-2 valve configuration at the start of the Run 1 test is shown in Figure 5-197. {{

}}2(a),(b),(c),ECI

The sequence of events for the Run 1 test is shown in Table 5-19.

RSI 15

Table 5-19 NIST-2 Run 1 sequence of events

{{

}}(a),(b),(c),ECI

5.3.7.7 Run 1 Test Results

Figure 5-220 through Figure 5-240 show the results of the code-to-data comparisons for Run 1.

Figure 5-220 shows the core power. Figure 5-221 shows the SG/DHRS active loop inventory. {{

}}2(a),(c)

RSI 15

Figure 5-229 NIST-2 Run 1 decay heat removal system heat exchanger inlet and outlet temperatures comparison

{{

}}2(a),(b),(c),ECI

RSI 15

Figure 5-230 NIST-2 Run 1 steam generator secondary side inlet and outlet temperatures comparison

{{

}}2(a),(b),(c),ECI

Figure 5-242 NIST-2 Run 1 decay heat removal system heat exchanger tube bottom fluid temperatures - data only

{{

}}2(a),(b),(c),ECI

RSI 15

5.3.7.8 Run 2 Test Description

The NIST-2 facility had the following initial conditions at the start of the Run 2 test:

{{

}}2(a),(b),(c),ECI

- {{

}}2(a).(b).(c).ECI

The valve configuration and execution of the Run 2 test was the same as described for Run 1 in Section 5.3.7.6. The sequence of events of the Run 2 test is shown in Table 5-20.

RSI 15

Table 5-20 NIST-2 Run 2 sequence of events

	{{		
		}}(a).(b).(c).ECI	

RSI 15

5.3.7.9 Run 2 Test Results

RSI 15

Figure 5-243 through Figure 5-264 show the code-to-data comparison of the key parameters for Run 2.

RSI 15

Figure 5-243 shows the core power. Figure 5-244 shows the SG/DHRS active loop inventory. {{

}}2(a).(c) The active loop inventory is discussed in greater detail for Run 1 in Section 5.3.7.7.

RSI 15

Figure 5-245 and Figure 5-246 show the DHRS heat exchanger and SG power comparison for the long-term and short-term, respectively. Figure 5-247 and Figure 5-248 show the SG/DHRS loop flow comparison for the long-term and short-term, respectively. {{

}}2(a).(c)

{{ }}2(a),(c) The results are consistent with those observed in Run 1 in Section 5.3.7.7.

RSI 15

{{

}}2(a),(c) Figure 5-249 compares the DHRS loop flow data without time average with the NRELAP5 results. Both are DHRS condensate line flow rates. {{

RSI 15

}}2(a),(c)

Figure 5-250 shows the differential pressure across the DHRS condensate line flow meter. {{

RSI 15

RSI 15

}}2(a),(c)

RSI 15

Figure 5-251 shows the code-to-data comparison for the pressurizer pressure and secondary side pressure near the steam drum. {{

}}2(a),(c) Overall the secondary side pressure has reasonable to excellent agreement with the test data.

RSI 15

Figure 5-252 shows the code-to-data comparison for the DHRS heat exchanger level and SG level. {{

}}2(a),(c) Overall, the predicted DHRS heat exchanger and SG levels have reasonable to excellent agreement with the test data.

RSI 15

Figure 5-253 shows the code-to-data comparison for the DHRS heat exchanger inlet and outlet temperatures. Figure 5-254 shows the code-to-data comparison for the SG secondary side inlet and outlet temperatures. {{

}}2(a),(c) The code predictions of these two temperatures both have reasonable to excellent agreement with the data, similar to the secondary side pressure.

RSI 15

From Figure 5-253 and Figure 5-254, {{

}}2(a),(c)

RSI 15

Figure 5-256 shows the code-to-data comparison of the RCS primary temperatures. {{

}}2(a),(c)

{{

}}2(a),(c)

RSI 15

Figure 5-257 shows the code-to-data comparison of the PZR level. Figure 5-258 shows the code-to-data comparison of the RPV level. {{

}}2(a),(c)

RSI 15

Figure 5-259 shows the code-to-data comparison of the RCS primary flow. The prediction has excellent agreement with the data during the transient. {{

}}2(a),(c)

RSI 15

Figure 5-260 shows the code-to-data comparison of the CPV level. The prediction has excellent agreement with data {{

}}2(a),(c)

RSI 15

Figure 5-263 shows the code-to-data comparison of the DHRS steam line differential pressure. Figure 5-264 shows the comparison of the DHRS steam line orifice differential pressure. Reasonable to excellent agreements are shown {{

}}2(a),(c)

RSI 15

Figure 5-243 NIST-2 Run 2 core power comparison

{{

}}2(a),(b),(c),ECI

RSI 15

Figure 5-244 NIST-2 Run 2 steam generator and decay heat removal system active loop inventory comparison

{{

}}2(a),(b),(c),ECI

RSI 15

Figure 5-245 NIST-2 Run 2 steam generator and decay heat removal system heat exchanger power comparison

{{

}}2(a),(b),(c),ECI

RSI 15

Figure 5-246 NIST-2 Run 2 steam generator and decay heat removal system heat exchanger power comparison - short-term

{{

}}2(a),(b),(c),ECI

RSI 15

Figure 5-247 NIST-2 Run 2 steam generator and decay heat removal system loop flow comparison

{{

}}2(a),(b),(c),ECI

RSI 15

Figure 5-248 NIST-2 Run 2 steam generator and decay heat removal system loop flow comparison - short-term

{{

}}2(a),(b),(c),ECI

RSI 15

Figure 5-249 NIST-2 Run 2 decay heat removal system condensate line flow comparison (without time average)

{{

}}2(a),(b),(c),ECI

RSI 15

Figure 5-250 NIST-2 Run 2 decay heat removal system condensate line differential pressure comparison

{{

}}2(a),(b),(c),ECI

RSI 15

Figure 5-251 NIST-2 Run 2 primary and secondary pressure comparison

{{

}}2(a),(b),(c),ECI

RSI 15

Figure 5-252 NIST-2 Run 2 steam generator and decay heat removal system level comparison

{{

}}2(a),(b),(c),ECI

RSI 15

Figure 5-253 NIST-2 Run 2 decay heat removal system heat exchanger inlet and outlet temperatures comparison

{{

}}2(a),(b),(c),ECI

RSI 15

Figure 5-254 NIST-2 Run 2 steam generator secondary side inlet and outlet temperatures comparison

{{

}}2(a),(b),(c),ECI

RSI 15

Figure 5-255 NIST-2 Run 2 steam generator secondary side saturation temperature comparison

{{

}}2(a),(b),(c),ECI

RSI 15

Figure 5-256 NIST-2 Run 2 steam generator primary side inlet and outlet temperatures comparison

{{

}}2(a),(b),(c),ECI

RSI 15

Figure 5-257 NIST-2 Run 2 pressurizer level comparison

{{

}}2(a),(b),(c),ECI

RSI 15

Figure 5-258 NIST-2 Run 2 reactor pressure vessel level comparison

{{

}}2(a),(b),(c),ECI

RSI 15

Figure 5-259 NIST-2 Run 2 primary flow rate comparison

{{

}}2(a),(b),(c),ECI

RSI 15

Figure 5-260 NIST-2 Run 2 cooling pool vessel level comparison

{{

}}2(a),(b),(c),ECI

RSI 15

Figure 5-261 NIST-2 Run 2 cooling pool vessel level 5 temperature comparison

{{

}}2(a),(b),(c),ECI

RSI 15

Figure 5-262 NIST-2 Run 2 cooling pool vessel level 6 temperature comparison

{{

}}2(a),(b),(c),ECI

RSI 15

Figure 5-263 NIST-2 Run 2 decay heat removal system steam line differential pressure comparison

{{

}}2(a),(b),(c),ECI

RSI 15

Figure 5-264 NIST-2 Run 2 decay heat removal system steam line orifice differential pressure comparison

{{

}}2(a),(b),(c),ECI

RSI 15

5.3.7.10 Run 3 Test Description

The NIST-2 facility had the following initial conditions at the start of the Run 3 test:

RSI 15

{{

}}2(a),(b),(c),ECI

- {{

}}2(a).(b).(c).ECI

RSI 15

The valve configuration and execution of the Run 3 test was the same as described for Run 1 in Section 5.3.7.6. The sequence of events of the Run 3 test is shown in Table 5-21.

RSI 15

Table 5-21 NIST-2 Run 3 sequence of events

	{{		
		}}(a).(b).(c).ECI	

RSI 15

5.3.7.11 Run 3 Test Results

RSI 15

Figure 5-265 through Figure 5-285 show the code-to-data comparison of the key parameters for Run 3.

RSI 15

Figure 5-265 shows the core power. Figure 5-266 shows the SG/DHRS active loop inventory. {{

}}2(a).(c) The active loop inventory is discussed in greater detail for Run 1 in Section 5.3.7.7.

RSI 15

Figure 5-267 and Figure 5-268 show the DHRS heat exchanger and SG power comparison for the long-term and short-term, respectively. Figure 5-269 and Figure 5-270 show the SG/DHRS loop flow comparison for the long-term and short-term, respectively. {{

}}2(a).(c)

{{

}}2(a),(c) The results are consistent with those observed in Run 1 in Section 5.3.7.7.

RSI 15

{{

}}2(a),(c) Figure 5-271 compares the DHRS condensate line flow data without time average with the NRELAP5 results. {{

}}2(a),(c)

RSI 15

Figure 5-272 shows the code-to-data comparison for the pressurizer pressure and secondary side pressure near the steam drum. {{

}}2(a),(c) The predicted secondary side pressure shows excellent agreement with the test data for the entire transient, including the peak pressure.

RSI 15

Figure 5-273 shows the code-to-data comparison for the DHRS heat exchanger level and SG level. {{

}}2(a),(c) Overall the predicted DHRS heat exchanger and SG levels have reasonable to excellent agreement with the test data.

RSI 15

Figure 5-274 shows the code-to-data comparison for the DHRS heat exchanger inlet and outlet temperatures. Figure 5-275 shows the code-to-data comparison for the SG secondary side inlet and outlet temperatures. {{

}}2(a),(c) The code predictions of these two temperatures both have reasonable to excellent agreement with the data, similar to the secondary side pressure.

RSI 15

From Figure 5-274 and Figure 5-275, {{

}}2(a),(c)

RSI 15

Figure 5-277 shows the code-to-data comparison of the RCS primary temperatures. {{

}}2(a),(c)

RSI 15

Figure 5-278 shows the code-to-data comparison of the PZR level. Figure 5-279 shows the code-to-data comparison of the RPV level. {{

}}2(a),(c) The predictions have reasonable agreement with test data.

RSI 15

Figure 5-280 shows the code-to-data comparison of the RCS primary flow. The prediction has excellent agreement with the data during the transient. {{

}}2(a),(c)

RSI 15

Figure 5-281 shows the code-to-data comparison of the CPV level. The prediction has excellent agreement with data {{

}}2(a),(c)

RSI 15

Figure 5-284 shows the code-to-data comparison of the DHRS steam line differential pressure. Figure 5-285 shows the comparison of the DHRS steam line orifice differential pressure. Predicted differential pressures have reasonable to excellent agreement with test data.

RSI 15

Figure 5-265 NIST-2 Run 3 core power comparison

{{

}}2(a),(b),(c),ECI

RSI 15

Figure 5-266 NIST-2 Run 3 steam generator and decay heat removal system active loop inventory comparison

{{

}}2(a),(b),(c),ECI

RSI 15

Figure 5-267 NIST-2 Run 3 steam generator and decay heat removal system heat exchanger power comparison

{{

}}2(a),(b),(c),ECI

RSI 15

Figure 5-268 NIST-2 Run 3 steam generator and decay heat removal system heat exchanger power comparison - short-term

{{

}}2(a),(b),(c),ECI

RSI 15

Figure 5-269 NIST-2 Run 3 steam generator and decay heat removal system loop flow comparison

{{

}}2(a),(b),(c),ECI

RSI 15

Figure 5-270 NIST-2 Run 3 steam generator and decay heat removal system loop flow comparison - short-term

{{

}}2(a),(b),(c),ECI

RSI 15

Figure 5-271 NIST-2 Run 3 decay heat removal system condensate line flow comparison (without time average)

{{

}}2(a),(b),(c),ECI

RSI 15

Figure 5-272 NIST-2 Run 3 primary and secondary pressure comparison

{{

}}2(a),(b),(c),ECI

RSI 15

Figure 5-273 NIST-2 Run 3 steam generator and decay heat removal system level comparison

{{

}}2(a),(b),(c),ECI

RSI 15

Figure 5-274 NIST-2 Run 3 decay heat removal system heat exchanger inlet and outlet temperatures comparison

{{

}}2(a),(b),(c),ECI

RSI 15

Figure 5-275 NIST-2 Run 3 steam generator secondary side inlet and outlet temperatures comparison

{{

}}2(a),(b),(c),ECI

RSI 15

Figure 5-276 NIST-2 Run 3 steam generator secondary side saturation temperature comparison

{{

}}2(a),(b),(c),ECI

RSI 15

Figure 5-277 NIST-2 Run 3 steam generator primary side inlet and outlet temperatures comparison

{{

}}2(a),(b),(c),ECI

RSI 15

Figure 5-278 NIST-2 Run 3 pressurizer level comparison

{{

}}2(a),(b),(c),ECI

RSI 15

Figure 5-279 NIST-2 Run 3 reactor pressure vessel level comparison

{{

}}2(a),(b),(c),ECI

RSI 15

Figure 5-280 NIST-2 Run 3 primary flow rate comparison

{{

}}2(a),(b),(c),ECI

RSI 15

Figure 5-281 NIST-2 Run 3 cooling pool vessel level comparison

{{

}}2(a),(b),(c),ECI

RSI 15

Figure 5-282 NIST-2 Run 3 cooling pool vessel level 5 temperature comparison

{{

}}2(a),(b),(c),ECI

RSI 15

Figure 5-283 NIST-2 Run 3 cooling pool vessel level 6 temperature comparison

{{

}}2(a),(b),(c),ECI

RSI 15

Figure 5-284 NIST-2 Run 3 decay heat removal system steam line differential pressure comparison

{{

}}2(a),(b),(c),ECI

RSI 15

Figure 5-285 NIST-2 Run 3 decay heat removal system steam line orifice differential pressure comparison

{{

}}2(a),(b),(c),ECI

SCP1-3277

5.3.7.12 NIST-2 Decay Heat Removal System Integral Effects Testing Summary

RSI 15

Based on the overall comparison between NRELAP5 and the NIST-2 test data for the simulated LOFW transients, there is reasonable to excellent agreement between code prediction and data. Predicted SG-DHRS loop flow and DHRS heat exchanger and SG power match the test data very closely during quasi steady state. Predicted secondary side pressure and temperatures, as well as DHRS heat exchanger and SG levels, have reasonable to excellent agreement with test data. SG-DHRS loop differential pressures are also predicted with reasonable to excellent agreement to test data. The comparisons demonstrate that NRELAP5 has the capability to accurately predict SG-DHRS performance during transients.

{{

}}2(a),(c)

Key conclusions from the NIST-2 SG/DHRS tests and NRELAP5 assessments are as follows.

RSI 15

- {{

RSI 15

}}2(a),(c)

Table 4-17 Top-Down Assessment for Extended ECCS Phenomena (Continued)

{{

}}2(a),(c)

RSI 15

Response to Request for Additional Information
Docket: 99902078

RAI No.: RSI
Date of RAI Issue: 03/27/2023

NRC Question No.: RSI-16

Analyses are missing for the potential impact of steam generator density wave oscillations on CHF, primary pressure, coolant mixture level, and subcriticality when power is above 100%. The Non-LOCA LTR, and SDAA Chapter 15 sections where core power exceeds 100% power during the progress of the event are missing evaluations of the potential impact of steam generator density wave oscillations above 100% power. Since higher power levels are achieved during the 72 hour period following some AOOs, analyses must be performed to assess the impacts on system safety. The DWO LTR only covers the methodology to detect the on-set of DWO for steady state and off-normal power levels between 20-100% power.

NuScale Response:

Response Summary:

This request for supplemental information (RSI) is focused on the impacts on transient analyses from potential secondary side component-level and system-level instabilities when reactor power is above 100 percent. The premise of the RSI is that the impacts are significant. This response demonstrates that the impacts of potential secondary side instabilities are not significant on key safety analysis figures of merit addressed in the final safety analysis report (FSAR) Chapter 15 sections, and the loss of coolant accident (LOCA) and non-LOCA topical reports. The technical justification for this conclusion is based on qualitative explanations, stability analyses using the PIM code, review of Società Informazioni Esperienze Termoidrauliche S.p.A. (SIET) TF-2 test data, and NRELAP5 sensitivity studies. Oscillatory behavior that may occur in the secondary side does not meaningfully impact the plant conditions that are used to assess relevant acceptance criteria. Additional modeling or special treatment of

oscillatory behavior beyond that already included in the safety analysis methodology topical reports is not required to ensure the adequacy of the safety analyses.

Detailed Response:

The focus of this RSI is on the impacts on transient analyses from potential secondary side component-level and system-level instabilities, from phenomena such as density wave oscillation (DWO), during design-basis transient events at full power or that could exceed 100 percent power; however, the conclusions are applicable for transients at all power levels above 20 percent. During such events at high powers, margin to specified applicable fuel design limits (SAFDLs), particularly minimum critical heat flux ratio (MCHFR), is of particular interest. Note that the RSI mentions coolant mixture level and subcriticality as parameters of interest. However, these specific parameters are only of interest in the longer-term transient response following reactor trip, when powers are at decay heat levels (i.e., they are not relevant when power is greater than or equal to 100 percent). Coolant mixture level remains well above the top of the core when the reactor is at or above full power. The response to RSI 15 addresses the impact of potential secondary side instabilities at low power conditions, including during decay heat removal system (DHRS) operation.

In the standard design approval application (SDAA) US460 design, limiting MCHFR conditions occur during either a reactivity insertion event (FSAR Section 15.4) or during a rapid blowdown condition with one or more emergency core cooling system (ECCS) valves opening (FSAR Section 15.6). Cooldown events (FSAR Section 15.1) that increase power and could challenge MCHFR are also considered. For completeness, the range of design-basis events and the primary and secondary system maximum pressure acceptance criteria are also considered in this RSI response. Qualitative discussion of NuScale Power Module (NPM) steady-state operation, and then NPM behavior during design-basis events, considering effects of DWO, is provided. Quantitative justification, including sensitivity calculations {{

}}[2(a),(c)] are provided to verify the described qualitative behavior.

Qualitative Analysis of Potential Secondary Side Instabilities

For non-LOCA transient events, {{

}}[2(a),(c)] These three phases correspond to before reactor trip,

after reactor trip during DHRS actuation, and during effective DHRS cooling with stable natural circulation, respectively, as described in non-LOCA topical report Section 5.1.3. As part of the response to this RSI and RSI 15, the non-LOCA topical report PIRT discussions in Section 5.1 are revised to add further disposition of potential instabilities. The non-LOCA topical report markups are provided with the response to RSI 15.

During the US600 design certification application (DCA) review and approval, supplemental information was provided in LO-1216-52161, Revision 0, on the role the SG has on stability of the NPM primary flow. The information supplemented the stability topical report, TR-0516-49417-P-A, Appendix A. As identified in FSAR Table 15.0-9, the NRC-approved stability topical report is referenced and is applicable for the SDAA. Based on the stability topical report and supplemental information previously provided, there is no closed-loop feedback process between the SG and the primary flow that can cause undamped instability in the primary flow.

As a natural circulation reactor, the NPM primary side temperature distribution and flow rate are affected by the reactor coolant system (RCS) loop pressure losses, the operating power level, and by the secondary side conditions that affect the thermal center of the SG. Key characteristics of the natural circulation NPM include:

- Higher power levels result in higher flow rate conditions as well as a higher temperature change over the core as shown in Figure 1.
- For a given power level and secondary side thermal center elevation, higher RCS loop pressure losses result in a lower RCS flow rate and a larger temperature change over the core and SG.
- A change in the secondary side boiling length, and therefore thermal center, has a second-order effect on the primary side flow rate and temperature distribution compared to changes in power or RCS loop pressure losses. The secondary side conditions indirectly affect the primary side due to changes in the natural circulation driving force (i.e., the elevation head between the hot region thermal center in the core and the cold region thermal center in the SG secondary side). For a constant average primary temperature, a reduced effective heat transfer coefficient from the primary-to-secondary in the SG extends the boiling length, elevating the thermal center, and therefore increases the RCS flow rate and decreases the temperature rise over the core.
    - When average temperature is controlled to be constant, if DWO occurs in the SG and primary-to-secondary heat transfer degrades slightly, the RCS flow increases.

    - As the driving force changes and primary flow changes, the temperature distribution on the primary side adjusts to maintain heat removal. The higher primary flow rate reduces the maximum temperature in the riser and the maximum temperature over the SG, which also affects the boiling length. Figure 1 shows the RCS temperature distribution for minimum and maximum flow conditions.
- The SG heat transfer affects the steam temperature distribution and superheat.

{{

}}2(a),(c)

Figure 1:
Hot and Cold Primary Coolant Temperatures as a Function of Reactor Power

where: BOL = Beginning-of-life
EOL = End-of-life
MIN = Minimum flow rate (higher loop resistance)
MAX = Maximum flow rate (lower loop resistance)

DWO may be postulated to cause a reduction in the heat transfer coefficient from the primary to the secondary. For otherwise constant secondary conditions, this reduction in heat removal is similar to a mild heat up event. Therefore, to assess the effect of postulated DWO on the FSAR Chapter 15 transient analyses and MCHFR margin, {{

}}2(a),(c)

Reactivity Insertion and Cooldown Events

As described above, reactor power may exceed 100 percent for reactivity insertion (FSAR Section 15.4) and cooldown (FSAR Section 15.1) events. For reactivity insertion events that require transient analysis, limiting MCHFR conditions occur around the time of reactor trip due to high power or a combination of high power and high temperature conditions near the module protection system (MPS) limits. The limiting primary side conditions for MCHFR occur due to the effects of reactivity insertion rate, the effects of reactivity feedback, the control rod response to varying temperature conditions, and the pressurizer spray response to increasing pressure conditions. As identified in the non-LOCA topical report, nominal SG heat transfer is modeled for reactivity insertion events {{

}}2(a),(c) (TR-0516-49416-P, Revision 4, Tables 7-60, 7-64, 7-68, and 7-70). {{

}}2(a),(c)

Control rod ejection event (FSAR Section 15.4.8) analyses simulate rapid reactivity insertions mitigated primarily by Doppler feedback, where limiting conditions and actuation of reactor trip occur on timescales too rapid for secondary side conditions to influence the transient. For example, the high power conditions during a rod ejection last for a few seconds (FSAR Figure 15.4-18), whereas the loop transit time for RCS flow at full power is more than one minute (FSAR Section 15.9.4). Lower rod worth control rod ejection events are similar to single rod withdrawal event analyses where nominal SG heat transfer is modeled (TR-0516-49416-P, Revision 4, Table 7-68).

Similar to the reactivity insertion event (FSAR Section 15.4) analyses described above, the cooldown event (FSAR Section 15.1) analyses that have reactivity feedback and can result in higher power levels, where MCHFR is challenged, model nominal SG heat transfer

(TR-0516-49416-P, Revision 4, Tables 7-7, 7-19, 7-24, and 7-28). Nominal SG heat transfer is modeled {{

}}[2(a),(c)] For the increase in feedwater flow event (FSAR Section 15.1.2), the SG heat transfer is varied as identified in TR-0516-49416-P, Revision 4, Table 7-14. Accordingly, the US460 calculations for the increase in feedwater flow event include sensitivity cases examining the effect of higher and lower SG heat transfer coefficients. Table 1 summarizes results {{

}}[2(a),(c)]

the limiting MCHFR case for the increase in feedwater flow event biases the SG heat transfer high as shown in FSAR Table 15.1-6. These results indicate that a degradation of SG heat transfer due to potential DWO would increase margin to MCHFR in this event. Neglecting the potential impacts of DWO is therefore reasonable and appropriate.

Table 1:
Increase in Feedwater Flow Event (FSAR Section 15.1.2)
Sensitivity Calculation Results for Steam Generator Heat Transfer

{{

}}2(a),(c)

ECCS Valve Opening Events

Design-basis events where ECCS valves open, either as the initiating event (FSAR Section 15.6.6) or in response to a LOCA (FSAR Section 15.6.5), do not result in an increase in power after event initiation. However, these events can be limiting for MCHFR acceptance criteria. Therefore, the potential effects of secondary side instabilities are considered here.

For the design-basis events with a rapid high-pressure blowdown through the ECCS valves, the limiting MCHFR conditions occur in the first few seconds after event initiation (i.e., less than 5 seconds as shown in FSAR Tables 15.6-8 and 15.6-14). {{

}}2(a),(c)

As part of the assessment of the effects of a loss of augmented direct current power (EDAS) described in Section 15.0.0.6.5.3, calculations were performed comparing the effects of non-LOCA Chapter 15 events with a coincident loss of EDAS to the analyses in FSAR Section 15.6.6. The calculation results summarized in Table 2 {{

}}2(a),(c) Transient results of the comparisons in Table 2 are shown in Figure 2 through Figure 6. {{

}}2(a),(c) The potential impact of DWO does not need to be addressed in the Chapter 15 short-term analyses using the LOCA topical report methodology.

{{

}}2(a),(c)

Table 2:
Inadvertent Actuation of Emergency Core Cooling System Phase 0
Sensitivity Calculation Results for Concurrent Secondary Side Transient

{{

}}2(a),(c)

{{

}}2(a),(c)

Figure 2:
Inadvertent Actuation of Emergency Core Cooling System Phase 0
Sensitivity Calculation Results for Concurrent Secondary Side Transient
Minimum Critical Heat Flux Ratio

{{

}}2(a),(c)

Figure 3:
Inadvertent Actuation of Emergency Core Cooling System Phase 0
Sensitivity Calculation Results for Concurrent Secondary Side Transient
Reactor Power

{{

}}2(a),(c)

Figure 4:
Inadvertent Actuation of Emergency Core Cooling System Phase 0
Sensitivity Calculation Results for Concurrent Secondary Side Transient
Reactor Coolant System Pressure

{{

}}2(a),(c)

Figure 5:
Inadvertent Actuation of Emergency Core Cooling System Phase 0
Sensitivity Calculation Results for Concurrent Secondary Side Transient
Core Inlet Flow

{{

}}2(a),(c)

Figure 6:
Inadvertent Actuation of Emergency Core Cooling System Phase 0
Sensitivity Calculation Results for Concurrent Secondary Side Transient
Steam Generator Pressure (one of two SGs)

Based on these non-LOCA and LOCA sensitivity calculation results, it is concluded that changes in primary-to-secondary heat transfer due to effects of DWO, if it were to potentially occur during a transient event prior to reactor trip and associated power reduction, do not result in challenges to limiting MCHFR conditions occurring around the time of reactor trip.

The overall scope of design-basis event analyses in FSAR Chapter 15 is also considered. DWO in the SG during a transient could result in a decrease in primary-to-secondary side heat transfer coefficient. The design-basis events in FSAR Chapter 15 already include initiating events that result in a decrease in heat removal from the secondary side (FSAR Section 15.2), such as decreases in (or complete loss of) feedwater flow or loss of alternating current (AC) power. These events do not challenge SAFDLs for the NPM. Primary pressure acceptance criteria are challenged for decrease in heat removal events (FSAR Section 15.2) and increase in primary inventory events (FSAR Section 15.5). For events other than the SG tube failure, secondary side pressure peaks after DHRS actuation. In the SG tube failure event, maximum secondary pressure occurs after pressure equalization with the primary side. Primary and secondary pressure acceptance criteria are met based on the fundamentals of the NPM design. Specifically, the reactor safety valves (RSVs) protect against increases in primary pressure, and the design of the SG to have the same design pressure as the reactor pressure vessel (RPV) protects against increases in secondary pressure. The broad range of initiating events evaluated in FSAR Chapter 15 demonstrate the capacity of the NPM design to accommodate a wide range of conditions without challenging SAFDLs or design pressure limits, including the potential impact of instabilities. This conclusion is consistent with the safety evaluation report (SER) for the stability topical report (TR-0516-49417-P-A), where the NRC staff found that:

> *"Because there is no resonant interaction, the primary-side response to a change in oscillatory flow would match the primary-side response to a monotonic change in secondary-side flow of the same magnitude. Therefore, the staff finds that no special consideration is needed in those analyses to address the possible primary-side flow instability. Demonstration of adequate thermal margin in Chapter 15 of the FSAR is adequate to show that thermal margins are maintained during postulated changes in the secondary-side flow. In turn, this is sufficient to confirm that adequate thermal margins would be maintained during postulated secondary-side flow oscillations."*

Stability Analysis Sensitivities

The NRC-approved stability topical report (TR-0516-49417-P-A, Revision 1) includes the methodology for analyzing NPM stability with the PIM code. FSAR Section 15.9 includes the results of stability analyses for the US460 design. The results demonstrate that perturbations in

the secondary side do not result in instability in the primary side. FSAR Section 15.9.3.2 describes the analysis of a step decrease in feedwater flow, resulting in a step decrease in heat removal by the secondary system. {{

}}2(a),(c)

To supplement the FSAR Section 15.9 results {{

}}2(a),(c) sensitivity calculations are performed {{

}}2(a),(c) {{

}}2(a),(c),ECI {{

}}2(a),(c)

The magnitude of the core power and core flow oscillations are evaluated {{

}}2(a),(c) in Figure 7 through Figure 11. {{

}}2(a),(c)

{{

}}[2(a),(c)]

These stability sensitivity results confirm the stability topical report SER findings cited above for the US460 design. Specifically, there is no resonant interaction between potential secondary side oscillations and the primary side response.

Note that these analyses consider low power conditions (i.e., 20 percent and below) when the reactor is critical and there is forced feedwater flow. As discussed in the response to RSI 15, Chapter 15 events initiating from these low powers are typically less limiting than the events initiating from higher power levels. For similarly low power levels associated with post-trip decay heat, the secondary system removes heat using the DHRS in a natural circulation mode. The response to RSI 15 includes consideration of secondary side oscillations during DHRS operation.

{{

}}[2(a),(c)]

Figure 7:

Core Power Response {{ }}[2(a),(c)]

Initial Core Power of 5 percent

{{

}}2(a),(c)

Figure 8:

Core Power Response {{ }}2(a),(c)

Initial Core Power of 20 percent

{{

}}2(a),(c)

Figure 9:

Core Power Response {{ }}2(a),(c)

Initial Core Power of 25 percent

{{

}}[2(a),(c)]

Figure 10:

Core Power Response {{ }}[2(a),(c)]

Initial Core Power of 50 percent

{{

}}2(a),(c)

Figure 11:

Core Power Response {{ }}2(a),(c)

Initial Core Power of 100 percent

{{

}}2(a),(c)

Figure 12:

Transient Core Power Response {{

}}2(a),(c)

Initial Core Power of 5 percent at End of Cycle

{{

}}2(a),(c)

Figure 13:

Transient Core Power Response {{

}}2(a),(c)

Initial Core Power of 20 percent at End of Cycle

{{

}}2(a),(c)

Figure 14:

Transient Core Power Response {{

}}2(a),(c)

Initial Core Power of 25 percent at End of Cycle

{{

}}2(a),(c)

Figure 15:

Transient Core Power Response {{

}}2(a),(c)

Initial Core Power of 50 percent at End of Cycle

{{

}}2(a),(c)

Figure 16:

Transient Core Power Response {{

}}2(a),(c)

Initial Core Power of 100 percent at End of Cycle

Review of SIET TF-2 Data

The DWO topical report (TR-131981-P, Revision 0) describes SIET TF-2 testing performed in 2022. The effects of DWO that may be relevant to the safety analyses are investigated based on review of the SIET TF-2 data. {{

}}$^{2(a),(c),ECI}$ Results of the test data analysis for the oscillation period and magnitude are shown in Figure 17. {{

}}$^{2(a),(c),ECI}$

{{

}}$^{2(a),(c)}$

{{

}}2(a),(c),ECI

Figure 17:
Calculated Oscillations in Secondary Heat Transfer from SIET TF-2 Test Data

Design-Basis Event Transient Response to Imposed Heat Transfer Degradation

Sensitivity calculations with NRELAP5 were performed to further quantify the NPM behavior if DWO were assumed to occur during a transient event. These calculations provide additional quantitative demonstration that the potential effects of DWO are not significant with respect to margin to SAFDLs or peak RCS pressure acceptance criteria for design-basis event analysis. Maximum secondary side pressure occurs after reactor trip with secondary side isolation and DHRS actuation in the NPM design and is discussed in the response to RSI 15.

Secondary side conditions during operation and transients are constrained by the MPS actuations on steam pressure and steam superheat, particularly for reactor trip and secondary side isolation or DHRS actuation. It is expected that changes in secondary side conditions due to DWO that degrade SG performance could result in earlier MPS actuations based on these secondary conditions. The existing Chapter 15 analyses use a range of assumptions and conditions to explore a large range of possible MPS actuation times. Therefore, earlier actuation of MPS and reactor trip during a scenario would result in mitigation of the event when conditions are less limiting. For example, if an event with increasing power trips earlier, the power level will be lower than the scenario where the trip is delayed. The sensitivity studies described below demonstrate that variation in secondary side conditions in the NPM design due to DWO does not significantly reduce margin to SAFDLs or maximum primary pressure acceptance criteria.

The effects of DWO are evaluated {{

}}$^{2(a),(c)}$ are summarized in Table 3.

Two Chapter 15 events are selected as representative for the sensitivity calculation {{

}}$^{2(a),(c)}$

- Partial loss of feedwater event (FSAR Section 15.2.7)
- Uncontrolled control rod assembly withdrawal from power (FSAR Section 15.4.2)

A loss of feedwater event is representative of heatup events described in FSAR Section 15.2. {{

}}[2(a),(c)] Although power does not increase to levels above 100 percent during this event (i.e., the region of concern identified in this RSI), this event nevertheless provides insight into the potential effect of DWO at full power.

An uncontrolled control rod assembly withdrawal at power event is representative of reactivity insertion events described in FSAR Section 15.4. The bank withdrawal from power results in an increase in reactor power and RCS temperature. {{

}}[2(a),(c)] The bank withdrawal event results in power levels above 100 percent (i.e., the region of concern identified in this RSI). Cooldown events in FSAR Section 15.1 also can result in power levels above 100 percent. The bank withdrawal event is therefore also representative of cooldown events for consideration of potential DWO.

Events that increase primary side inventory (FSAR Section 15.5) can challenge primary pressure limits but do not affect core conditions and do not challenge MCHFR margins or secondary side pressure limits. Non-LOCA events that decrease primary side inventory (FSAR Sections 15.6.2 and 15.6.3) are not limiting for primary pressure limits or MCHFR margins. LOCA and IORV events that decrease primary side inventory (FSAR Sections 15.6.5 and 15.6.6) are addressed as described earlier in this response. Therefore, the two events selected above are appropriate to investigate the impact of potential DWO during a Chapter 15 event transient progression.

Table 3:
Secondary Side Oscillation – Methods for Sensitivity Calculations

{{

}}2(a),(c)

Partial Loss of Feedwater Flow Sensitivities

The sensitivity calculations for the partial loss of feedwater event are discussed first. The cases analyzed, and associated results, are provided in Table 4.

{{

}}2(a),(c)

Figure 18 through Figure 29 show transient results from the partial loss of feedwater {{

}}2(a),(c)

{{

}}2(a),(c)

The spectrum of responses observed in the sensitivity results is comparable to the spectrum of responses observed in the loss of feedwater analysis already performed in support of FSAR Section 15.2.7, where a range of feedwater reductions is modeled to determine limiting cases. Therefore, the range of loss of feedwater events analyzed in FSAR Chapter 15 ensure that the limiting conditions for acceptance criteria are identified, without requiring a specific analysis of subsequent secondary side oscillations during the transient progression. In the limiting case for peak RCS pressure, as presented in FSAR Section 15.2.7, a large rapid loss of feedwater results in rapid pressurization (FSAR Figure 15.2-28), and the RSVs lift to relieve pressure and maintain margin to the primary pressure acceptance criteria (FSAR Table 15.2-20). Comparing the results of these sensitivities {{ }}2(a),(c) to the limiting FSAR Section 15.2.7 analysis results demonstrates that the transient effects of DWO on primary pressure response are bounded within the existing design-basis calculations. As a representative heatup event, the conclusion of this loss of feedwater sensitivity can be extended in general to the heatup events considered in FSAR Section 15.2.

Table 4:
Sensitivity Calculations for Effects of Feedwater Oscillations
Loss of Feedwater Flow Event – Cases and Results

{{

}}2(a),(c)

{{

}}2(a),(c)

Figure 18:
Sensitivity Calculations for Effects of Feedwater Oscillations
Loss of Feedwater Flow Event {{ }}2(a),(c)
Feedwater Flow

{{

}}2(a),(c)

Figure 19:
Sensitivity Calculations for Effects of Feedwater Oscillations
Loss of Feedwater Flow Event {{ }}2(a),(c)
Core Power

{{

}}2(a),(c)

Figure 20:
Sensitivity Calculations for Effects of Feedwater Oscillations
Loss of Feedwater Flow Event {{ }}2(a),(c)
Reactor Coolant System Flow

{{

}}2(a),(c)

Figure 21:
Sensitivity Calculations for Effects of Feedwater Oscillations
Loss of Feedwater Flow Event {{ }}2(a),(c)
Reactor Coolant System Average Temperature

{{

}}2(a),(c)

Figure 22:
Sensitivity Calculations for Effects of Feedwater Oscillations
Loss of Feedwater Flow Event {{ }}2(a),(c)
Reactor Pressure Vessel Lower Plenum Pressure

{{

}}2(a),(c)

Figure 23:
Sensitivity Calculations for Effects of Feedwater Oscillations
Loss of Feedwater Flow Event {{ }}2(a),(c)
Pressurizer Level

{{

}}2(a),(c)

Figure 24:
Sensitivity Calculations for Effects of Feedwater Oscillations
Loss of Feedwater Flow Event {{ }}2(a),(c)
Total Pressurizer Spray Flow

{{

}}2(a),(c)

Figure 25:
Sensitivity Calculations for Effects of Feedwater Oscillations
Loss of Feedwater Flow Event {{ }}2(a),(c)
Steam Generator Power

{{

}}2(a),(c)

Figure 26:
Sensitivity Calculations for Effects of Feedwater Oscillations
Loss of Feedwater Flow Event {{ }}2(a),(c)
Steam Generator Pressure (one of two SGs)

{{

}}2(a),(c)

Figure 27:
Sensitivity Calculations for Effects of Feedwater Oscillations
Loss of Feedwater Flow Event {{ }}2(a),(c)
Steam Generator Superheat (one of two SGs)

{{

}}2(a),(c)

Figure 28:
Sensitivity Calculations for Effects of Feedwater Oscillations
Loss of Feedwater Flow Event {{ }}2(a),(c)
Steam Generator Level (one of two SGs)

{{

}}2(a),(c)

Figure 29:
Sensitivity Calculations for Effects of Feedwater Oscillations
Loss of Feedwater Flow Event {{ }}2(a),(c)
Decay Heat Removal System Flow (one of two DHRS trains)

The second set of sensitivities for the loss of feedwater event {{

}}[2(a),(c)] {{

}}[2(a),(c),ECI] Results are provided in Table 4 and Figure 30 through Figure 41.

{{

}}[2(a),(c)] The results of these sensitivity cases demonstrate that postulated oscillation in the primary-to-secondary heat transfer does not result in a limiting condition with respect to primary or secondary pressure limits or SAFDLs.

{{

}}[2(a),(c)]

{{

}}2(a),(c)

{{

}}2(a),(c)

Figure 30:
Sensitivity Calculations for Effects of Feedwater Oscillations
Loss of Feedwater Flow Event {{ }}2(a),(c)
Feedwater Flow

{{

}}2(a),(c)

Figure 31:
Sensitivity Calculations for Effects of Feedwater Oscillations
Loss of Feedwater Flow Event {{ }}2(a),(c)
Core Power

{{

}}2(a),(c)

Figure 32:
Sensitivity Calculations for Effects of Feedwater Oscillations
Loss of Feedwater Flow Event {{ }}2(a),(c)
Reactor Coolant System Flow

{{

}}2(a),(c)

Figure 33:
Sensitivity Calculations for Effects of Feedwater Oscillations
Loss of Feedwater Flow Event {{ }}2(a),(c)
Reactor Coolant System Average Temperature

{{

}}2(a),(c)

Figure 34:
Sensitivity Calculations for Effects of Feedwater Oscillations
Loss of Feedwater Flow Event {{ }}2(a),(c)
Reactor Pressure Vessel Lower Plenum Pressure

{{

}}2(a),(c)

Figure 35:
Sensitivity Calculations for Effects of Feedwater Oscillations
Loss of Feedwater Flow Event {{ }}2(a),(c)
Pressurizer Pressure (extended duration)

{{

}}2(a),(c)

Figure 36:
Sensitivity Calculations for Effects of Feedwater Oscillations
Loss of Feedwater Flow Event {{ }}2(a),(c)
Pressurizer Level

{{

}}2(a),(c)

Figure 37:
Sensitivity Calculations for Effects of Feedwater Oscillations
Loss of Feedwater Flow Event {{ }}2(a),(c)
Total Pressurizer Spray Flow

{{

}}2(a),(c)

Figure 38:
Sensitivity Calculations for Effects of Feedwater Oscillations
Loss of Feedwater Flow Event {{ }}2(a),(c)
Steam Generator Power

{{

}}2(a),(c)

Figure 39:
Sensitivity Calculations for Effects of Feedwater Oscillations
Loss of Feedwater Flow Event {{ }}2(a),(c)
Steam Generator Pressure (one of two SGs)

{{

}}2(a),(c)

Figure 40:
Sensitivity Calculations for Effects of Feedwater Oscillations
Loss of Feedwater Flow Event {{ }}2(a),(c)
Steam Generator Superheat (one of two SGs)

{{

}}2(a),(c)

Figure 41:
Sensitivity Calculations for Effects of Feedwater Oscillations
Loss of Feedwater Flow Event {{ }}2(a),(c)
Steam Generator Levels (one of two SGs)

Uncontrolled Control Rod Assembly Withdrawal at Power Sensitivities

Similar to the loss of feedwater flow sensitivities previously discussed, sensitivity calculations are performed for the uncontrolled control rod assembly withdrawal event. The transient is initiated from full power by adding reactivity at a constant rate to the core, simulating withdrawal of a control rod assembly bank. The cases analyzed, and associated results, are provided in Table 5.

The analyses of the rod withdrawal at power event in FSAR Section 15.4.2 consider a wide range of reactivity insertion rates. For large reactivity insertion rates, the reactor trip occurs shortly after event initiation. For example, the case that is limiting for linear heat generation rate (LHGR) described in FSAR Table 15.4-6 and Table 15.4-7 results in a reactor trip within 5 seconds on high power rate. {{

}}2(a),(c)

Figure 42 through Figure 53 show transient results from the uncontrolled control rod assembly withdrawal at power {{

}}2(a),(c)

{{

}}[2(a),(c)] Comparing the results of these sensitivities {{ }}[2(a),(c)] to the limiting FSAR Section 15.4.2 analysis results demonstrates that the transient effects of DWO on primary pressure response are bounded within the existing design-basis calculations reported in the FSAR. As a representative reactivity insertion event, the conclusion of this uncontrolled control rod assembly withdrawal at power sensitivity can be extended in general to the reactivity insertion events from high power conditions considered in FSAR Section 15.4. Similarly, these sensitivity analysis results are applicable to cooldown events in FSAR Section 15.1 that result in an increase in power during the event progression.

Table 5:
Sensitivity Calculations for Effects of Feedwater Oscillations
Uncontrolled Control Rod Assembly Withdrawal at Power Event – Cases and Results

{{

}}2(a),(c)

{{

}}2(a),(c)

Figure 42:
Sensitivity Calculations for Effects of Feedwater Oscillations
Uncontrolled Control Rod Assembly Withdrawal {{ }}2(a),(c)
Feedwater Flow

{{

}}2(a),(c)

Figure 43:
Sensitivity Calculations for Effects of Feedwater Oscillations
Uncontrolled Control Rod Assembly Withdrawal {{ }}2(a),(c)
Core Power

{{

}}2(a),(c)

Figure 44:
Sensitivity Calculations for Effects of Feedwater Oscillations
Uncontrolled Control Rod Assembly Withdrawal {{ }}2(a),(c)
Reactor Coolant System Flow

{{

}}2(a),(c)

Figure 45:
Sensitivity Calculations for Effects of Feedwater Oscillations
Uncontrolled Control Rod Assembly Withdrawal {{ }}2(a),(c)
Reactor Coolant System Average Temperature

{{

}}2(a),(c)

Figure 46:
Sensitivity Calculations for Effects of Feedwater Oscillations
Uncontrolled Control Rod Assembly Withdrawal {{ }}2(a),(c)
Reactor Pressure Vessel Lower Plenum Pressure

{{

}}2(a),(c)

Figure 47:
Sensitivity Calculations for Effects of Feedwater Oscillations
Uncontrolled Control Rod Assembly Withdrawal {{ }}2(a),(c)
Pressurizer Level

{{

}}2(a),(c)

Figure 48:
Sensitivity Calculations for Effects of Feedwater Oscillations
Uncontrolled Control Rod Assembly Withdrawal {{ }}2(a),(c)
Total Pressurizer Spray Flow

{{

}}2(a),(c)

Figure 49:
Sensitivity Calculations for Effects of Feedwater Oscillations
Uncontrolled Control Rod Assembly Withdrawal {{ }}2(a),(c)
Steam Generator Power

{{

}}2(a),(c)

Figure 50:
Sensitivity Calculations for Effects of Feedwater Oscillations
Uncontrolled Control Rod Assembly Withdrawal {{ }}2(a),(c)
Steam Generator Pressure (one of two SGs)

{{

}}2(a),(c)

Figure 51:
Sensitivity Calculations for Effects of Feedwater Oscillations
Uncontrolled Control Rod Assembly Withdrawal {{ }}2(a),(c)
Steam Generator Superheat (one of two SGs)

{{

}}2(a),(c)

Figure 52:
Sensitivity Calculations for Effects of Feedwater Oscillations
Uncontrolled Control Rod Assembly Withdrawal {{ }}2(a),(c)
Steam Generator Level (one of two SGs)

{{

}}2(a),(c)

Figure 53:
Sensitivity Calculations for Effects of Feedwater Oscillations
Uncontrolled Control Rod Assembly Withdrawal {{ }}2(a),(c)
Decay Heat Removal System Flow (one of two DHRS trains)

The second set of sensitivities for the uncontrolled control rod assembly withdrawal at power event {{

}}2(a),(c) {{

}}2(a),(c),ECI Results are provided in Table 5 and Figure 54 through Figure 65.

{{

}}2(a),(c)

The results of these sensitivity cases demonstrate that {{

}}2(a),(c) do not result in a limiting condition with respect to primary or secondary pressure or SAFDLs. Therefore, modeling of nominal secondary side conditions and behavior is an adequate analysis assumption for reactivity insertion events that challenge MCHFR. As a representative reactivity insertion event, the conclusion of this uncontrolled control rod assembly withdrawal at power sensitivity can be extended in general to the reactivity insertion events from high power conditions considered in FSAR Section 15.4. Similarly, these sensitivity analysis results are applicable to cooldown events in FSAR Section 15.1 that result in an increase in power during the event progression.

{{

}}2(a),(c)

Figure 54:
Sensitivity Calculations for Effects of Feedwater Oscillations
Uncontrolled Control Rod Assembly Withdrawal {{ }}2(a),(c)
Feedwater Flow

{{

}}2(a),(c)

Figure 55:
Sensitivity Calculations for Effects of Feedwater Oscillations
Uncontrolled Control Rod Assembly Withdrawal {{ }}2(a),(c)
Core Power

{{

}}2(a),(c)

Figure 56:
Sensitivity Calculations for Effects of Feedwater Oscillations
Uncontrolled Control Rod Assembly Withdrawal {{ }}2(a),(c)
Reactor Coolant System Flow

{{

}}2(a),(c)

Figure 57:
Sensitivity Calculations for Effects of Feedwater Oscillations
Uncontrolled Control Rod Assembly Withdrawal {{ }}2(a),(c)
Reactor Coolant System Average Temperature

{{

}}2(a),(c)

Figure 58:
Sensitivity Calculations for Effects of Feedwater Oscillations
Uncontrolled Control Rod Assembly Withdrawal {{ }}2(a),(c)
Reactor Pressure Vessel Lower Plenum Pressure

{{

}}2(a),(c)

Figure 59:
Sensitivity Calculations for Effects of Feedwater Oscillations
Uncontrolled Control Rod Assembly Withdrawal {{ }}2(a),(c)
Pressurizer Level

{{

}}2(a),(c)

Figure 60:
Sensitivity Calculations for Effects of Feedwater Oscillations
Uncontrolled Control Rod Assembly Withdrawal {{ }}2(a),(c)
Total Pressurizer Spray Flow

{{

}}2(a),(c)

Figure 61:
Sensitivity Calculations for Effects of Feedwater Oscillations
Uncontrolled Control Rod Assembly Withdrawal {{ }}2(a),(c)
Steam Generator Power

{{

}}2(a),(c)

Figure 62:
Sensitivity Calculations for Effects of Feedwater Oscillations
Uncontrolled Control Rod Assembly Withdrawal {{ }}2(a),(c)
Steam Generator Pressure (one of two SGs)

{{

}}2(a),(c)

Figure 63:
Sensitivity Calculations for Effects of Feedwater Oscillations
Uncontrolled Control Rod Assembly Withdrawal {{ }}2(a),(c)
Steam Generator Superheat (one of two SGs)

{{

}}2(a),(c)

Figure 64:
Sensitivity Calculations for Effects of Feedwater Oscillations
Uncontrolled Control Rod Assembly Withdrawal {{ }}2(a),(c)
Steam Generator Level (one of two SGs)

{{

}}2(a),(c)

Figure 65:
Sensitivity Calculations for Effects of Feedwater Oscillations
Uncontrolled Control Rod Assembly Withdrawal {{ }}2(a),(c)
Decay Heat Removal System Flow (one of two DHRS trains)

Summary of Technical Justification

In summary, considering: (1) the range of SG heat transfer sensitivities covered in the existing safety analyses, (2) the PIM stability analyses that demonstrate minimal primary impact from secondary oscillations at high frequencies (small periods), (3) the impact of DWO on primary-to-secondary heat transfer determined from SIET TF-2 test data testing, (4) the results of NRELAP5 sensitivity studies that include {{ }}[2(a),(c)], and (5) the results of NRELAP5 sensitivity studies that evaluate {{ }}[2(a),(c)], it is concluded that oscillatory behavior that may occur in the SG does not impact the margins for relevant acceptance criteria for Chapter 15 design-basis events, including events where power may exceed 100 percent. Specifically, oscillatory behavior that may occur in the secondary side does not meaningfully impact the plant conditions that are used to assess SAFDLs or peak pressures. Additional modeling or special treatment of oscillatory behavior beyond that already included in the safety analysis methodology topical reports is not required to ensure the adequacy of the safety analyses in the FSAR.

Impact on US460 SDA:

There are no impacts to US460 SDA as a result of this response.

Additional Information:

Topical report TR-0516-49416, Non-Loss-of-Coolant Accident Analysis Methodology, is revised to include further discussion of potential instabilities. The markups are provided with the response to RSI 15.

Response to Request for Additional Information
Docket: 99902078

RAI No.: RSI
Date of RAI Issue: 03/27/2023

NRC Question No.: RSI-17

Missing sufficient information on updates to scaling analyses in the LOCA and non-LOCA LTRs due to the changed design. No sufficient scaling analysis updates are included to capture higher power operations for RCS, containment and cooling pool in NPM-20 and NIST-2. No sufficient details are provided to justify extending the similarity of NPM-160/NIST-1 to NPM-20/NIST-2 in terms of the distortion analysis of important phenomena. This scaling analysis is discussed in the justification for applicability of the NRELAP5 code but not provided in the submission. The scaling analyses regarding DHRS operation with the modeling of DWO or other two-phase instabilities on the steam generator secondary side when DHRS is activated are not included in the LTRs.

NuScale Response:

Response Summary:

The relevant topical reports are revised to include further discussion of the scaling analyses. Qualitative explanations and quantitative studies demonstrate that the scaling analyses are adequate regardless of the potential for secondary side instabilities.

Detailed Response:

Scaling analyses are performed for the loss-of-coolant accident (LOCA) and non-LOCA topical reports to support the standard design approval application (SDAA) submittals. The topical reports describe that the scaling analyses support the applicability of the NRELAP5 code, but do not provide details of the scaling analyses in the reports themselves. Additional information about the LOCA and inadvertent opening of a reactor valve (IORV) scaling analyses is added to the LOCA topical report as shown in the markups included with the response to this request for

supplemental information (RSI). Similarly, additional information about the non-LOCA scaling analyses is added to the non-LOCA topical report as shown in the markups included with the response to RSI 15.

This RSI requests information regarding the use of scaling analyses to address density wave oscillation (DWO) or other two-phase instabilities on the steam generator (SG) secondary side when the decay heat removal system (DHRS) is operation. As described in Section 5.3.7.3 of the non-LOCA topical report, the DHRS behavior during non-LOCA events is applicable to the behavior of LOCAs during DHRS operation prior to emergency core cooling system (ECCS) actuation. Therefore, scaling analyses associated with the DHRS are performed as part of the non-LOCA applicability assessments. The extended passive cooling (XPC) topical report, Section 4.4, also refers to the NRELAP5 validation basis developed for non-LOCA. Therefore, the focus of this response is on the non-LOCA evaluation model (EM) scaling basis as it relates to the NIST-2 facility, because the code validation against the NIST-2 facility test data, and examination of NuScale Power Module (NPM) DHRS heat transfer during LOCA and non-LOCA events, provides confidence in the NRELAP5 prediction of DHRS heat transfer during design-basis events.

As part of the non-LOCA EM development to evaluate EM adequacy, a top-down scaling analysis is performed. Note that the complete scaling analysis, ER-126485, is provided in the electronic reading room (eRR) as part of the response to SDAA audit question A-NonLOCA.LTR-3. The scaling analysis compares dimensionless Π groups for the governing field equations of liquid mass, total energy, and total momentum balances in the DHRS loop. Comparisons are made between {{

}}2(a),(c),ECI

The SG/DHRS loop is a boiling/condensation-driven natural circulation system. {{

}}2(a),(c),ECI

{{

}}2(a),(c),ECI

The instantaneous Π group balance equations for the total liquid mass in the SG and DHRS loop are given by Equations 1 and 2, respectively. {{

}}2(a),(c),ECI

The instantaneous Π group balance equation for the total energy balance is given in Equation 3. {{

}}2(a),(c),ECI

The instantaneous Π group balance equation for the total two-phase mixture fluid momentum conservation in the SG/DHRS loop is given in Equation 4. {{

}}2(a),(c),ECI

{{

}}2(a),(c),ECI

{{

}}2(a),(c)

{{

}}2(a),(c),ECI

{{

}}2(a),(c),ECI

Figure 1:
Normalized Time-Averaged Π groups for Decay Heat Removal System Energy Balance

{{ }}2(a),(c),ECI

where: {{

}}2(a),(c),ECI

{{

}}2(a),(c),ECI

Figure 2:
Normalized Time-Averaged Π groups for Decay Heat Removal System Momentum Balance

{{ }}2(a),(c),ECI

where: {{

}}2(a),(c),ECI

The post-test scaling analysis is performed for the NIST-2 Run 1 test, {{

}}[2(a),(c),ECI] Sensitivity studies varying liquid region form losses, which would similarly change the resistance in this region, indicate negligible impact on NPM or NIST-2 behavior during DHRS operation:

- The response to RSI 14 provides NPM sensitivity calculation results with varying SG inlet flow restrictor losses that change the liquid region line form losses in the SG. Although performed for the SG inlet rather than the DHRS condensate line, the sensitivity calculation results show negligible impact on the NPM from increased liquid region line form losses.
- Sensitivity studies were performed for NIST-2 prior to testing to determine the impact of the form loss from the flow meter in the DHRS condensate line. The condensate line form loss was increased and decreased by a factor of {{ }}[2(a),(c)]. Results for the increased form loss are shown in Figure 3 through Figure 8 and results for the decreased form loss are shown in Figure 9 through 14. The NIST-2 sensitivity results demonstrate that the impact of the condensate line form loss is minimal over a wide range of conditions.

Therefore, it is concluded that condensate line flow (velocity) oscillations would not affect the conclusions of the scaling analysis.

{{

}}2(a),(c)

Figure 3:
NIST-2 Decay Heat Removal Sensitivity Study for Loss of Feedwater Event
Core, Steam Generator, and Decay Heat Removal System Heat Exchanger Powers

where: {{

}}2(a),(c)

{{

}}[2(a),(c)]

Figure 4:
NIST-2 Decay Heat Removal Sensitivity Study for Loss of Feedwater Event
Decay Heat Removal System Flow

where: {{

}}[2(a),(c)]

{{

}}2(a),(c)

Figure 5:
NIST-2 Decay Heat Removal Sensitivity Study for Loss of Feedwater Event
Steam Generator and Decay Heat Removal System Heat Exchanger Levels

where: {{

}}2(a),(c)

{{

}}2(a),(c)

Figure 6:
NIST-2 Decay Heat Removal Sensitivity Study for Loss of Feedwater Event
Decay Heat Removal System Heat Exchanger Temperatures

where: {{

}}2(a),(c)

{{

}}2(a),(c)

Figure 7:
NIST-2 Decay Heat Removal Sensitivity Study for Loss of Feedwater Event
Steam Generator Secondary Inlet and Outlet Temperatures

where: {{

}}2(a),(c)

{{

}}2(a),(c)

Figure 8:
NIST-2 Decay Heat Removal Sensitivity Study for Loss of Feedwater Event
Steam Generator Primary Inlet and Outlet Temperatures

where: {{

}}2(a),(c)

{{

}}[2(a),(c)]

Figure 9:
NIST-2 Decay Heat Removal Sensitivity Study for Loss of Feedwater Event
Core, Steam Generator, and Decay Heat Removal System Heat Exchanger Powers

where: {{

}}[2(a),(c)]

{{

}}2(a),(c)

Figure 10:
NIST-2 Decay Heat Removal Sensitivity Study for Loss of Feedwater Event
Decay Heat Removal System Flow

where: {{

}}2(a),(c)

{{

}}2(a),(c)

Figure 11:
NIST-2 Decay Heat Removal Sensitivity Study for Loss of Feedwater Event
Steam Generator and Decay Heat Removal System Heat Exchanger Levels

where: {{

}}2(a),(c)

{{

}}2(a),(c)

Figure 12:
NIST-2 Decay Heat Removal Sensitivity Study for Loss of Feedwater Event
Decay Heat Removal System Heat Exchanger Temperatures

where: {{

}}2(a),(c)

{{

}}2(a),(c)

Figure 13:
NIST-2 Decay Heat Removal Sensitivity Study for Loss of Feedwater Event
Steam Generator Secondary Inlet and Outlet Temperatures

where: {{

}}2(a),(c)

{{

}}2(a),(c)

Figure 14:
NIST-2 Decay Heat Removal Sensitivity Study for Loss of Feedwater Event
Steam Generator Primary Inlet and Outlet Temperatures

where: {{

}}2(a),(c)

The response to RSI 15 includes sensitivity studies with {{ }}[2(a),(c)] oscillations in the SG/DHRS loop. The sensitivity study results demonstrate that the SG/DHRS loop continues to remove heat and margin to the figures of merit predicted by NRELAP5 are not affected. These results are reasonable considering the bottom-up assessment of NRELAP5 models and correlations to predict high-ranked phenomena such as {{

}}[2(a),(c)] The NIST-2 data scales well to the NPM for all major momentum and energy balance Π groups. Assessment of the NIST-2 data, included with the response to RSI 15, shows reasonable to excellent agreement between NRELAP5 prediction of overall heat transfer and the test data {{

}}[2(a),(c),ECI]

In conclusion, the scaling analyses for the NPM-20 SG/DHRS operation are adequate to support the non-LOCA, LOCA, and XPC EMs considering the potential effects of boiling/condensing loop oscillations.

Impact on US460 SDA:

There are no impacts to US460 SDA as a result of this response.

Additional Information:

Topical reports TR-0516-49422, Loss-of-Coolant Accident Evaluation Model, and TR-0516-49416, Non-Loss-of-Coolant Accident Analysis Methodology, are revised to include further discussion of the scaling analyses. The markups for TR-0516-49422, Loss-of-Coolant Accident Evaluation Model, are provided in this response. The markups for TR-0516-49416, Non-Loss-of-Coolant Accident Analysis Methodology, are provided with the response to RSI 15.

{{

}}2(a),(c)

8.2.22.2 Technical Evaluation

{{

}}2(a),(c)

8.3 Evaluation of Integral Performance (Top-Down Assessment)

There are three primary areas addressed by the top-down assessment.

- {{

RSI 17

}}2(a),(c)

To ensure maximum fidelity of the assessments, the NRELAP5 NIST and NPM input models were developed using consistent nodalization and option selection. Code assessments are also performed against SETs to establish code capabilities for predicting local behavior within unique NPM components. Assessments against SETs are addressed in Section 8.2.1.

RSI 17

These Π groups were evaluated in LOCA Phase 1a and Phase 1b based on NRELAP5 simulations of the NPM and as built NIST facility for the following events:

- 100 percent discharge line break on the CVCS line (similar to NIST-1 HP-06 and NIST-2 Run 1)
- 100 percent high point vent line break (Similar to NIST-1 HP-07 and NIST-2 Run 2)
- Inadvertent opening of a single RVV (Similar to NIST-1 HP-09 and NIST-2 Run 3)

RSI 17

- Inadvertent opening of a single RRV (Similar to NIST-1 HP-49 and NIST-2 Run 4)

RSI 17

Phase-wise time-averaged Π groups comparing dominant phenomena between NPM designs (NPM-160 and NPM-20) are shown in Figure 8-15 through Figure 8-18 for a liquid space discharge line break (HP06). Similar scaling analysis results are shown in Figure 8-19 through Figure 8-22 for a vapor space inadvertent RVV opening event (HP09). {{

}}$^{2(a),(c)}$ Comparisons of phase-wise time averaged Π groups comparing dominant phenomena between the NPM and NIST facility (specifically NPM-20 and NIST-2) are shown in Figure 8-23 through Figure 8-26 for HP06 and in Figure 8-27 through Figure 8-30 for HP09. These scaling analysis results are representative of results for a spray line break or inadvertent RRV opening. The below discussion was originally developed for the NPM-160 to NIST-1 comparison; {{

}}$^{2(a),(c)}$ The key conclusions of this analysis are summarized below.

1. {{

}}$^{2(a),(c)}$

{{

RSI 17

RSI 17

RSI 17

RSI 17

}}2(a),(c)

6. {{

RSI 17

RSI 17

RSI 17

RSI 17

}}[2(a),(c)] The scaling and distortion analysis methodology presented above

is used to analyze the impact of biases in initial and boundary conditions and differences in operating procedures of the final NIST-1 IET data used in Section 8.3.4.

RSI 17

The IORV Phase 0 top-down scaling analysis focuses on the RPV depressurization. {{

}}2(a),(c) Three representative events are analyzed:

RSI 17

1. Opening of a single RVV
2. Opening of a single RRV
3. Opening of all ECCS valves (for an NPM design with no IABs on any ECCS valves)

RSI 17

The Π groups are averaged over Phase 0 and normalized to unity by the maximum value of the Π groups within the mass (inventory) or energy (pressure) balances. The phase-wise time-averaged normalized Π group results are shown in Figure 8-31, Figure 8-32, and Figure 8-33 for the RVV opening, RRV opening, and all ECCS valve opening cases, respectively.

RSI 17

{{

RSI 17

}}2(a),(c)

RSI 17

{{

}}2(a),(c)

RSI 17

Based on this scaling and distortion analysis, it is concluded that distortions between model and prototype are understood and acceptable, and the initial RCS depressurization in Phase 0 can be well-simulated at the NIST facility.

RSI 17

Figure 8-15 NuScale Power Module comparisons of phase-wise time-averaged and normalized Π groups for reactor pressure vessel mixture/liquid mass, HP06, Phases 1a and 1b

{{

}}2(a),(c)

RSI 17

Figure 8-16 NuScale Power Module comparisons of phase-wise time-averaged and normalized Π groups for reactor pressure vessel pressure, HP06, Phases 1a and 1b

{{

}}2(a),(c)

RSI 17

Figure 8-17 NuScale Power Module comparisons of phase-wise time-averaged and normalized Π groups for containment vessel mixture/liquid mass, HP06, Phases 1a and 1b

{{

}}2(a),(c)

RSI 17

Figure 8-18 NuScale Power Module comparisons of phase-wise time-averaged and normalized Π groups for containment vessel pressure, HP06, Phases 1a and 1b

{{

}}2(a),(c)

RSI 17

Figure 8-19 NuScale Power Module comparisons of phase-wise time-averaged and normalized Π groups for reactor pressure vessel mixture/liquid mass, HP09, Phases 1a and 1b

{{

}}2(a),(c)

RSI 17

Figure 8-20 NuScale Power Module comparisons of phase-wise time-averaged and normalized Π groups for reactor pressure vessel pressure, HP09, Phases 1a and 1b

{{

}}2(a),(c)

RSI 17

Figure 8-21 NuScale Power Module comparisons of phase-wise time-averaged and normalized Π groups for containment vessel mixture/liquid mass, HP09, Phases 1a and 1b

{{

}}2(a),(c)

RSI 17

Figure 8-22 NuScale Power Module comparisons of phase-wise time-averaged and normalized Π groups for containment vessel pressure, HP09, Phases 1a and 1b

{{

}}2(a),(c)

RSI 17

Figure 8-23 NuScale Power Module to NIST comparisons of phase-wise time-averaged and normalized Π groups for reactor pressure vessel mixture/liquid mass, HP06, Phases 1a and 1b

{{

}}2(a),(c)

RSI 17

Figure 8-24 NuScale Power Module to NIST comparisons of phase-wise time-averaged and normalized Π groups for reactor pressure vessel pressure, HP06, Phases 1a and 1b

{{

}}2(a),(c)

RSI 17

Figure 8-25 NuScale Power Module to NIST comparisons of phase-wise time-averaged and normalized Π groups for containment vessel mixture/liquid mass, HP06, Phases 1a and 1b

{{

}}2(a),(c)

RSI 17

Figure 8-26 NuScale Power Module to NIST comparisons of phase-wise time-averaged and normalized Π groups for containment vessel pressure, HP06, Phases 1a and 1b

{{

}}2(a),(c)

RSI 17

Figure 8-27 NuScale Power Module to NIST comparisons of phase-wise time-averaged and normalized Π groups for reactor pressure vessel mixture/liquid mass, HP09, Phases 1a and 1b

{{

}}2(a),(c)

RSI 17

Figure 8-28 NuScale Power Module to NIST comparisons of phase-wise time-averaged and normalized Π groups for reactor pressure vessel pressure, HP09, Phases 1a and 1b

{{

}}2(a),(c)

RSI 17

Figure 8-29 NuScale Power Module to NIST comparisons of phase-wise time-averaged and normalized Π groups for containment vessel mixture/liquid mass, HP09, Phases 1a and 1b

{{

}}2(a),(c)

RSI 17

Figure 8-30 NuScale Power Module to NIST comparisons of phase-wise time-averaged and normalized Π groups for containment vessel pressure, HP09, Phases 1a and 1b

{{

}}2(a),(c)

RSI 17

Figure 8-31 NuScale Power Module to NIST comparisons of phase-wise time-averaged and normalized Π groups for reactor pressure vessel mass and energy, inadvertent opening of a single reactor vent valve, Phase 0

{{

}}2(a),(c)

RSI 17

Figure 8-32 NuScale Power Module to NIST comparisons of phase-wise time-averaged and normalized Π groups for reactor pressure vessel mass and energy, inadvertent opening of a single reactor recirculation valve, Phase 0

{{

}}2(a),(c)

RSI 17

Figure 8-33 NuScale Power Module to NIST comparisons of phase-wise time-averaged and normalized Π groups for reactor pressure vessel mass and energy, inadvertent opening of all emergency core cooling system valves, Phase 0

{{

}}2(a),(c)

{{

}}2(a),(c)

8.3.5 Calculation of Peak CNV pressure

RSI 17

Since containment is an integral part of the NPM ECCS, Section 4.3 identifies peak containment pressure as one of the LOCA EM FOMs. ~~However, as identified earlier in Section 4.3~~As described in Section 5.6, the peak containment pressure and temperature for containment performance are calculated with biased geometry, and initial and boundary conditions to maximize mass and energy release from the RPV and CNV pressurization response.~~a different methodology (Containment Response Analysis Methodology - Reference 109).~~ The top-down scaling analysis of Π groups representing the inventory and energy balance equations (Section 8.3.2) can be used to provide more insights on the processes/phenomena governing the peak containment pressure. It is observed that the CNV pressurization during Phase 1a of the liquid space break is governed by {{

}}2(a),(c). As described in Section 9.0 of this report, the peak CNV pressure occurs following ECCS actuation in liquid space breaks. It is observed that the major processes that contribute to CNV pressurization during the early part of Phase 1b are {{

}}2(a),(c)

8.4 Summary of Adequacy Findings

8.4.1 Findings from Bottom-Up Evaluation

The bottom-up evaluation focused on determining the pedigree, applicability, fidelity to SET data, and scalability of the NRELAP5 closure relations and correlations that model the high-ranked phenomena as determined by the PIRT panel.

The pedigree of the identified closure relations and correlations was first established based on their historical development and subsequent assessment in the literature. Assessment cases were then identified to demonstrate the capability of NRELAP5 to

Enclosure 3:

Affidavit of Mark W. Shaver, AF-145426

NuScale Power, LLC
1100 NE Circle Blvd., Suite 200 Corvallis, Oregon 97330 Office 541.360.0500 Fax 541.207.3928
www.nuscalepower.com

NuScale Power, LLC

AFFIDAVIT of Mark W. Shaver

I, Mark W. Shaver, state as follows:

(1) I am the Director of Regulatory Affairs of NuScale Power, LLC (NuScale), and as such, I have been specifically delegated the function of reviewing the information described in this Affidavit that NuScale seeks to have withheld from public disclosure, and am authorized to apply for its withholding on behalf of NuScale

(2) I am knowledgeable of the criteria and procedures used by NuScale in designating information as a trade secret, privileged, or as confidential commercial or financial information. This request to withhold information from public disclosure is driven by one or more of the following:

(a) The information requested to be withheld reveals distinguishing aspects of a process (or component, structure, tool, method, etc.) whose use by NuScale competitors, without a license from NuScale, would constitute a competitive economic disadvantage to NuScale.

(b) The information requested to be withheld consists of supporting data, including test data, relative to a process (or component, structure, tool, method, etc.), and the application of the data secures a competitive economic advantage, as described more fully in paragraph 3 of this Affidavit.

(c) Use by a competitor of the information requested to be withheld would reduce the competitor's expenditure of resources, or improve its competitive position, in the design, manufacture, shipment, installation, assurance of quality, or licensing of a similar product.

(d) The information requested to be withheld reveals cost or price information, production capabilities, budget levels, or commercial strategies of NuScale.

(e) The information requested to be withheld consists of patentable ideas.

(3) Public disclosure of the information sought to be withheld is likely to cause substantial harm to NuScale's competitive position and foreclose or reduce the availability of profit-making opportunities. The accompanying responses reveal distinguishing aspects about the method by which NuScale develops its evaluation model for determining density wave oscillation (DWO) onset, as well as the treatment of DWO within the US460 design.

NuScale has performed significant research and evaluation to develop a basis for this evaluation method and has invested significant resources, including the expenditure of a considerable sum of money.

The precise financial value of the information is difficult to quantify, but it is a key element of the design basis for a NuScale plant and, therefore, has substantial value to NuScale.

If the information were disclosed to the public, NuScale's competitors would have access to the information without purchasing the right to use it or having been required to undertake a similar expenditure of resources. Such disclosure would constitute a misappropriation of NuScale's intellectual property, and would deprive NuScale of the opportunity to exercise its competitive advantage to seek an adequate return on its investment.

(4) The information sought to be withheld is in the enclosed responses entitled NuScale Power, LLC Submittal of Responses to NRC RSIs on Topical Report, "Methodology for the Determination of the Onset of Density Wave Oscillation (DWO)." The enclosure contains the designation "Proprietary" at the top of each page containing proprietary information. The information considered by NuScale to be proprietary is identified within double braces, "{{ }}" in the document.

(5) The basis for proposing that the information be withheld is that NuScale treats the information as a trade secret, privileged, or as confidential commercial or financial information. NuScale relies upon the exemption from disclosure set forth in the Freedom of Information Act ("FOIA"), 5 USC § 552(b)(4), as well as exemptions applicable to the NRC under 10 CFR §§ 2.390(a)(4) and 9.17(a)(4).

(6) Pursuant to the provisions set forth in 10 CFR § 2.390(b)(4), the following is provided for consideration by the Commission in determining whether the information sought to be withheld from public disclosure should be withheld:

(a) The information sought to be withheld is owned and has been held in confidence by NuScale.

(b) The information is of a sort customarily held in confidence by NuScale and, to the best of my knowledge and belief, consistently has been held in confidence by NuScale. The procedure for approval of external release of such information typically requires review by the staff manager, project manager, chief technology officer or other equivalent authority, or the manager of the cognizant marketing function (or his delegate), for technical content, competitive effect, and determination of the accuracy of the proprietary designation. Disclosures outside NuScale are limited to regulatory bodies, customers and potential customers and their agents, suppliers, licensees, and others with a legitimate need for the information, and then only in accordance with appropriate regulatory provisions or contractual agreements to maintain confidentiality.

(c) The information is being transmitted to and received by the NRC in confidence.

(d) No public disclosure of the information has been made, and it is not available in public sources. All disclosures to third parties, including any required transmittals to NRC, have been made, or must be made, pursuant to regulatory provisions or contractual agreements that provide for maintenance of the information in confidence.

(e) Public disclosure of the information is likely to cause substantial harm to the competitive position of NuScale, taking into account the value of the information to NuScale, the amount of effort and money expended by NuScale in developing the information, and the difficulty others would have in acquiring or duplicating the information. The information sought to be withheld is part of NuScale's technology that provides NuScale with a competitive advantage over other firms in the industry. NuScale has invested significant human and financial capital in developing this technology and NuScale believes it would be difficult for others to duplicate the technology without access to the information sought to be withheld.

I declare under penalty of perjury that the foregoing is true and correct. Executed on 7/14/2023.

Mark W. Shaver

Mark W. Shaver